Role of obesity in the pathology of pulmonary hypertension

Inaugural Dissertation
submitted to the

Faculty of Medicine in partial fulfillment of the
requirements

for the PhD-Degree

of the Faculties of Veterinary Medicine and Medicine of
the Justus Liebig University Giessen

by

Balram Neupane

बलराम न्यौपाने

of

Syangja, Nepal

Giessen 2016

From the Institute of Pulmonary Pharmacotherapy

Director / Chairman: Prof. Dr. rer. nat. Ralph Schermuly

of the Faculty of Medicine of the Justus Liebig University Giessen

First Supervisor and Committee Member: Prof. Dr. Ralph Schermuly

Second Supervisor and Committee Member: Prof. Dr. Christiane Herden

Committee Members: Prof. Dr. Martin Diener
Prof. Dr. Ralph Schermuly
Prof. Dr. Christiane Herden

Date of Doctoral Defense: 21 November, 2016

Table of contents

Index of figures

Index of tables

Preface

Pulmonary hypertension (PH) is a condition where the pulmonary artery pressure is elevated. This condition develops due to various known and unknown factors. Pulmonary vascular constriction due to hypoxia or other factors give rise to acute pulmonary hypertension whereas progressive pulmonary vascular remodeling is more prominent feature in the chronic form of this disease. To simplify the diagnosis and treatment of PH, the disease has been classified into various groups according to its etiology. Among various factors, obesity has also been linked with pulmonary hypertension. Obesity, a condition where excess of adipose tissue accumulates in the body, exerts oxidative stress and inflammation in the body tissues. Since both important features of obesity, such as oxidative stress and increased inflammation, play a role in the pathophysiology of pulmonary hypertension, it has been speculated that obesity might contribute to the initiation, propagation or exacerbation of pulmonary hypertension.

Obesity is prevalent in many countries. It is alarmingly increasing due to food processing as well as change of life styles. Obesity itself is associated with myriad of morbid states in heart such as hypertension, obstructive sleep apnea, obesity hypoventilation syndrome, coronary heart disease, heart failure, diabetes and insulin resistance. Nevertheless, research till date does not provide an explicit correlation between pulmonary hypertension and obesity. Conversely, some cohort studies have even shown beneficial effects of increased body weight in long term mortality due to pulmonary hypertension. However, proper research and convincing results are still missing in these circumstances.

With these interesting but still unresolved issue, the present work aims to unveil the mechanisms and proper relationship between obesity and pulmonary hypertension. The results and conclusion obtained from this study may help to understand the underlying mechanisms and potential link of obesity and pulmonary hypertension. It may also open the door to find out the right therapeutic option in pulmonary hypertension patients who also suffer from various degree of dysregulated body weight.

1. Introduction

Pulmonary hypertension (PH) and obesity are two obstinate diseases that may coexist in clinical practice. Intromitted by the disturbances of several molecular pathways, PH is characterized by increased vascular cell growth and inflammation culminating to right heart failure and death (Simonneau et al., 2013; Schermuly et al., 2011). Obesity, on the other hand, is a condition of excessive fat accumulation in the body, which has an established association with cardiovascular diseases, diabetes, renal dysfunction and several pulmonary disorders namely chronic obstructive pulmonary disease (COPD), sleep apnea and pulmonary embolism (Irwin et al., 2014). Although obesity has a long-familiar positive correlation with systemic hypertension, there are insufficient data with regard to obesity as a potential player for PH (Summer et al., 2012).

The degree of adiposity of all levels has been alarmingly increasing in most part of the world. In spite of the fact that overweight and obesity predispose many cardiovascular diseases namely systemic hypertension, heart failure and coronary heart disease, the "obesity paradox" exists, which shows significant higher short or long term survival in obese patients than their lean counterparts (Lavie et al., 2014). Till date, no data have been able to show an effective role of obesity in PH. These studies are clearly missing and therefore this research is targeted to understand and find the proper correlation and molecular link between obesity and PH.

Once thought to be a predominant female oriented disease in relatively younger age, the recent results on pulmonary arterial hypertension (PAH) suggest a more even ratio of male to female (Hoeper et al., 2013). Therefore, the current thesis also aims to unravel the important but not fully understood arena of female obesity in relation to PH in a murine model of male and female obesity. Surprisingly, in humans, the survival rate of females after the diagnosis of PH is shown to be higher than in males (Austin et al., 2013). Presuming the uniqueness of female hormones and physiology versus male, diversity of etiology and pathomechanism of PH, it would be crucial and exciting to explore the potential gender specific association of PH.

1.1 Pulmonary circulation

The pulmonary circulation, along with systemic circulation and lymphatic circulation, is a part of the circulatory system. The pulmonary circulation comprises heart, pulmonary arteries and veins, and lungs. The pulmonary artery receives the deoxygenated blood from the right ventricle. It then transfers blood to the pulmonary capillaries via the artery network system where the oxygen exchange takes place. The oxygenated blood is pumped back to the left ventricle via the pulmonary veins from where it is distributed to the systemic circulation (Guyton and Hall, 2006).

Various cardio-pulmonary diseases are related to abnormalities in the pulmonary circulation. Pulmonary hypertension is a medical condition where abnormally higher pulmonary artery pressure is seen due to various factors. Key parts are disturbed mitochondrial functions, inflammation and disordered growth factors which may or may not be genetically acquired. The structure and the function of the right ventricle plays an important role for the patient survival (Tuder et al., 2013). Hence, the diagnosis and treatment of diseases related to pulmonary circulation needs research focus not only on the lung but also on the heart. Especially, underlying genetic, epigenetic as well as molecular mechanisms have to be examined (Vonk-Noordegraaf et al., 2013).

1.2 Anatomy and physiology of heart and lung

Structure and function of heart and lung constitute the cardio-pulmonary system (Fig. 1). The heart is a muscular four chambered organ consisting of two each - atria and ventricles. Atria (singular: atrium) and ventricles are separated into right and left parts by interatrial and interventricular septum, respectively. The heart tissue consists of three layers - epi-, myo- and endo-cardium. It is protected by an outer double layered pericardium (Scanlon and Sanders, 2007). The right atrium first collects the deoxygenated blood and then transfers it to the right ventricle via tricuspid valve. The right ventricle then ejects the blood towards the lungs via pulmonary artery. The left atrium collects the oxygenated blood and forwards to the left ventricle via bicuspid / mitral valve, where the left ventricle pumps the

blood into the systemic circulation through the aorta. This whole process is initiated by the generation of electric impulses from the sino-atrial node (SA node). The excitation is conducted via the cardiomyocytes to the atrioventricular node. This node functions as a "bodyguard" and forwards only a certain amount of impulses. These continue their way through the Tawara's branches and finally reach the chamber myocardium via purkinje fibers. An electromechanical coupling generates the transduction from the electronic impulses into mechanical movement of the heart muscle (Guyton and Hall, 2006).

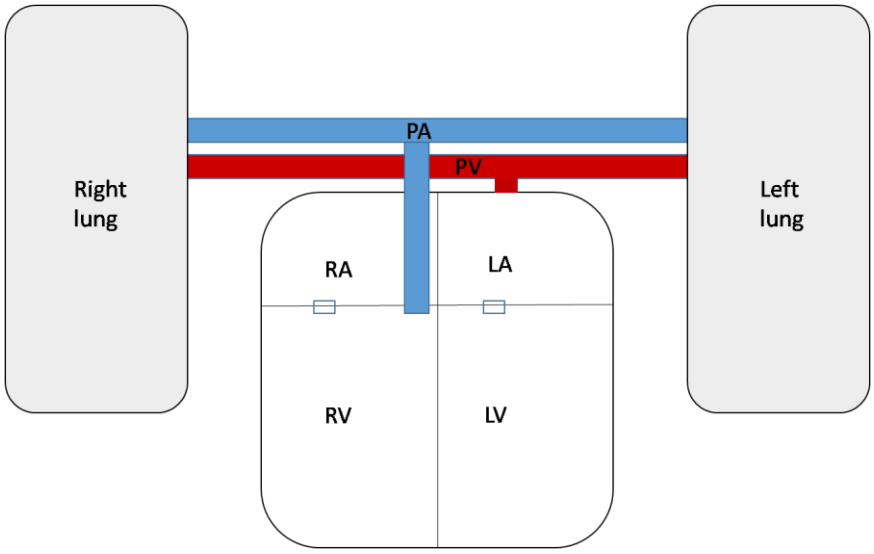

Fig. 1: Schematic diagram of the cardio-pulmonary system. PA = pulmonary artery, PV = pulmonary vein, RA = right atrium, LA = left atrium, RV = right ventricle, LV = left ventricle

In humans, the lungs are situated inside the thoracic cavity and are divided into right and left lungs. The right and left lungs are further divided into three and two lobes respectively. The heart lies in the mediastinum between the right and left lung. The cardiac notch in the left lung accommodates the pericardium. With a tremendous architectural design, the lungs consist of around 480 million gas exchange units - the alveoli, putting the total area for gas exchange to a huge 130 square meters. Maintained by primarily two types, type I and type II alveolar cells, the majority of the alveolar wall is covered by type I cells. These are able to maintain a meager thickness of 1.6 micrometer (Weibel, 2009).

The spatial pattern and distribution of alveoli makes the lung a very sophisticated organ for the gas exchange. The internal lining of the airways is covered with epithelial cells which not only give physical protection to outside pathogen or foreign particles, but also assist by releasing antimicrobials and inflammatory mediators as well as recruiting immune cells. Other cell types, such as basal cells and clara cells also have adequate potentiality to proliferate and self regenerate into various cell types. This become important when external damage occurs in the epithelium (Tam et al., 2011). In addition to various protective functions such as detoxification, inflammation control, mucociliary clearance and maintenance of ciliated epithelial cells, clara cells also secrete surfactant proteins, cytokines, chemokines, antimicrobials and mucins (Reynolds and Malkinson, 2010).

Although advancements in the knowledge and understanding of the cardio-vascular system have taken a long stride, the knowledge about the pathomechanisms behind pulmonary hypertension and pulmonary vascular diseases are still progressing. A deeper understanding of the pathobiology of pulmonary hypertension with respect to its etiology is more than needed for an effective treatment with lower side effects to the patients in future.

1.3 Pulmonary hypertension

Pulmonary hypertension is the condition of increased blood pressure in the pulmonary artery and is characterized by morbid and gradual growth, progression and increased motility of pulmonary vascular smooth muscle cells (Dahal et al., 2010; Schermuly et al., 2005). Clinically, PH is defined as the mean pulmonary artery pressure of greater or equal to 25 mm Hg measured at a resting condition and measured through right heart catheterization. Right heart catheterization is established as the "gold standard" for diagnosis of PH. An additional measurement of pulmonary artery wedge pressure (PAWP) or pulmonary artery capillary pressure (PACP) is performed during the right heart catheterization to differentiate between pre-capillary and post-capillary PH (Hoeper et al., 2013).

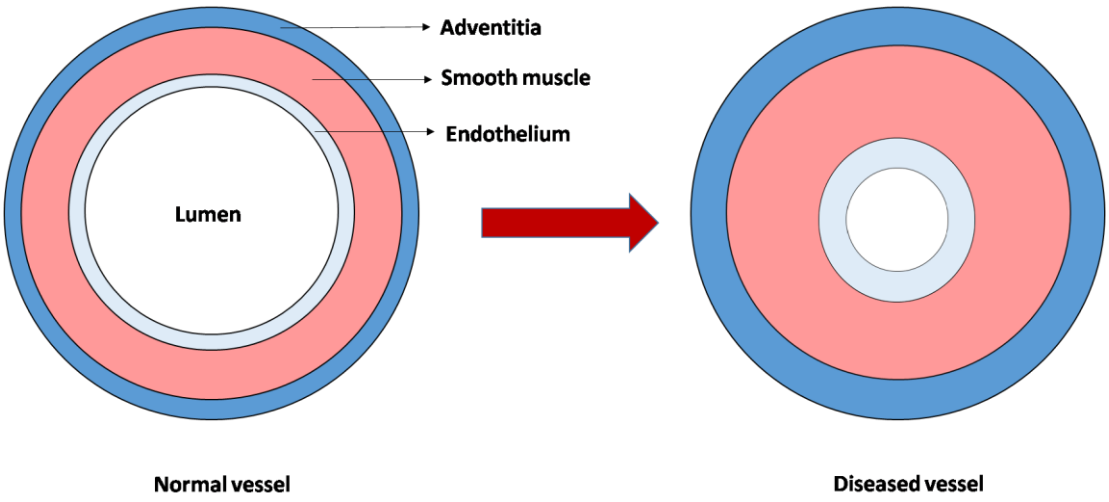

Fig. 2: Schematic diagram showing increased thickness of pulmonary vessels and loss of cross sectional area.

Associated with an acute form of vasoconstriction or a chronic phase of pulmonary vascular remodeling, PH results in the decrement of cross-sectional area of the vascular lumen, thereby increasing the right ventricle afterload. The abnormal pulmonary vascular remodeling is observed in all the three layers of the vessels - *intima, media and adventitia*. A decrease in the content/functions of various vasodilatory molecules such as prostaglandin I_2 or nitric oxide and an increase in vasoconstrictive mediators such as thromboxane, serotonin and endothelin I, increase of growth factors such as vascular endothelial growth factor (VEGF), basic fibroblast growth factor (bFGF), transforming growth factor - beta (TGF-β), platelet derived growth factor (PDGF), as well as involvement of inflammatory mediators, monocytes, macrophages, mast cells and disturbed cytokine and chemokine profiles play role in the development and patho-mechanism of PH (Schermuly et al., 2011).

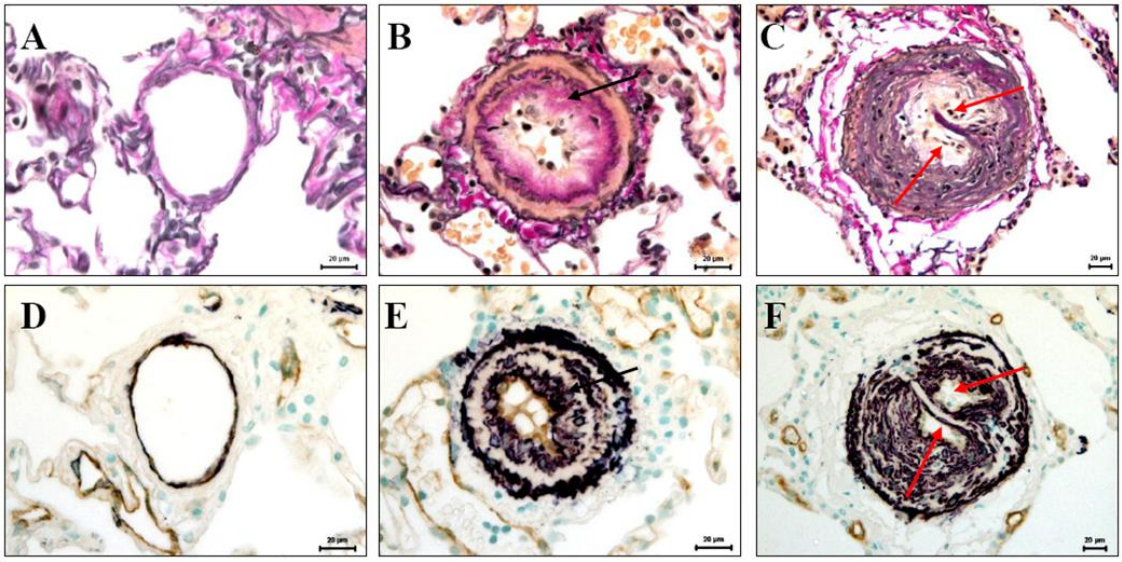

Fig. 3: Severe histo-pathological features of the pulmonary vasculature found in the patients with pulmonary arterial hypertension (PAH). Neointima formation (**B**, **E**; indicated by black arrows) and plexiform lesions (**C**, **F**; indicated by red arrows), in comparison to the normal vessels (**A**, **D**). **A**, **B**, **C**: Elastica van Gieson staining; **D**, **E**, **F**: immunohistochemical staining (α-smooth muscle actin (violet color) and von Willebrand factor (brown color)). Scale bars = 20 µm. (Used with permission from the dissertation of Dr. Djuro Kosanovic (2011)).

With all the changes in pulmonary artery remodeling, pulmonary hypertension leads to increased right heart afterload with compensatory mechanisms. However, the compensatory mechanisms become gradually insufficient giving rise to right ventricle (RV) failure. This RV failure ultimately determines the prognosis of patients (Vonk-Noordegraaf et al., 2013). Largely endorsed by symptomatic care, an effective and optimized treatment for pulmonary hypertension is still missing (Ghofrani et al., 2009).

1.4 Updated classification of pulmonary hypertension

To possess a common attribute for the characteristics and management of PH, clinical classifications have been made since 1998 in World Symposium on PH held in Evian, France. This classification has been updated with the advancement of knowledge in the pathobiology of this disease. The latest clinical classification of PH, which includes some

modifications and updates from the previous versions, comes from the 5th World Symposium held in 2013 in Nice, France. Based on the etiology, PH is classified into five groups. The first group include PAH with various causes, pulmonary veno-occlusive disease and/or pulmonary capillary hemangiomatosis and persistent PH of the newborn. The second group consists of PH due to left heart disease. PH due to lung diseases and/or hypoxia is included in the third group. The fourth and fifth group comprise the chronic thromboembolic PH and PH with unclear multifactorial mechanisms respectively. The classification is presented in the table (Simonneau et al., 2013).

1. Pulmonary arterial hypertension
Idiopathic PAH
Heritable PA:
BMPR2
ALK-1, ENG, SMAD9, CAV1, KCNK3
Unknown
Drug and toxin induced
Associated with:
Connective tissue disease
HIV infection
Portal hypertension
Congenital heart disease
Schistosomiasis
1'. Pulmonary veno-occlusive disease and/or pulmonary capillary hemangiomatosis
1''. Persistent PH of the newborn
2. Pulmonary hypertension due to left heart disease
Left ventricular systolic dysfunction
Left ventricular diastolic dysfunction
Valvular disease
Congenital/acquired left heart inflow/outflow tract obstruction and congenital cardiomyopathies
3. Pulmonary hypertension due to lung diseases and/or hypoxia
Chronic obstructive pulmonary disease
Interstitial lung disease
Other pulmonary diseases with mixed restrictive and obstructive pattern
Sleep-disordered breathing
Alveolar hypoventilation disorders
Chronic exposure to high altitude
Developmental lung diseases
4. Chronic thromboembolic pulmonary hypertension

5. Pulmonary hypertension with unclear multi-factorial mechanisms
Hematologic disorders: chronic hemolytic anemia, myeloproliferative disorders, splenectomy
Systemic disorders: sarcoidosis, pulmonary histiocytosis, lymphangioleiomyomatosis
Metabolic disorders: glycogen storage disease, Gaucher disease, thyroid disorders
Others: tumoral obstruction, fibrosing mediastinitis, chronic renal failure, segmental PH

Table 1: Updated clinical classification of pulmonary hypertension as adopted by the 5th world symposium on pulmonary hypertension, Nice, France, 2013 (Simonneau et al., 2013).

1.5 Current treatment for pulmonary hypertension

With limited therapeutic options in the past, the evolution of treatment algorithms for pulmonary hypertension have advanced. At present, the main focus on the treatment relies on several areas such as rehabilitation and exercise training, application of drugs approved by the respective countries and the response and adjustments to the applied therapies (Galie et al., 2013). Currently, the main treatment regimes for pulmonary arterial hypertension and pulmonary hypertension relies on the endothelin receptor antagonists (such as ambrisentan, bosentan and macitentan) (Galie et al., 2013)., nitric oxide and prostacyclin pathways (such as selexipag) (Sitbon et al., 2015). Research on additional pathways has also allowed to utilize the tyrosine kinase inhibitors, Rho kinase inhibitors and serotonin receptor blockers for the potential future treatment of pulmonary hypertension (Dahal et al., 2010; Pulido et al., 2016).

Soluble guanylate cyclase stimulators such as riociguat have been shown to significantly improve the 6 minute walk distance, pulmonary vascular resistance as well as WHO functional class in both naive pulmonary arterial hypertension patients as well as those who were receiving endothelin receptor antagonists (Ghofrani et al., 2013). Sildenafil, a phosphodiesterase 5 inhibitor (PDE5 inhibitor) has shown efficacy in the treatment of lung fibrosis, pulmonary arterial hypertension as well as portopulmonary hypertension. PDE5 inhibitors works by acting on the nitric oxide and cyclic guanosine monophosphate

(cGMP) pathways thereby increasing the cGMP levels and exerting vasodilatory and antiproliferative effects (Ghofrani et al., 2004; Ghofrani et al., 2002; Reichenberger et al., 2006).

The complexity and patient response has lead to combination therapy with more than one classes of medicine with additional supports such as rehabilitation, exercise training or oxygen therapy to maintain the correct arterial blood oxygen pressure.

1.6 Role of inflammation and oxidative stress in pulmonary hypertension

Intensive research in the past years clearly suggested that increased inflammation plays a role both in experimental and clinical forms of pulmonary hypertension (Dahal et al., 2011; Kosanovic et al., 2014; Pullamsetti et al., 2011; Savai et al., 2012). Imbalance of serum cytokines in a study done in idiopathic and familial PAH patients indicated the involvement of a wide range of inflammatory mediators in PH (Soon et al., 2010).

Furthermore, a significant increase of CD68 +ve macrophages, CD14+ve macrophages/monocytes, mast cells, CD209 +ve dendritic cells, CD3 +ve T cells, CD8 +ve cytotoxic T cells and CD4 +ve helper T cells were found in perivascular regions of various vascular categories (20-50 µm, 51-150 µm and > 150 µm) in the lungs of idiopathic PAH patients compared to that of healthy controls. This apparently suggests an altered infiltration and distribution of various inflammatory cells in PAH (Savai et al., 2012). In agreement to these findings, mast cells were also shown to be upregulated in the perivascular regions of the lungs of PH patients (Dahal et al, 2011; Kosanovic et al., 2014). Likewise, interleukin-6 is involved in the regulation of pulmonary arterial hypertension rendering the possibility to treat idiopathic pulmonary hypertension by intervening with this pathway (Furuya et al., 2010). The cytokines - tumor necrosis factor-alpha (TNF-α) and monocyte chemoattractant protein-1 (MCP-1) are also associated with pulmonary arterial hypertension and their interference allow beneficial effects in experimental monocrotaline model of PH in rats (Ikeda et al., 2004; Itoh et al., 2006; Wang et al., 2013).

These data further strengthen the fact of the involvement of inflammatory mediators in pulmonary hypertension (Fig. 4).

Along with inflammation and inflammatory mediators, to check the presence of oxidative stress in the lung tissues of patients with severe PH, Bowers et al. measured and demonstrated elevated levels of nitrotyrosine and 5-oxo-eicosatetraenoic acid. This study suggested that the lung tissues of patients with severe PH are under oxidative stress (Bowers et al., 2004). The group of Peter Dorfmüller also presented a novel idea of immunologic responses to oxidative stress in experimental pulmonary hypertension associating the influx of oxidative stress causing mast cells and dendritic cells to the affected vascular regions in the lungs (Dorfmüller et al., 2011). Ellagic acid, a compound with anti-oxidative, anti-inflammatory and anti-proliferative properties effectively improved the monocrotaline induced pulmonary hypertension in rats suggesting the involvement of inflammatory pathways in this disease (Tang et al., 2014).

In patients with an active pulmonary arterial hypertension, a controlled and non-randomized clinical research has shown the presence of inflammation and oxidative stress supported by increase in lipid peroxidation, reduced glutathione and vitamin E (Reis et al., 2013). Also, the treatment with chronic prostacyclin infusion showed anti-inflammatory effects in patients with severe pulmonary hypertension (Bowers et al., 2004). Inflammatory cells are known to produce metabolites of arachidonic acid, cytokines and chemokines, which further trigger the recruitment of inflammatory cells at the damaged site along with the production of more reactive species, thus playing a role in oxidative stress-induced inflammation (Reuter et al., 2010).

The findings on clinical or experimental pulmonary hypertension of different origins suggest a certain involvement of inflammation and oxidative stress in the pathology of the disease (Bowers et al., 2004; Dahal et al., 2011; Musaad and Haynes 2007). Therefore, anti-inflammatory drugs may show beneficial effects and represent future targets for the treatment of patients suffering from pulmonary hypertension.

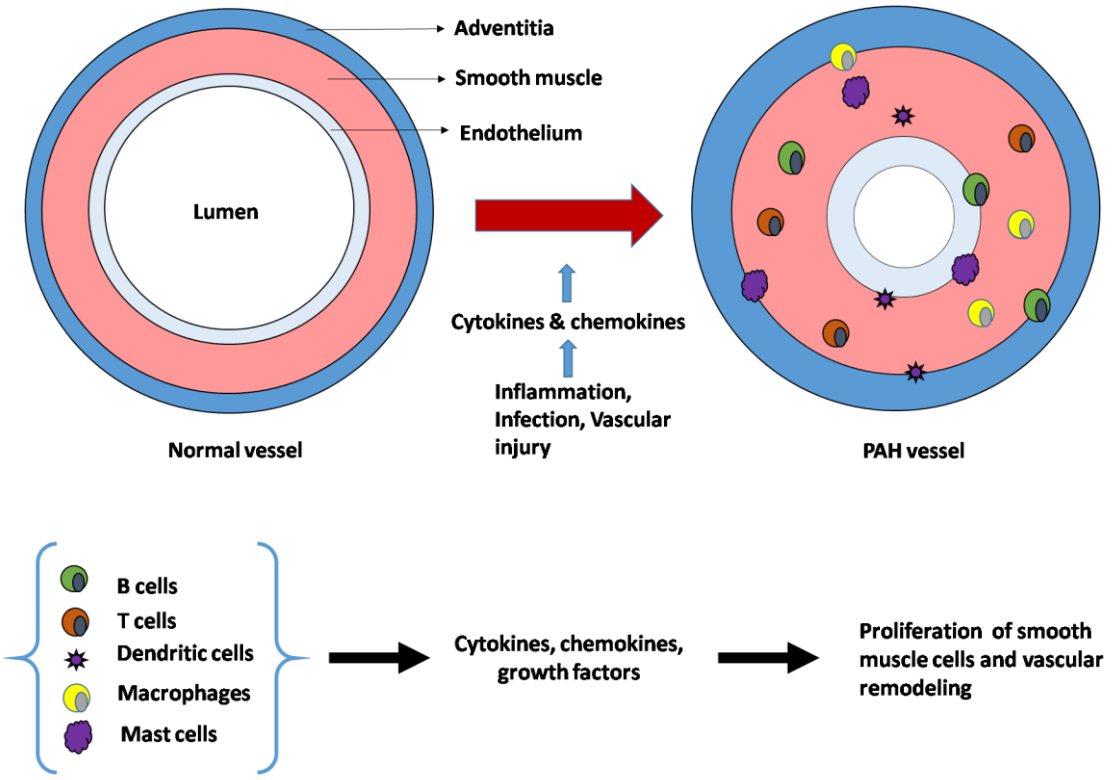

Fig. 4: Schematic diagram showing the role of inflammation in PAH and the types of cells involved.

1.7 Animal models of pulmonary hypertension

Animal models have long been used to mimic human disease. Both large animals and small animals have been used for the research purposes. However, choosing small mammals such as mice, rats and guinea pigs makes it much easier for the researcher in terms of space, money, maintenance as well as handling. Use of animals in studies make sure that humans are safe but yet able to learn and investigate the most important diseases which otherwise would not be possible.

Although some of the models employing rats and mice depict certain features common to human form of pulmonary hypertension, none of the animal models can precisely mimic the human conditions (Schermuly et al., 2011). Various models from environmentally or toxically induced models, as well as genetically modified models are currently used as models for pulmonary hypertension. Hypoxia induced pulmonary hypertension in mice, monocrotaline induced pulmonary hypertension in rats, bone morphogenetic protein

receptor 2 knockout mice, over-expressing interleukin 6 mice, cigarette smoke exposure, bleomycin induced pulmonary hypertension, pulmonary artery banding, transverse aortic constriction are some of the popular and successfully implied models for pulmonary hypertension (Pak et al., 2010).

Many essential pathological characteristics of pulmonary hypertension can be revealed by smaller animal models. However, certain types such as persistent pulmonary hypertension of the newborn are best suited in comparatively larger ovine and swine animal models. Although difficult to manipulate, they have a distinct advantage of handling larger instruments or later collecting ample amount of tissues (Steinhorn, 2010). Likewise, certain congenitally acquired left to right shunting induced pulmonary hypertension is best described by chronic systemic to pulmonary shunting in piglets. This animal model recapitulates naturalistic features of pulmonary hypertension in few months which may require decades in humans to be noticeable (Dewachter and Naeije, 2010). As such, animal models are need to be chosen very carefully and pragmatically according to the type and pathology of the disease. Two of the animal models used in the study are described in the following sections.

1.7.1 Hypoxia induced pulmonary hypertension

Hypoxia is a condition of reduced oxygen level in the tissues. People living or ascending high altitudes frequently experience lower oxygen pressure and may develop acute mountain sickness or PH. The lungs respond to hypoxia with a compensatory mechanism where pulmonary vasoconstriction occurs allowing to redistribute the pulmonary artery blood into the area where higher oxygen exchange capability is available. Known as von Euler-Liljestrand mechanism, this process of initial hypoxia adaptation, optimizes the oxygen exchange in the lungs (Sommer et al., 2008).

A chronic hypoxia exposure for a longer time will eventually lead to complex molecular and cellular alterations in the lung vasculature that contributes for the proliferation and remodeling of the pulmonary vessels (Stenmark et al., 2006). Taking advantage of the same

effect, hypoxia models are widely and successfully used as a model of pulmonary hypertension with a very high reproducible rate, mostly rats and mice (Dahal et al., 2011; Dahal et al., 2010; Schermuly et al., 2005). Nevertheless, the hypoxia injury and remodeling varies between different species of animal models (Stenmark et al., 2009).

Chronic hypoxia in rats and mice acquire mild to moderate type of pulmonary hypertension and do not represent the complex manifestation as that of human forms. It is crucial to indicate that the classical chronic exposure of mice and rats basically mimics the group 3 of the current clinical classification of PH. To overcome this problem and to find closer model for PAH (group 1), a combination of different factors are applied to achieve the best representation of the disease. SU5416 (3-[(2,4-dimethylpyrrol-5-yl) methylidenyl]-indolin-2-one), a synthetic vascular endothelial growth factor receptor (VEGFR) - 2 inhibitor, in combination with chronic hypoxia, has been shown to manifest severe pulmonary hypertension in rats. The establishment of this model ensured the appearance of pre-capillary occlusion by the proliferation of endothelial cells which are also the characteristics of the human form (Taraseviciene-Stewart et al., 2001). SU5416, in combination with hypoxia, also show similar effects in mice and persists more than 10 weeks after the return of normoxic conditions, albeit without further worsening of pulmonary hypertension or right ventricular dysfunction (Vitali et al., 2015).

1.7.3 Monocrotaline induced pulmonary hypertension

Monocrotaline is a pyrrolizidine alkaloid commonly found in many species of the Crotalaria plant and it is toxic to birds and mammals. Administration of monocrotaline in rats causes a cascade of events resulting in a severe form of pulmonary hypertension (Wilson et al., 1992). The precise and accurate explanation for the mechanism of action of monocrotaline is still not clear, but it has been suggested that the drug after entering the liver, is converted into monocrotaline pyrrole form and after traveling the lung vasculature, causes injury to the endothelium, finally activating the pathways responsible for proliferation and remodeling of pulmonary vessels. Monocrotaline induced pulmonary

hypertension is clearly seen in rats, but its effects on mice appear meek showing species differences of toxicity from this toxin (Dumitrascu et al., 2008).

Higher doses of subcutaneous monocrotaline injections show dose dependent toxicity and mortality in mice. Microscopic anatomy revealed severe interstitial pneumonia and lung fibrosis showing the advancement of disease in a non-reversible way indicating a possible model for lung cancers related to pulmonary fibrosis (Hayashi et al., 1995). Studies have also been done on cell cultures. Monocrotaline exposure to bovine pulmonary artery endothelial cells caused abnormal enlargement of cells characterized by enlarged Golgi, mislocalization of endothelial nitric oxide synthase and decreased nitric oxide indicating both Golgi and sub-cellular trafficking dysfunction (Lee et al., 2009). Study on human pulmonary arterial endothelial cells treated with monocrotaline pyrrole showed decreased expression of bone morphogenetic protein receptor II and transient expression of Smad (Suppressor of mothers against decapentaplegic) signaling pathways providing the evidence of resemblance to human pulmonary hypertension characteristics and the usefulness of this molecule in in-vitro model to exhibit molecular mechanism of pulmonary hypertension (Ramos et al., 2008).

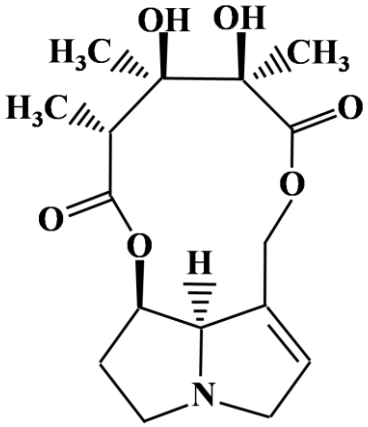

Fig. 5: Monocrotaline (Synonym: crotaline). Structure reconstructed from D. W. Wilson, Department of Pathology, College of Veterinary Medicine, University of California-Davis, USA (Wilson et al., 1992).

The monocrotaline model is being widely used in rats as a model for pulmonary arterial hypertension and it represents a historical model used in our research group for years (Dahal et al., 2010; Kosanovic et al., 2011; Schermuly et al., 2005). Keeping in mind the complexity and versatility of pulmonary hypertension in humans, this model should be carefully used to depict the underlying mechanisms and interpretations should be made by acquiring data from other models.

1.8 Obesity

Obesity is the condition of excessive accumulation of adipose tissue in the body. Generally estimated by means of body mass index, it gives an idea about the general condition. Obesity contributes myriads of adverse effects in the body such as psychological stress, insulin resistance, type II diabetes, leptin resistance, systemic hypertension, certain types of cancers and cardiovascular disease the deterioration of health condition and reduced life expectancy. The rate of obesity is alarmingly increasing and associated with numerous factors including sedentary life style, higher intake of processed and fast foods as well as genetic makeup (Yazdi et. al., 2015).

Adipose tissue is a loose connective tissue regarded as an endocrine organs due to fact that it secretes a wide range of adipokines as well as pro- and anti-inflammatory mediators such as leptin, adiponectin, interleukin-1 beta, interleukin-10 and tumor necrosis factor. Increase in adipose tissue or obesity leads to disorganization of these hormones or proteins with a variety of complications for example adverse effects on hemodynamics and cardiovascular structure and function, chronic inflammation, reduced insulin sensitivity, pre-diabetes and lower adiponectin levels. These effects due to obesity warrants complex metabolic syndrome (Grant and Dixit, 2015; Lavie, Milani, and Ventura, 2009).

Recently, it has also been suggested that the obesity related co-morbidities are different in obese subjects depending upon whether they are responders or non-responders indicating a biological variance within the obese groups. Interestingly, similar pattern are also seen in the lean counterparts in terms of metabolic diseases, where the two groups respond in a

dissimilar manner (Grant and Dixit, 2015). Elucidation on these variations in cellular and molecular levels would resolve many findings and provide insights on the involvedness of obesity with its associated morbidities.

Various obese models of rats and mice are available for obesity research. The models can either be genetically prone to obesity or special food diets higher in total fat percentage can be given to induce obesity.

Male and female obesity also have different characteristics and processes for deposition of adipose tissues in the body and it has been deemed important to include both sexes in basic research or clinical trials. Males have the tendency to accumulate more adipose tissues in the visceral region, while females conglomerate in the subcutaneous region (Palmer and Clegg, 2015). An experiment with high fat fed diet induced obesity presented the dimorphism of the increase in left ventricular mass in mice. This left ventricular mass was significantly higher in the male mice (Böhm et al., 2013). A nationwide study in United Sates of America showed that female patients had higher asthma prevalence than male in class III obesity (Wang et al., 2015). These data suggest that male versus female obesity may have different physiological features and pathologies.

1.8.1 Body mass index as a measure for obesity

Body mass index (BMI) is a system to measure the degree of obesity. It is calculated by dividing the weight in kilogram by the height square in meter. It is accepted worldwide with some differences between the countries. The calculation of BMI requires only height and weight, so its calculation can be easily done. Because BMI does not consider factors like the type and location of tissues or fat within the body, it is only used for screening and not for the diagnostic value (http://www.cdc.gov/healthyweight/assessing/bmi/adult_bmi/, assessed on 23 April, 2016).

International BMI calculation for adults given by world health organization (WHO):

Body mass index (Kg/m^2)	Status
< 18.5	Under-weight
18.5 - 24.99	Normal weight
25.0 - 29.99	Overweight / Pre-obese
30.0 - 34.99	Class I obesity
35.0 - 39.99	Class II obesity
> 40.0	Class III obesity

Table 2: Classification of adult obesity. (http://apps.who.int/bmi/index.jsp?introPage=intro_3.html, retrieved on 18 Feb, 2016)

Determining the body mass index for infants, toddlers and teenagers are different than those of adults. Suggestions for the body mass index chart for different age groups have also been made which will assist in the tracking and advising for the weight balance during the different growth periods. These kind of charts might also bring a way for body mass index screening for necessary adjustment in children and adults (Elizabeth and Muraleedharan, 2003).

The body mass index in rodents are usually calculated as weight in gram divided by length square in centimeter (gm/cm^2). Length is measured from the tip of nose to the base of tail.

1.10 Current understanding of obesity in pulmonary hypertension

The evidence up to date is not sufficient to relate obesity and pulmonary hypertension thoroughly. The frequency of patients with pulmonary hypertension and co-morbidity such as obesity is increasing (Poms et al., 2013). However, long term statistical studies have shown either less risk of death or low mortality of obese pulmonary hypertension patients (Badri et al., 2012; Poms et al., 2013; Zafrir et al., 2013). Whether or not obesity has direct consequences to pulmonary hypertension is still an undecided question.

Obesity also is one of the many causes for leptin resistance. Leptin which is secreted by the adipose tissue is a key hormone for energy regulation (Banks et al., 2004; Berbari et al., 2013). With an adjustment to obesity or body mass index, pulmonary arterial hypertension patients with high leptin levels have higher survival rates and lower leptin levels are linked with high mortality (Tonelli et al., 2012). Ghrelin, another hormone related to energy regulation, also stimulates adiposity in experimental conditions (Tschöp et al., 2000) suggesting that impairment of these energy regulating hormones might play a role in the development of pulmonary hypertension.

Obesity expresses the possibility of developing the conditions of obesity hypoventilation syndrome (Kauppert et al., 2013) and obstructive sleep apnea (Vgontzas et al., 2000) which are more concerning and intriguing disease sequela. The formal classification of PH also lists sleep disordered breathing and alveolar hypoventilation disorder as possible etiology of pulmonary hypertension (Simonneau et al., 2013). Also the data from pulmonary hypertension arising due to obstructive sleep apnea or obesity hypoventilation syndrome suggest that these patients only suffer from mild to moderate form of the disease (Kauppert et al., 2013; Kessler et al., 1996). This milder form of disease may explain the obesity paradox where less mortality of obese patients is seen after the first diagnosis.

Adiponectin, an anti-inflammatory cytokine, secreted primarily by adipose tissues, is down-regulated in various clinical conditions such as pulmonary hypertension, type II diabetes, insulin resistance, obesity, coronary artery disease or other cardiovascular diseases (Li et al., 2007; Medoff et al., 2009; Summer et al., 2009). Adiponectin through its beneficial effects on pulmonary artery smooth muscle cells, is shown to inhibit the remodeling process in the context of pulmonary hypertension (Weng et al., 2011). The role of adiponectin has also been demonstrated in lung injury and inflammation in adiponectin deleted mice model (Konter et al., 2012). Therefore, adiponectin, due to similar alteration pattern in both obesity and pulmonary hypertension, may represent a potential link between these two medical conditions.

Another evidenced pathway for adiponectin is the suppression of C-reactive protein from the endothelial cells. Adiponectin also inhibits the activity of nuclear factor-κB (nuclear factor kappa-light-chain-enhancer of activated B cells) (Devaraj et al., 2008). Higher expression of C-reactive protein and nuclear factor-κB are related to obesity and cardiovascular abnormalities with higher expression of interleukins and cell adhesion mediates (Devaraj et al., 2008; Ouchi and Walsh, 2008). This higher levels of interleukins leads to vasoconstriction by inhibiting eNOS (endothelial nitric oxide synthase) pathway (Hansmann and Rabinovitch, 2010).

In addition to pulmonary hypertension, adiponectin appears to be a common molecule which has been attributed to down-regulation of various clinical conditions such as diabetes, insulin resistance and obesity. It can be speculated that this exclusive molecule is the common factor which has the molecular connection between pulmonary hypertension and obesity, diabetes and insulin resistance. Nevertheless, proper evidences need to plausibly connect this interaction.

Fat diet induced obesity in rats has also been shown to cause increased oxidative stress in the pulmonary artery wall, as well as elevated inflammatory cytokines in the blood plasma (Irwin et al., 2014). It has also been postulated that obesity might play crucial role in the pathobiology of pulmonary diseases through the involvement of pro-inflammatory mediators contributing a low grade systemic inflammation (Mancuso, 2010).

Obese mice showed increased cardiac expression of prepro-endothelin-1 mRNA (micro ribonucleic acid), protein as well as endothelin receptors A and B mRNA compared to their lean counterparts (Catar et. al., 2014) suggesting that increase in adipose tissues can be important later for the disease development and its further complications. Importantly, the altered endothelin system is described in the context of PH (Kosanovic et al., 2011).

Musaad and Haynes have elaborated the importance of obesity derived inflammation and oxidative stress in the tissues and organs of the body taking into account the environmental and genetic background of the subjects. Increase of adipose tissue mass leads to increased

levels of oxidized low density lipoprotein, IL-6, TNF-α and CRP as well as decrease in adiponectin levels, subsequently increasing the cardiovascular risk in general (Musaad and Haynes, 2007).

Pulmonary hypertension, on the other hand, is also closely connected with chronic inflammatory processes with the infiltration of various inflammatory cells, such as mast cells, macrophages and dendritic cells. Increased expressions of pro-inflammatory cytokines and chemokines also contribute to the pulmonary vascular remodeling processes (Dahal et al., 2011; Pullamsetti et al., 2011; Savai et al., 2012). In addition, PH is indeed a disease which considers oxidative stress, as one of its features (Bowers et al., 2004).

Therefore, the current understanding apparently suggests that both obesity and pulmonary hypertension are characterized by altered inflammation and oxidative stress, potentially showing a possible interaction between these two conditions (Fig. 6).

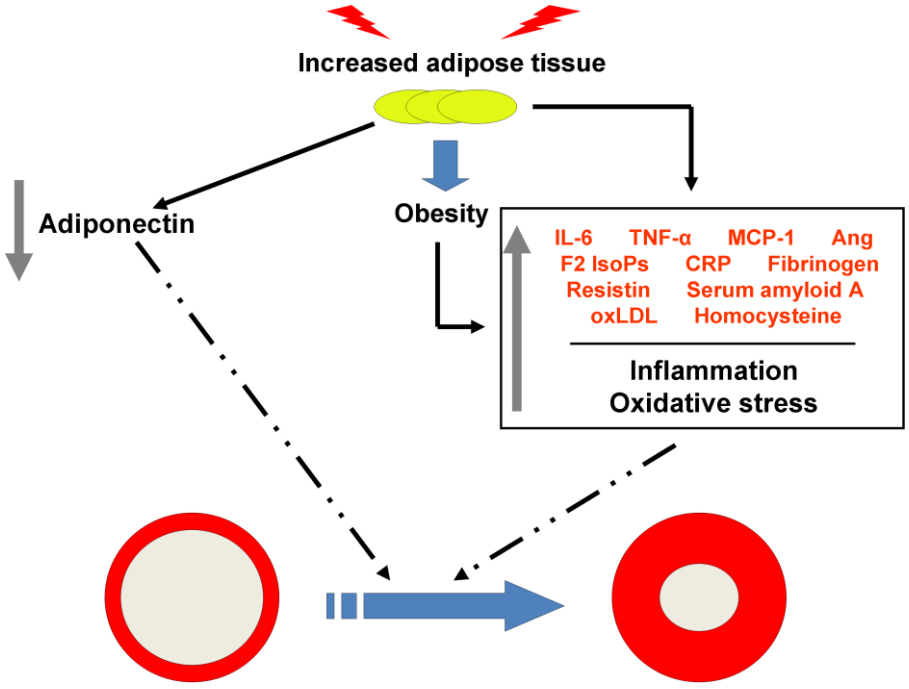

Fig. 6: Schematic diagram for the obesity - pulmonary hypertension possible pathway. IL-6 = interleukin-6, TNF-α = tumor necrosis factor - alpha, MCP-1 = monocyte chemoattractant protein - 1, Ang = angiotensinogen, F2 IsoPs = F2 isoprostanes, CRP = C-reactive protein, oxLDL = oxidized low density lipoprotein. (Neupane et. al., PVRI Chronicle, 2014)

1.11 Metabolic dysfunction, gender and endocrine players

The metabolic activities within a normal cell or organ are tightly and precisely maintained. Cardiac dysfunction with altered metabolism and differences in nature and form of degree of progress in pulmonary hypertension has been shown with regard to gender, animal models and well as female sex hormones (Bal et al., 2013; Belke et al., 2000; Stevan et al., 2009). Pulmonary hypertension in studies done decades before showed it to be primarily a female oriented (female : male :: 1.7 : 1) disease with only 10% of patients older than 60 years (Ghamra and Dweik, 2003). However, a more recent result suggest that the course of pulmonary hypertension has been shifted to older patients (greater than 65 years) with almost even female to male ratio (female : male :: 1.2 : 1), although the ratio of female to male in young diagnosed patients were higher (Hoeper, Huscher, et al., 2013).

Surprisingly, survival rates of females after diagnosis are higher (Austin et al., 2013). This asymmetrical characteristic of the disease has not been explained but the possibility of endocrine hormonal roles cannot be taken out. Experimentally induced monocrotaline model of pulmonary hypertension showed less severity of disease in female rats. Higher antioxidant defense capacity of female rats was thought to play the protective role (Bal et al., 2013). Protective effects of estrogen has been shown in monocrotaline model of pulmonary hypertension in female Sprague-Dawley rats and ovariectomized females were more prone to pulmonary hypertension (Yuan et al., 2013).

Because of the diversity of etiology and patho-mechanism of pulmonary hypertension, a single factor may not be able to explain the course of disease.

1.12 Hypothesis, objectives and aims of the study

Therefore, based on the above mentioned knowledge and current understanding, the role or contribution of obesity to the pathogenesis of pulmonary hypertension is not accurately and profoundly described and systematic investigation is still missing. In the line with this thinking, I would like to hypothesize that increase in adipose tissue may represent an important factor of the patho-biology of pulmonary hypertension.

Objectives and aims of the study are:

- To investigate the role of obesity in development of experimental pulmonary hypertension, using two well-established models of the disease, such as monocrotaline (MCT)-induced pulmonary hypertension in rats and chronic hypoxia-induced pulmonary hypertension in mice.

- To reveal the potential differences between male and female obesity in the context of pulmonary hypertension.

Genetically modified obese male and female Zucker rats and their lean counterparts were used for the monocrotaline (MCT) model. Similarly, genetically modified obese male and female B6 mice and their lean counterparts were used for chronic hypoxia model. Invasive hemodynamic measurements, echocardiography and histological assessment were performed for measurement of right heart function and hypertrophy, hemodynamic parameters and pulmonary vascular remodeling. This study may reveal important details about potential involvement of obesity in experimental pulmonary hypertension and differences between male and female obesity.

2. Materials and methods

2.1 Materials

Table 3: Materials used for animal experiments, echocardiography, invasive hemodynamics and histology with semi-quantitative computer-based morphometry.

Substance	Supplier
Blood analyzer Rapid Lab 348	Siemens, Germany
High-resolution imaging system VEVO 2100	VisualSonics, Toronto, Canada
Transducers	B. Braun Melsungen, Melsungen, Germany
SAR-830/P Ventilator	IITH Life Science INC., CA, USA
Isoflurane Forene®	Abbott, Wiesbach, Germany
Braunoderm®	B. Braun Melsungen, Melsungen, Germany
Ultrasound transmission gel Aquasonic® 100	Parker Laboratories, Fairfield, NJ, USA
Physiological saline solution	DeltaSelect GmbH, Dreieich, Germany
Heparin	Ratiopharm GmbH, Germany
Dexpanthenol eye ointment	Bayer, Leverkusen, Germany
Monocrotaline (Crotaline®)	Sigma-Aldrich Biochemie GmbH, Steinheim, Germany
Ketamin-10%	Bela Pharm, Vechta, Germany
Physiological saline solution	B.Braun, Melsungen AG, Melsungen, Germany
Xylazin 2%	Ceva Tiergesundheit, Dusseldorf, Germany
Normoxic ventilation gas (21% O_2, 5.3% CO_2, balanced with N_2)	Praxair, Germany
Hypoxic ventilation gas (1% O_2, 5.3% CO_2, balanced with N_2)	Praxair, Germany
Domitor® 1mg/ml	Janssen Animal Health (Elanco) Bad Homburg, Germany
Baytril 2.5%	Bayer Leverkusen, Germany
Veet shaving creme	Bayer Leverkusen, Germany
EDTA Monovette	Sarstedt, Nümbrecht, Germany
Automated microtome RH 2255	Leica Microsystems, Wetzlar, Germany
Tissue embedding machine EG 1150H	Leica Microsystems, Wetzlar, Germany
Sakura cassette printer	Sakura finetek Germany
Tissue dehydrating machine TP1050	Leica Microsystems, Wetzlar, Germany
Cooling plate EG 1150 C	Leica Microsystems, Wetzlar, Germany
Flattening table HI 1220	Leica Microsystems, Wetzlar, Germany
Flattening bath for paraffin sections HI 1210	Leica Microsystems, Wetzlar, Germany

Hypoxic chambers Oxycycler Model A84XOV	Bio Spherix, New York, USA
Stereo light microscope DMLA 6000	Leica Microsystems, Wetzlar, Germany
Imaging workstation Q550IW	Leica Microsystems, Wetzlar, Germany
Imaging software QWin V3	Leica Microsystems, Wetzlar, Germany
Ethanol 70%, 95%, 99.6%	Otto Fischar GmbH, Saarbrücken, Germany
Coverslip	Menzel, Germany
2% acid fuchsin	
Avidin-Biotin blocking kit	Vector, Wertheim-Bettingen, Germany
DAB substrate kit	Vector, Wertheim-Bettingen, Germany
Dako Real™ proteinase K	Dako, Glostrup, Denmark
Eosin Y	Thermo scientific, Kalamazoo, USA
Formaldehyde 3.5 - 3.7%	Otto Fischar, Saarbrucken, Germany
Haemalaun, Sauer nach Mayer	Waldeck GmbH, Muenster, Germany
Hydrogen peroxide 30%	Merck, Darmstadt, Germany
ImPRESS kit anti-rabbit Ig	Vector, Wertheim-Bettingen, Germany
Isopropanol (99.8%)	Fluka Chemie, Buchs, Switzerland
Methanol	Sigma-Aldrich Biochemie GmbH, Steinheim, Germany
Methyl green	Vector, Wertheim-Bettingen, Germany
Mounting medium (Pertex®)	Medite GmbH, Burgdorf, Germany
Mouse-on-mouse HRP polymer	Biocare Medical, Concord, USA
Normal horse serum	Vector, Wertheim-Bettingen, Germany
Normal rabbit serum	Vector, Wertheim-Bettingen, Germany
PAP pen	Kisker Biotech, Steinfurt, Germany
Paraplast plus	Sigma Aldrich, Steinheim, Germany
Trypsin Digest all 2®	Zytomed, Berlin, Germany
Vector VIP substrate kit	Vector, Wertheim-Bettingen, Germany
Xylol	Roth, Karlsruhe, Germany
Glass slides (SuperFrost UltraPlus®)	Langenbrinck, Emmendingen, Germany
Embedding cassettes	Leica Microsystems, Nussloch, Germany
Microtom blades type A35	Feather Safety Razor Co. Ltd, Japan

Antibodies for immunohistochemistry.

Mouse anti-α-SMA, clone 1A4 monoclonal	Sigma Aldrich, Steinheim, Germany
Rabbit anti-von Willebrand factor	Dako Cytomation, Hamburg, Germany
Mouse anti-Rat CD68 (MCA341R)	AbD Serotec

Consumables

Napkins	Tork, Mannheim, Germany
Falcon tubes	Greiner bio-one, Frickenhausen, Germany
Single use gloves Microtouch	Ansell Healthcare Europe, Brussels, Belgium
Filter tips	Filter tips
Disposable feather scalpel	Feather safety razor Co. Ltd, Osaka, Japan
Pipette tips	EPPENDORF, Hamburg, Germany
Syringe Injekt®-F	Braun, Melsungen, Germany
Black thread no. 16	Coats GmbH, Kenzingen, Germany
Medical adhesive bands (3M™ Durapore™ Surgical tape	3M Health Care, St, Paul, MN, USA
Gauze balls size 6	Fuhrmann Verrbandstoffe GmbH, Munich, Germany
Surgical instruments	Fine Science Tools GmbH, Heidelberg, Martin Medizintechnik, Tuttlingen, Germany
Cannula for vein catheter support 22G	B. Braun Melsungen AG, Melsungen
Eppendorf tubes	Eppendorf, Hamburg, Germany

2.2 Methods

2.2.1 Animal models

Adult obese and lean male and female Zucker rats (Crl:ZUC-*Lepr*$^{fa)}$ were obtained from Charles River Laboratories (Sulzfeld, Germany). Similarly, ob/ob B6.Cg-*Lep*^{ob}/J obese and lean (C57BL6/J or B6) mice (male and female) were also obtained from Charles River. All animals were kept under controlled temperature (22 ± 2^{o}C and a daylight/night cycle of 14/10 hours with *ad libitum* food and water supply. The protocols were approved by the governmental Animal Ethics Committee: Regierungspraesidium Giessen, GI 20/10 Nr. 24/2014 and GI 20/10 Nr. 71/2012.

Fig. 7: Lean and obese Zucker rats. Left: lean male Zucker rat, Right: obese male Zucker rat.

2.2.2 Monocrotaline (MCT) induced pulmonary hypertension model in rats

MCT model is well-established in our research group and it was used in this study, as we previously described and published (Dahal et al., 2011; Dahal et al., 2010; Dumitrascu et al., 2008; Kosanovic et al., 2011; Schermuly et al., 2004; Schermuly et al., 2005). Pulmonary hypertension in the Zucker rats was induced by single subcutaneous injection of monocrotaline with a dose of 60mg/kg body weight as described previously (Schermuly et al., 2005). Monocrotaline (MCT) solution was prepared by dissolving the Monocrotaline (Crotaline®) in 1N HCl and 1N NaOH and pH was maintained at 7.4. The MCT solution was injected at day 0 subcutaneously in the neck. These MCT injected rats received 2.5% Baytril (antibiotic) in drinking water from 1st day to 15th day. Baytril solution was prepared by mixing 2ml of Baytril in 500ml of drinking water. As a healthy control, Zucker rats were injected with normal saline solution. The procedure were same for male and female rats.

2.2.3 Hypoxia induced pulmonary hypertension model in mice

Pulmonary hypertension in B6 ob/ob was induced by exposing the mice to hypoxia (10% O_2 fraction, FiO_2 10%) in normobaric hypoxic chamber for 5 weeks, as we previously described (Schermuly et al., 2005; Dahal et al., 2010; Dahal et al., 2011). The control mice were placed in the similar condition but in normoxic chamber (21% O_2 fraction, FiO_2 21%). The systems were regulated automatically to maintain the chamber normoxic and hypoxic. The procedure were similar for both male and female mice.

2.2.3.1 Experimental design

Experimental design for rats and mice is depicted below.

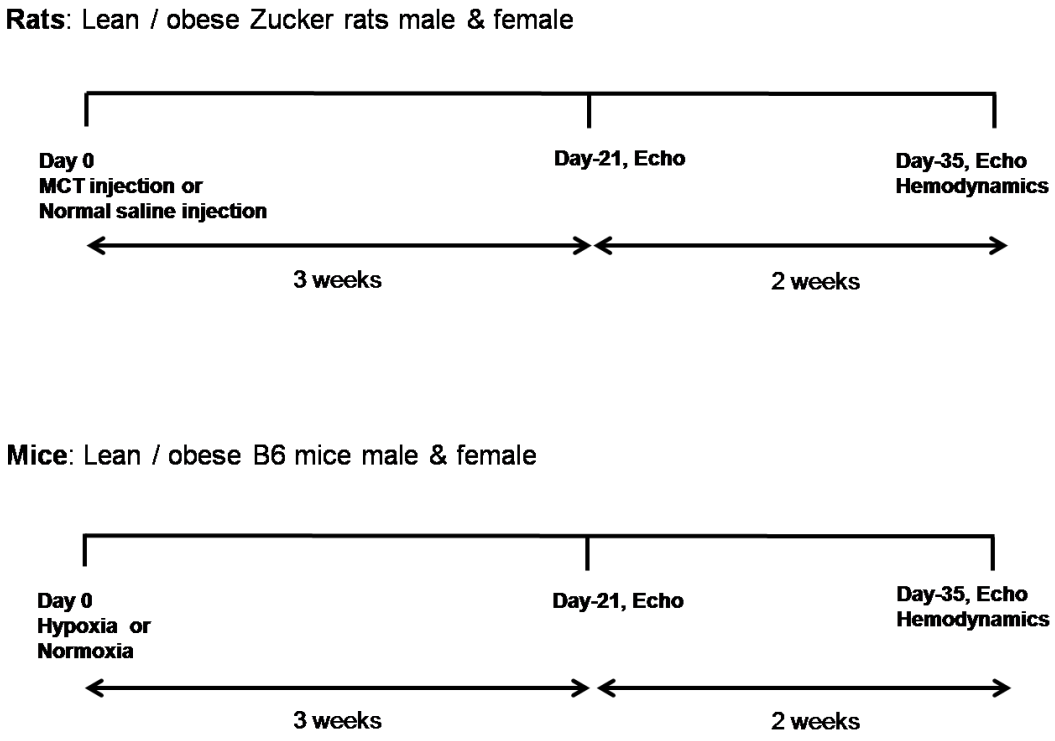

Fig. 8: Experimental design for all groups of Zucker rats and B6 mice

2.2.4 Echocardiography

Non-invasive measurement of several functional and morphometric parameters was performed by echocardiography, as we have previously described and published (Kojonazarov et al., 2013; Kosanovic et al., 2011; Savai et al., 2014). For this purpose, mouse or rat was anesthetized in the induction chamber supplied with 3% isoflurane in 100% oxygen. After the animal lost its reflex action, it was taken out and kept in supine position on a heating platform. The limbs of the animal were taped to ECG electrodes and the anesthesia was maintained with 1.5% isoflurane in 100% O_2 through a nose cone. The body temperature was monitored through a rectal probe. A dexpanthenol eye ointment (Bepanthen®) was applied in the eyes of animal to avoid their drying. A pre warmed ultrasound gel was applied over the chest wall after shaving the chest. Echocardiographic images were acquired with a VEVO2100 high resolution imaging system (Visual Sonics, Toronto, Canada) equipped with MicroScan linear array transducers MS550D (22-55 MHz) and MS250 (13-24 MHz). Following parameters were analyzed:

Right ventricle free wall thickness

It is the measure of the thickness of the right ventricle free wall. It is measured in millimeter and serves as a parameter of the right ventricle hypertrophy.

Right ventricle internal diameter

This is the distance between the inner linings of right ventricle free wall to the inner linings of interventricular septum towards the right ventricle. It is measured in millimeter and serves as a parameter of the right ventricle hypertrophy and dilatation.

Tricuspid annular plane systolic excursion (TAPSE)

TAPSE is the distance covered by right ventricle annular plane towards the apex and serves as a parameter of right ventricle longitudinal function. It is measured in millimeter. The normal value of TAPSE in humans is greater than 16 mm and decreases in heart failure or pulmonary hypertension. TAPSE is considered as an effective prognostic value for the survival of patients suffering from pulmonary hypertension. The mortality in patients with

TAPSE greater than 18 mm were significantly lower than those where the value were less than 18 mm (Forfia et al., 2006).

Pulmonary artery acceleration time (PAAT) / pulmonary artery ejection time (PAET)

PAAT is the time from the onset to peak velocity of pulmonary artery flow, obtained using pulsed wave Doppler echocardiography from the left parasternal short axis view. PAET is the full time required for the pulmonary outflow. The ratio of PAAT to PAET gives more reliable data because PAAT is dependent on heart rate. In humans, the normal heart rate is around 60-80 beats per minute, so the range is small. However, for small rodents, this range can be very high, even up to a difference of 200 beats per minute.

Cardiac output

It is the volume of blood ejected from the left ventricle or right ventricle into the circulation each minute. Cardiac output equals stroke volume, the volume of the blood ejected by the ventricle during each contraction, multiplied by the heart rate, the number of heart beats per minute. It can be calculated by the following formula:

CO = HR x SV, where CO = cardiac output, HR = heart rate, SV = stroke volume

The unit of measurement is liters/minute in humans and milliliters/minute in rodents.

Cardiac index

It is the ratio of cardiac output per unit area of the body. It estimates the performance to heart or the cardiac output according to the size of the body. Cardiac index can be calculated by the following formula:

CI = CO / BSA, where CI = cardiac index, CO = cardiac output, BSA = body surface area.

The unit of measurement is liters per minute per square meter in humans. In rodents, the cardiac index is given as cardiac output relative to body weight (milliliters/minute/gram body weight).

2.2.5 Hemodynamic measurements

The hemodynamic measurements were performed in full agreement and following the protocol that we have previously described and published (Dahal et al., 2011; Dahal et al., 2010; Kosanovic et al., 2011; Schermuly et al., 2005). Rats were anesthetized by intraperitoneal injection of combination of ketamine and domitor solution in the ratio of 10:1. The anesthetized animal was placed in supine position and neck and chest area were cleaned with Braunoderm®. After that the tracheotomy was performed and animal was artificially ventilated with a mixture of oxygen and nitrogen in the ratio 1:1 at a frequency of 60 breaths/min with an inspiratory flow rate of 500-600cc/min. The left carotid artery was isolated and small incision was made. To prevent blood coagulation, 0.5ml of heparin solution was administered. A cannula connected to a fluid filled transducer was inserted through the incision and systemic arterial pressure (SAP) was measured as described previously (Schermuly et al., 2005). Next the right jugular vein was isolated. A silicon catheter connected to a fluid filled transducer was inserted into the jugular vein through incision and right ventricular systolic pressure (RVSP) was measured. Before measuring RVSP, 0.5ml of heparin solution was administered through jugular vein. The computer software Labtech Notebook Runtime version 9.02 was used for recording the pressure for 5-10 minutes

For mice, the anesthesia dose combination was xylazin, ketamine and saline in the ratio of 1:1:2 and the rest of the procedure was similar. Before anesthetizing the mice, heparin was injected to reduce the blood coagulation.

2.2.6 Blood gas analysis / Hemoglobin concentration

During the hemodynamic procedure in Zucker rats, arterial and venous blood were taken separately and a blood gas analysis was performed in Rapidlab™ 348 for measuring the blood gas components. For B6 mice, arterial blood was taken in the hematocrit tube and analyzed in the Rapidlab™ 348 for measuring the hematocrit value.

2.2.7 Body mass index

Body mass index (BMI) was calculated in both mice and rats with the following formula:

$$BMI = \text{weight in grams} / \text{length in centimeters}^2$$

The length of the body of both mice and rats were considered from the tip of the nose until the base of the tail (Fig. 9).

Fig. 9: Depiction of the way by which the length of mice or rats was measured using a ruler.

2.2.8 Tissue harvesting / paraffin embedding / storage of tissues and plasma

At the end of hemodynamic procedure, animal was sacrificed. The chest cavity was opened. Lungs were flushed through pulmonary artery with 0.9% normal saline to make it free of blood. Right lung lobes were taken for molecular biology. For this it was taken out and frozen in liquid nitrogen and stored in -80^{o}C. The left lung was taken for histological analysis. For this the lung was taken in 3.5% formaldehyde and kept in 4^{o}C overnight. Then the tissue was changed to 1x PBS for 2 days. Finally, it was kept in embedding cassette in 70% alcohol for dehydration. The dehydration was done in automatic dehydration machine and embedded in paraffin.

In order to analyze the right heart hypertrophy, the Fulton's index (RV/(LV+S)) was assessed. Briefly, the heart was excised to left ventricle + Septum (LV+S) and right ventricle (RV) and taken weight. Main part of both tissues were snap frozen in liquid nitrogen as for lung. Small part were kept in formalin for embedding. The process was similar to lungs.

The blood collected was kept in the EDTA tubes and centrifuged in 10000 rpm for 10 minutes. The plasma was separated and stored in -20^{o}C.

2.2.9 Histology

The tissue embedded in paraffin were sectioned into 3µm slices in microtome and stored in 37^{O}C in the incubator.

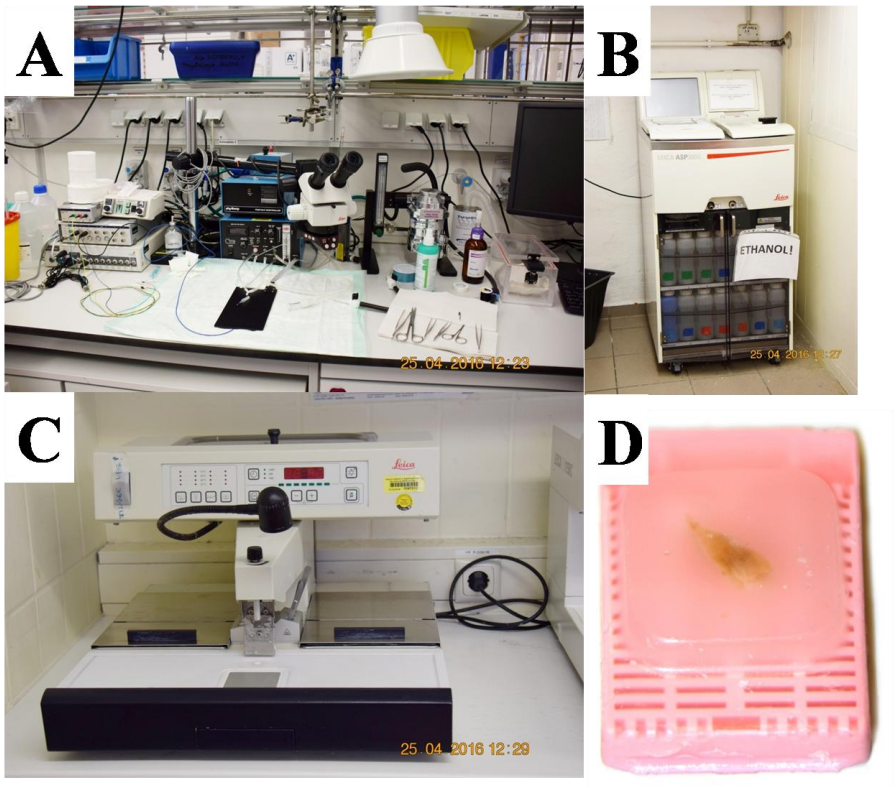

Fig. 10: Histology procedures. A. Setup for invasive hemodynamic measurements in rats or mice. B. Dehydration machine for tissues. C. Paraffin embedding machine D. Paraffin embedded lung sample in a cassette.

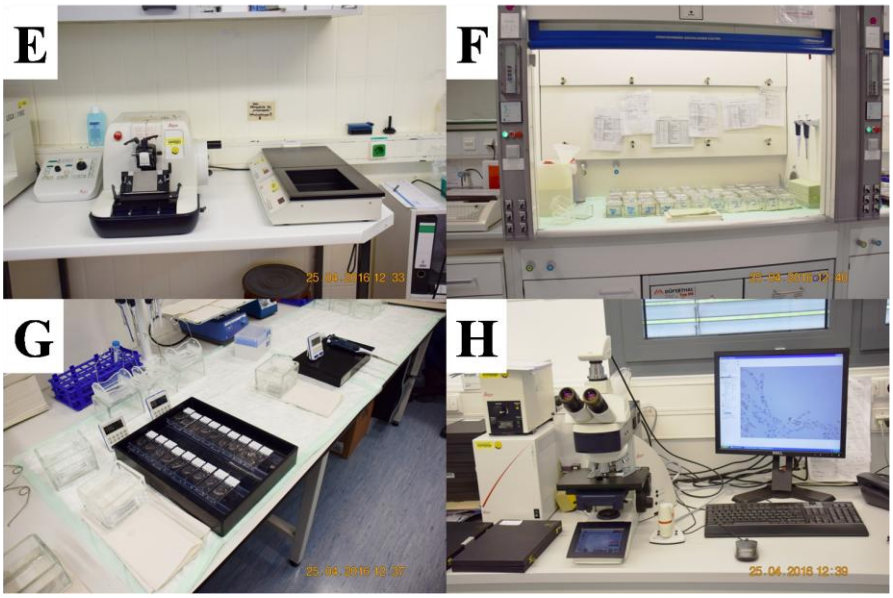

Fig. 11: Histology procedures. E. Microtome for cutting the paraffin embedded tissue samples into thin slices. F. Working place under the hood for staining of tissues. G. Antibody staining of the tissues. H. Light microscope and computer for analysis of the tissue sections.

2.2.10 Medial wall thickness

To assess the pulmonary vascular remodeling, the medial wall thickness analysis was performed, as we previously published and described (Dahal et al., 2011; Kosanovic et al., 2011; Schermuly et al., 2005; Dahal et al., 2010). Medial wall thickness of pulmonary vessels is defined as the distance between the lamina elastic interna and externa. To measure the medial wall thickness van Gieson's staining was used. The 3µm lung tissue sections were deparaffinised and rehydrated. After overnight staining in Resorcin-Fuchsin, the slides with the tissue sections were washed with water. The sections were immersed in Weigert's working solution of hematoxylin for 5 minutes. The Weigert's working is prepared by mixing equal volume of Weigert's Iron Hematoxylin A and Weigert's Iron Hematoxylin B (i.e. in the ratio of 1:1). The sections were washed with running water and then with aquadest. After washing, the slides were immersed in van Gieson solution for 10 minutes. The sections were dehydrated and immersed in xylol and coverslipped with

mounting medium (Pertex®). Vessels with outer diameter of 20-50µm were used for analysis. Light microscope with Leica Qwin V3 computer-assisted image analysis software was used for analysis. Elastic fibers and cell nuclei are stained dark blue or dark brown by the iron-hematoxylin stain. Collagen and muscle fibers are stained red by the van Gieson counterstain. Cytoplasm is stained yellow due to counterstain

2.2.11 Degree of Muscularization

Another well-established method for assessment of the pulmonary vascular remodeling, the degree of muscularization was performed, as we previously published and described (Dahal et al., 2011; Kosanovic et al., 2011; Schermuly et al., 2005; Dahal et al., 2010). Muscularization of pulmonary vessels was analyzed by performing double immuno-staining with anti-alpha smooth muscle actin (α SMA) antibody (Sigma Aldrich) and anti von-Willebrand factor (vWF) antibody (Dahal et al., 2010; Schermuly et al., 2005). 3µm lung tissue sections were deparaffinised and rehydrated. The endogenous peroxidase activity of the tissue was blocked by using freshly prepared solution of 30% hydrogen peroxide (H_2O_2) in methanol in 1:1 ratio. The sections were then washed with 1x PBS with pH 7.4. The composition of 20x PBS: NaCl: 80gm, KCl: 2gm, $Na_2HPO_4x2H_2O$: 11.5gm, KH_2PO_4: 2gm and A-dest: 900ml and stored for longer use. This stock solution was used to prepare 1x PBS. Antigen retrieval was performed with trypsin at 37^oC for 15 minutes and then washed with 1x PBS. To avoid the non-specific binding, the slides were first incubated with 10% BSA for 15 minutes and washed with PBS. Incubation with normal horse serum was done for 30 minutes to avoid the non-specific bindings caused by the immunoglobulin cross-reactivity. For staining of the pulmonary vascular smooth muscle, anti-alpha smooth muscle actin antibody was used in the dilution ratio of 1:900 in 10% BSA for 30 minute. Biotinylated secondary antibody was used for 30 minutes. VIP substrate was used to develop color by reaction with streptavidin peroxidase complex coupled to secondary antibody. Smooth muscle layer developed the purple/violet color. For staining the endothelium, the same slides were washed with 1x PBS, incubated with 10% BSA for 15 minutes and washed again. Incubation with 2.5 % normal horse serum (ImPRESS kit Anti-Rabbit Ig Peroxidase) was done for 30 minutes. The slides were

incubated with the primary antibody anti-von Willebrand factor in the dilution ratio of 1:1200 in 10% BSA for 30 minutes at 37^{o}C. After washing with 1x PBS, secondary antibody ImmPRESS reagent anti-rabbit peroxidase was added. Visualization of staining was done by DAB substrate which shows brown color of the vascular endothelium. The sections were counter stained with methyl green in the hot plate for 3 minutes and dehydrated, then cover-slipped with mounting medium. The sections were examined by light microscope using a computerized system (Qwin, Leica). Vessels with 20-50µm size were used for analysis. Each vessel was categorized as fully muscularized (70-100%), partially muscularized (5-70%) or non-muscularized (0-5%)

For mice, the 3µm lung tissue sections were deparaffinised and rehydrated similar to rat tissue. The endogenous peroxidase activity of the tissue was blocked by using freshly prepared solution of 30% hydrogen peroxide (H_2O_2) in methanol in 1:10 ratio. Other steps were similar till BSA blocking. As mouse primary antibody should be used in the mice tissues, so Mouse- on- Mouse HRP polymer kit was used to reduce the cross reactivity. This kit consisted of Rodent block M and MM HRP polymer. The Rodent block M was used for 30 minutes. For staining pulmonary vascular smooth muscle, anti-alpha smooth muscle actin antibody was used in the dilution ratio of 1:900 in 10% BSA for 30 minute. After washing with 1x PBS, the antigen antibody reaction was visualized by adding MM HRP polymer and then VIP substrate kit. Other steps were done similar as for rat tissues.

2.2.12 CD68 staining

To identify macrophages in the lung tissues, CD68 staining was performed, similarly as we published and described before (Savai et al., 2012). The 3µm section of lung tissue were deparaffinised and rehydrated. For antigen retrieval, the slides were cooked with citrate buffer 20x for 20 minutes. The citrate buffer solution was prepared with 95ml aquadest and 5 ml 20x citrate buffer with pH 6. The endogenous peroxidase activity of the tissue was blocked by using freshly prepared solution of 30% hydrogen peroxide (H_2O_2) in methanol in 1:1 ratio. The slides were washed with aquadest and 1x PBS. The slides were again incubated in proteinase K at room temperature for 15 minutes. The slides were washed

with aquadest and PBS and incubated with 10% BSA. The slides were then washed with 1x PBS and incubated with 2.5 % normal horse serum (ImPRESS kit Anti-Mouse Ig Peroxidase) for 30 minutes. The slides were incubated with the primary antibody anti-Rat CD68 (MCA341R, AbD Serotec) in the dilution ratio of 1:100 in 10% BSA overnight at 4^{o}C. After washing with 1x PBS, secondary antibody ImmPRESS reagent anti-mouse peroxidase was added. Visualization of staining was done by NovaRED substrate. Counter staining was done with hematoxylin and dehydration steps were performed. The procedure was completed by covering the slide with mounting medium and putting the coverslip. The CD68 positive cells would appear brown in the light microscope and counted manually.

2.2.13 Statistical analysis

Values are expressed as Mean ± SEM (Standard error of mean). The different experimental groups were compared by one way ANOVA (Analysis of variance). The Newman Keuls post hoc test was applied. A p value of less than 0.05 was considered significant in all cases.

3. Results

3.1 Body mass index of male Zucker rats

The body mass index was measured before the final hemodynamic measurements on day 35. The obese rats acquired significantly higher body mass index than their lean counterparts. However, there was a noticeably decreased value of the body mass index in both lean and obese groups of monocrotaline injected Zucker rats.

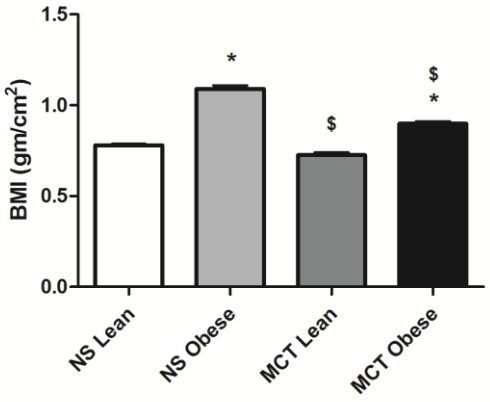

Fig. 12: Body mass index of lean and obese male Zucker rats was assessed after 5 weeks of either NS or MCT treatment. NS = normal saline, MCT = monocrotaline, BMI = body mass index. Data are mean ± SEM, p value ≤ 0.05 are significant, n = 8-11, *compared to lean, $compared to normal saline

3.2 Echocardiographic parameters of MCT induced PH in male Zucker rats

Echocardiography was done at two time points - 3 weeks and 5 weeks after normal saline or monocrotaline (MCT) injection to lean or obese male Zucker rats. In general, 5 weeks upon MCT injection both lean and obese Zucker rats developed PH, as evident by increased value of RVID and RVWT, and noticeably reduced values of TAPSE, PAAT/PAET and CI. On the other hand, minor differences were noticed between groups in echocardiography parameters such as RVID, RVWT, TAPSE and CI done in 3 weeks (Fig. 13-A, B, C and E). Interestingly, PAAT/PAET showed a remarkable difference in the MCT obese group between 3 and 5 weeks (Fig. 13-D).

A

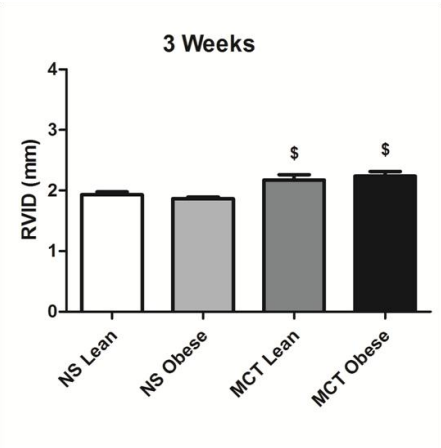
3 Weeks
RVID (mm)
0
1
2
3
4
$
$
NS Lean
NS Obese
MCT Lean
MCT Obese

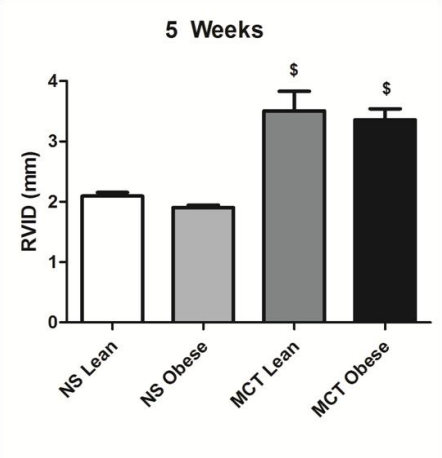
5 Weeks
RVID (mm)
0
1
2
3
4
$
$
NS Lean
NS Obese
MCT Lean
MCT Obese

B

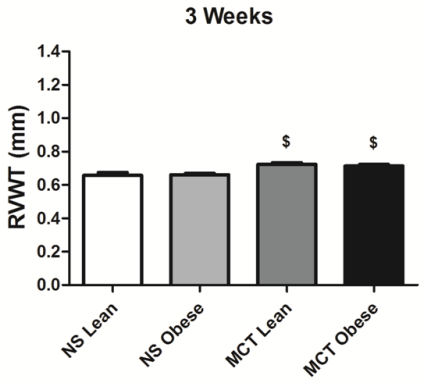
3 Weeks
RVWT (mm)
0.0
0.2
0.4
0.6
0.8
1.0
1.2
1.4
$
$
NS Lean
NS Obese
MCT Lean
MCT Obese

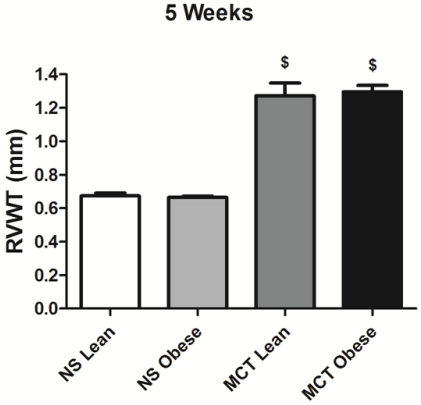
5 Weeks
RVWT (mm)
0.0
0.2
0.4
0.6
0.8
1.0
1.2
1.4
$
$
NS Lean
NS Obese
MCT Lean
MCT Obese

C

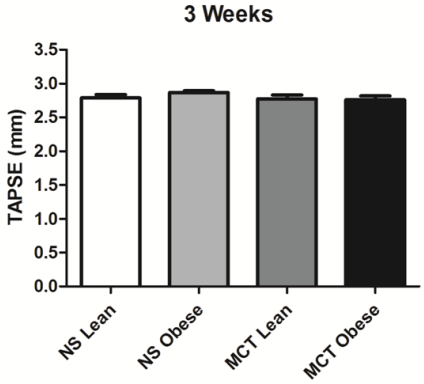
3 Weeks
TAPSE (mm)
0.0
0.5
1.0
1.5
2.0
2.5
3.0
3.5
NS Lean
NS Obese
MCT Lean
MCT Obese

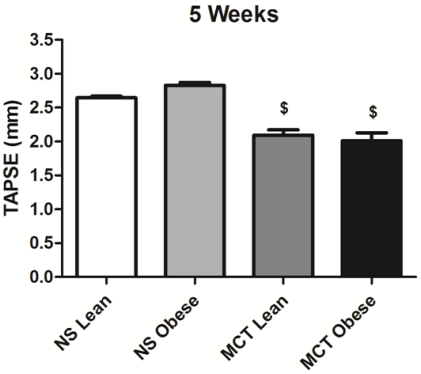
5 Weeks
TAPSE (mm)
0.0
0.5
1.0
1.5
2.0
2.5
3.0
3.5
$
$
NS Lean
NS Obese
MCT Lean
MCT Obese

D

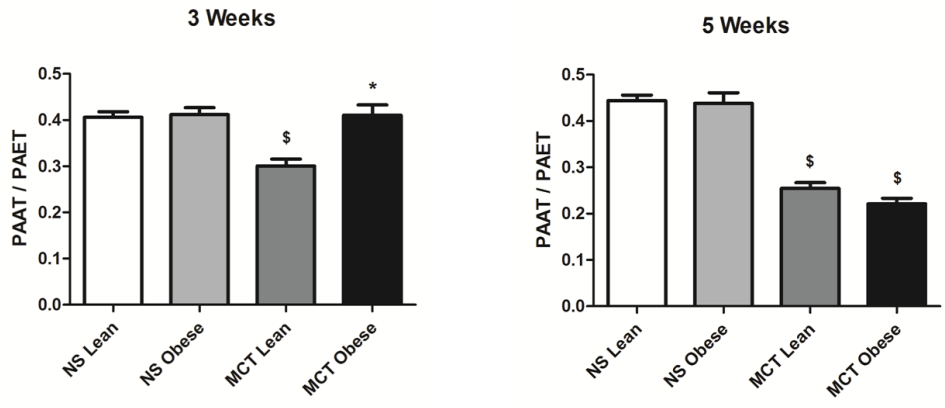

E

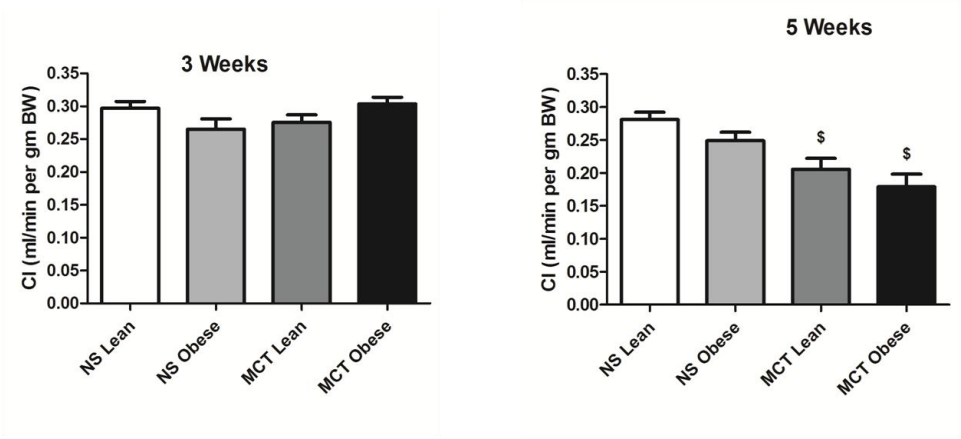

Fig. 13: Echocardiographic parameters of lean and obese male Zucker rats were assessed after 3 and 5 weeks of either NS or MCT treatment. **A. to E.** Right ventricular internal diameter, right ventricular free wall thickness, tricuspid annular plane systolic excursion, ratio of pulmonary artery acceleration time to ejection time and cardiac index respectively, measured at 3 and 5 weeks. NS = normal saline, MCT = monocrotaline, RVID = right ventricular internal diameter, RVWT = right ventricular free wall thickness, TAPSE = tricuspid annular plane systolic excursion, PAAT = pulmonary artery acceleration time, PAET = pulmonary artery ejection time, CI = cardiac index. Data are mean ± SEM, p value ≤ 0.05 are significant, n = 10-15, *compared to lean, $^{\$}$compared to normal saline

3.3 Hemodynamic and right heart hypertrophy features of MCT induced PH in male Zucker rats

Invasive hemodynamic and right ventricular hypertrophy parameters were assessed at 5 weeks of normal saline or monocrotaline injection. Minor differences were seen for the systemic arterial pressure. A significant increase in the RVSP as well as Fulton's index showed a prominent manifestation of PH in the MCT lean and obese groups of Zucker rats (Fig. 14-A and B), compared to their respective saline controls. No change between the MCT injected lean and obese groups was observed.

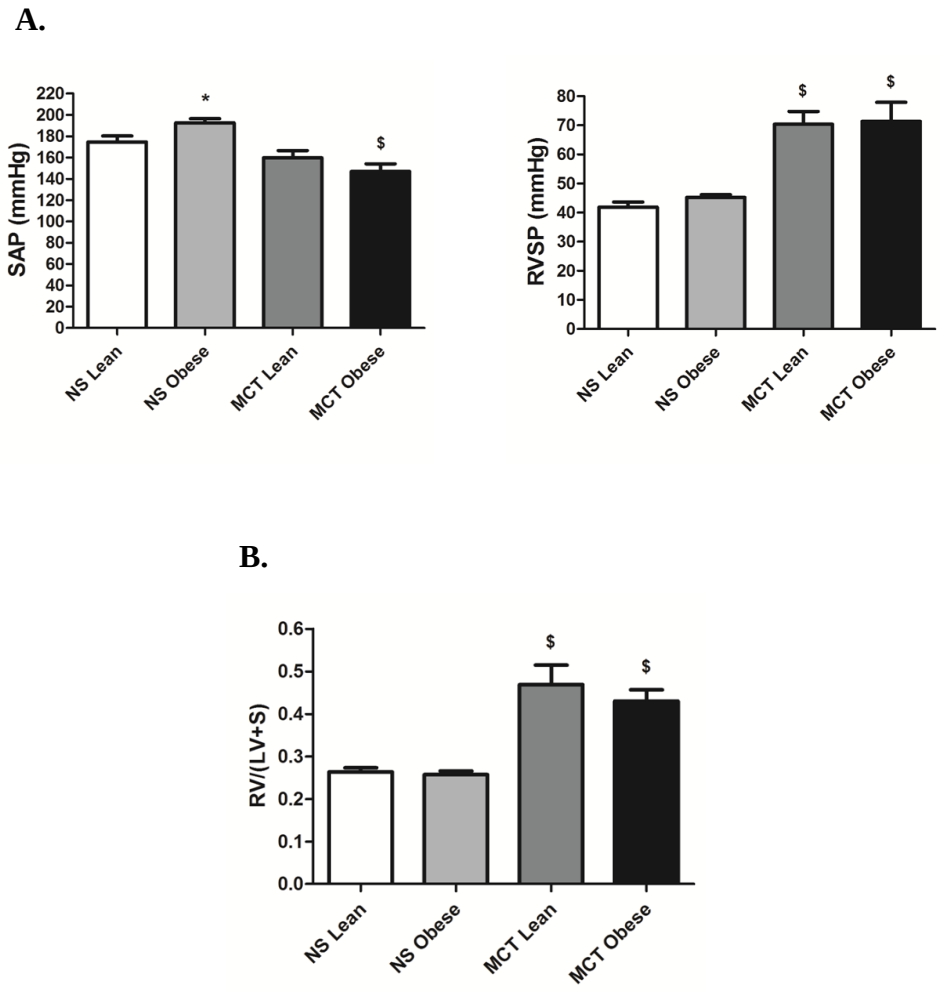

Fig. 14: Hemodynamic measurements and Fulton's index of lean and obese male Zucker rats were assessed after 5 weeks of either NS or MCT treatment. **A.** Systemic arterial pressure and right

ventricle systolic pressure measured invasively at 5 weeks after normal saline or monocrotaline injection. **B.** Ratio of right ventricle to left ventricle + septum measured at 5 weeks of normal saline or monocrotaline injection. NS = normal saline, MCT = monocrotaline, SAP = systemic arterial pressure, RV = right ventricle, LV = left ventricle, S = septum. Data are mean ± SEM, p value ≤ 0.05 are significant, n = 2-11, *compared to lean, $compared to normal saline

3.4 Survival rate in obese male Zucker rats

The overall mortality was higher for the obese male Zucker rats than their lean counterparts treated with MCT (Fig. 15). No mortality was seen in both the groups until 4 weeks. The mortality started later in the obese groups but with higher degree of severity.

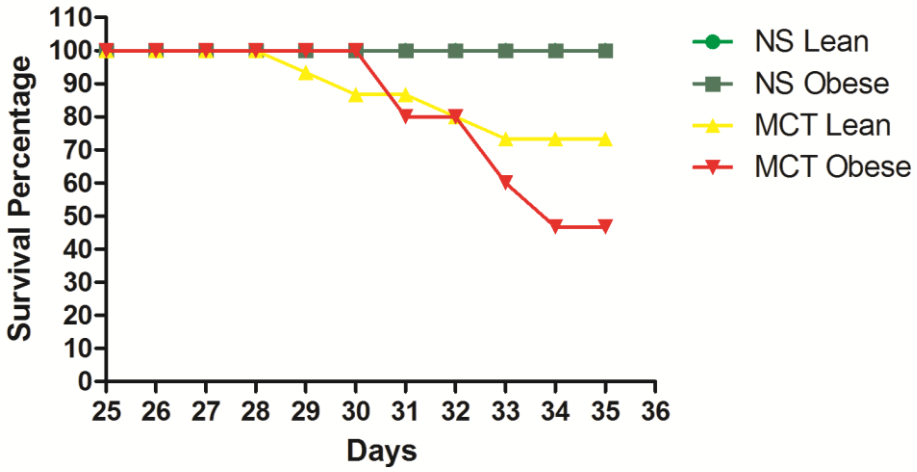

Fig. 15: Survival rate of lean and obese male Zucker rats. Survival percentage was evaluated until 5 weeks of either NS or MCT treatment. NS = normal saline, MCT = monocrotaline. Data are mean ± SEM, p value ≤ 0.05 are significant, n = 10-15, *compared to lean, $compared to normal saline

3.5 Pulmonary vascular remodeling effects of MCT in male Zucker rats

Pulmonary vascular remodeling in the distant pulmonary vessels was assessed via measuring the medial wall thickness and the degree of muscularization. In agreement with hemodynamic and non-invasive data, a substantial enhancement in medial wall thickness and fully muscularized vessels were found out in the MCT injected Zucker rats, compared

to their saline controls. However, no differences between the lean and obese groups were seen. On the other hand, the number of non-muscularized vessels was lower in both lean and obese MCT injected groups, in comparison to their respective saline controls (Fig. 16-B). Therefore, in agreement with hemodynamic, right heart hypertrophy and non-invasive echocardiographic parameters, pulmonary vascular remodeling also revealed that there was no difference in the PH severity between lean and obese rats.

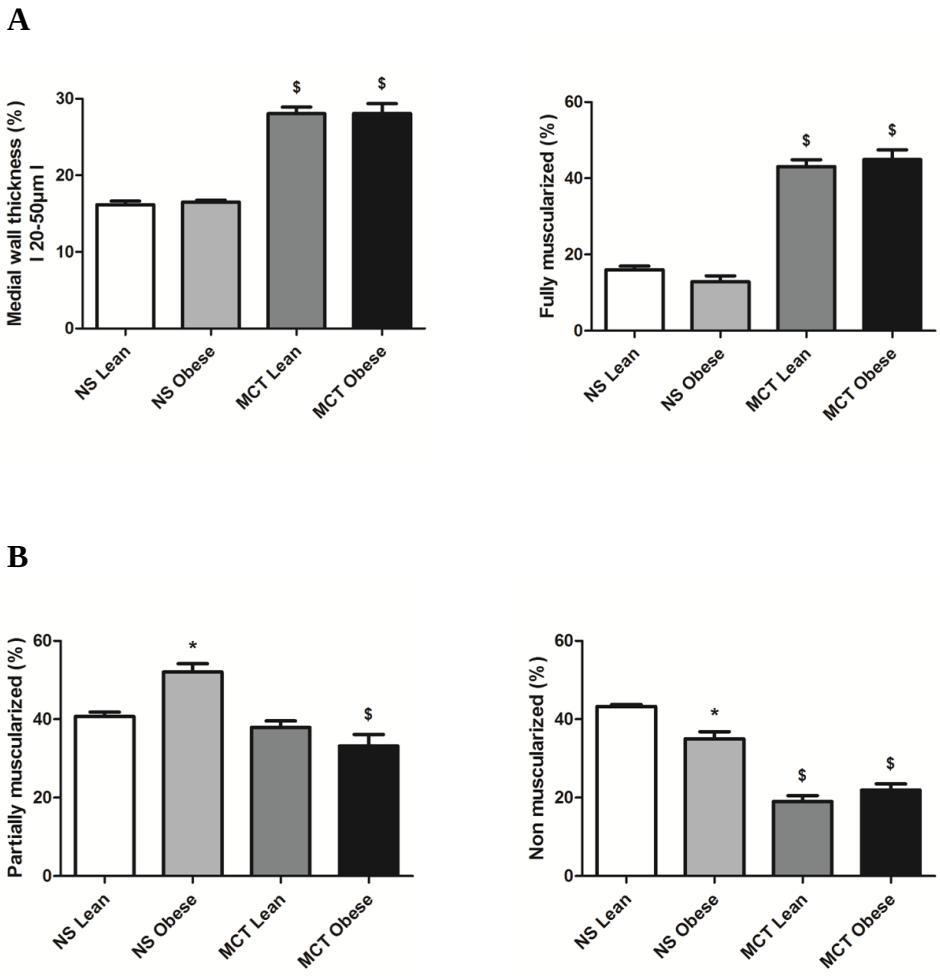

C

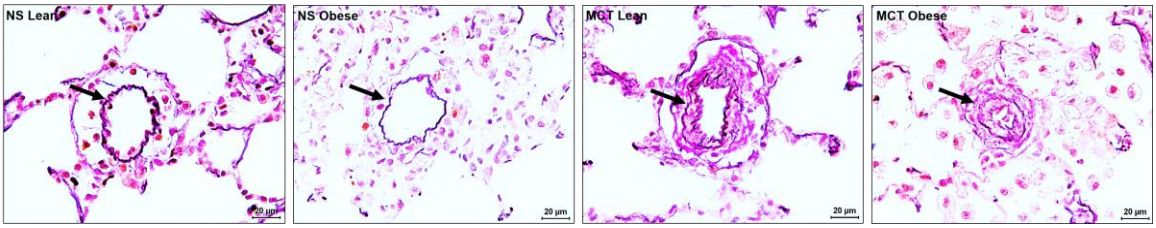

Fig. 16: Medial wall thickness and degree of muscularization in lean and obese male Zucker rats were assessed after 5 weeks of either NS or MCT treatment. Lung tissues were sliced at 3 µm sections for staining. van Gieson's staining was done to measure the medial wall thickness. The distance between lamina elastic interna and externa was measured. Double immuno-staining with anti-alpha smooth muscle actin (α SMA) antibody and anti-von-Willebrand factor (vWF) antibody was done to measure the degree of muscularization. **A and B.** Medial wall thickness and degree of muscularization for lean and obese male Zucker rats treated either with normal saline or monocrotaline solution. **C.** Representative images for medial wall thickness (arrows indicate the pulmonary vessel). NS = normal saline, MCT = monocrotaline. Data are mean ± SEM, p value ≤ 0.05 are significant, n = 6-11, *compared to lean, $^{\$}$compared to normal saline.

3.6 Inflammatory effect of MCT in obese male Zucker rats

The inflammatory effects of MCT were traced via the presence of CD68 (Cluster of Differentiation 68) positive macrophages. CD68 staining was done on the paraffin embedded lung tissues. High infiltration of CD68 positive cells were detected in both lean and obese MCT groups, compared to their respective saline controls. However, a significantly higher infiltration in the obese MCT group compared to the lean MCT group was observed (Fig. 17-A).

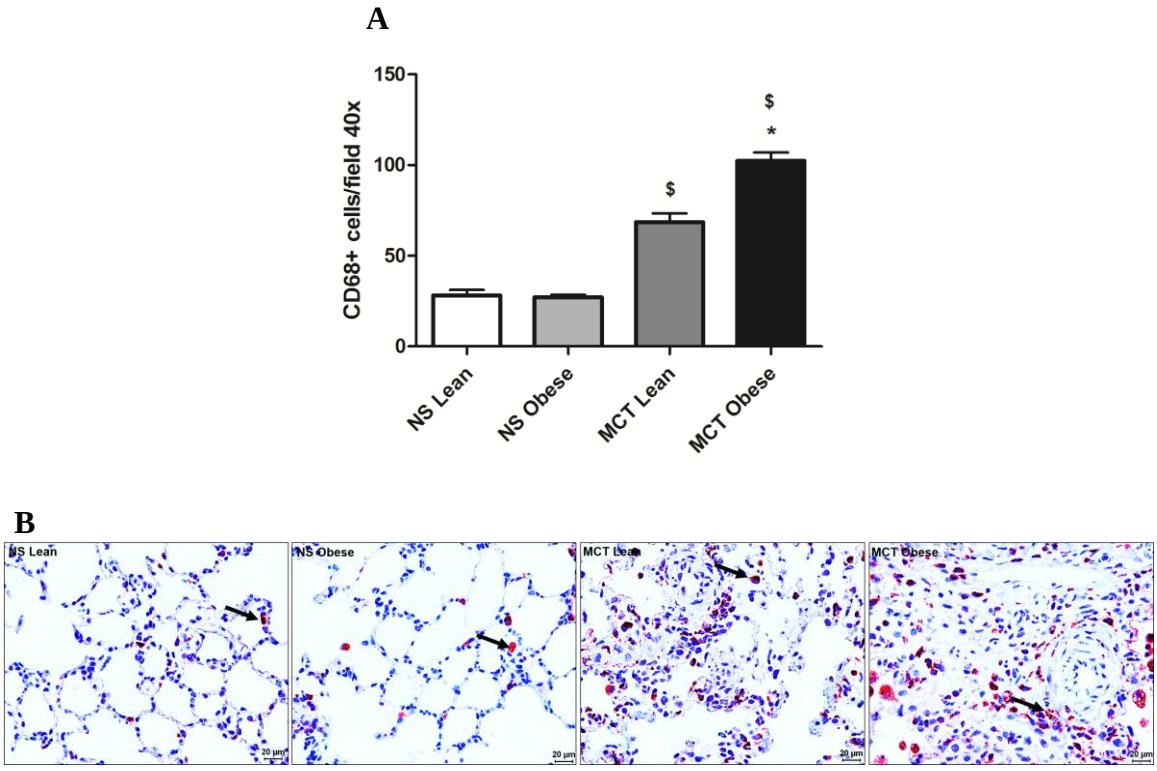

Fig. 17: CD68 (macrophages) positive cells counting in the lung tissues of lean and obese male Zucker rats was assessed after 5 weeks of either NS or MCT treatment. Lung tissues were sliced at 3 µm sections for staining. Staining with anti-CD68 antibody was done. **A.** Quantification of CD68 positive cells from paraffin embedded lung tissues from lean and obese male Zucker rats treated with either normal saline or monocrotaline. **B.** Representative images for CD68 staining in Zucker rats lung tissues (arrows indicate the CD68 positive cells). NS = normal saline, MCT = monocrotaline. Data are mean ± SEM, p value ≤ 0.05 are significant, n = 6-11, *compared to lean, $^{\$}$compared to normal saline.

3.7 Body mass index in obese female Zucker rats

The body mass index was measured before the final hemodynamic measurements on day 35. The obese female rats acquired significantly higher body mass index than their lean counterparts. Unlike in the case of male Zucker rats, MCT injection *per se* did not change noticeably the body mass index in female Zucker rats.

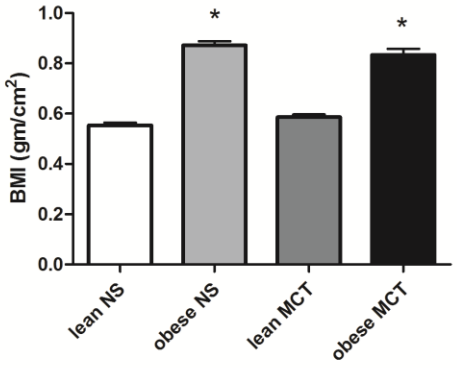

Fig. 18: Body mass index of lean and obese female Zucker rats was assessed after 5 weeks of either NS or MCT treatment. NS = normal saline, MCT = monocrotaline, BMI = body mass index. Data are mean ± SEM, p value ≤ 0.05 are significant, n = 10, *compared to lean, $compared to normal saline

3.8 Echocardiographic parameters of MCT induced PH in female rats

For female Zucker rats, echocardiography was also done at two instances - 3 weeks and 5 weeks after normal saline or MCT injection to lean or obese female Zucker rats. Increase in RVID and RVWT was evident from the third week of MCT injection and it was more prominent in the fifth week, compared to the saline controls. Importantly, both of the parameters, were more severe in the obese female Zucker rats (Fig. 19-A and B), compared to their lean controls. In agreement, PAAT/PAET was reduced after 5 weeks in MCT female Zucker rats in comparison to their saline controls, and even further decreased in obese versus lean MCT rats. Similarly, TAPSE was prominently reduced in obese MCT rats compared to the lean control. CI values were not dramatically different between groups.

A

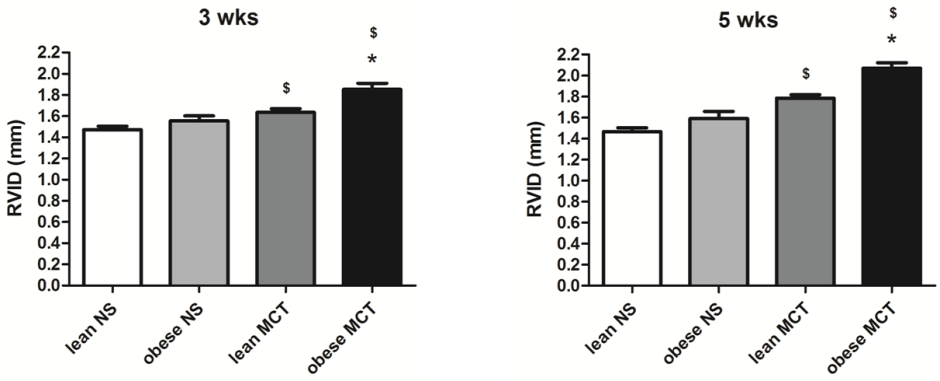
3 wks
5 wks
RVID (mm)
0.0
0.2
0.4
0.6
0.8
1.0
1.2
1.4
1.6
1.8
2.0
2.2
$
*
lean NS
obese NS
lean MCT
obese MCT

B

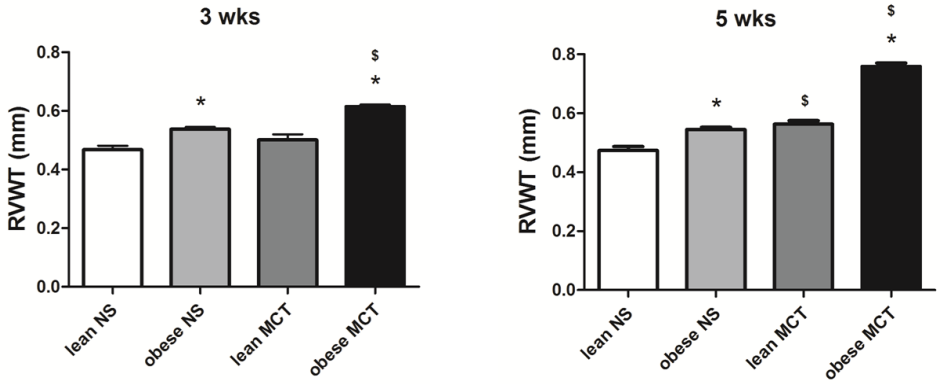
3 wks
5 wks
RVWT (mm)
0.0
0.2
0.4
0.6
0.8
*
$
lean NS
obese NS
lean MCT
obese MCT

C

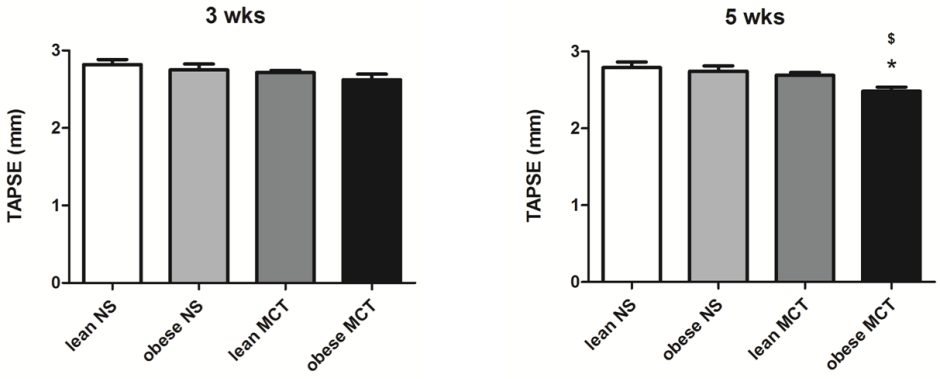
3 wks
5 wks
TAPSE (mm)
0
1
2
3
*
$
lean NS
obese NS
lean MCT
obese MCT

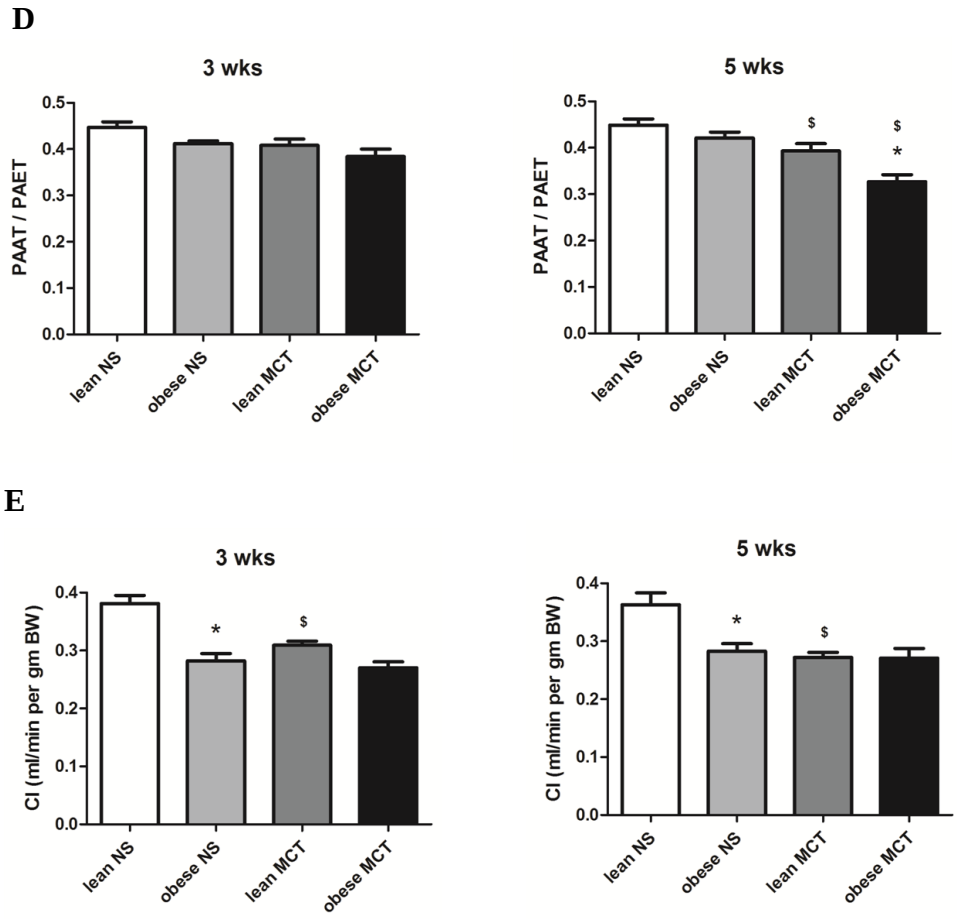

Fig. 19: Echocardiographic parameters of lean and obese female Zucker rats were assessed after 3 and 5 weeks of either NS or MCT treatment. **A. to E.** Right ventricular internal diameter, right ventricular free wall thickness, tricuspid annular plane systolic excursion, ratio of pulmonary artery acceleration time to ejection time, cardiac output and cardiac index respectively, measured at 3 and 5 weeks. NS = normal saline, MCT = monocrotaline, RVID = right ventricular internal diameter, RVWT = right ventricular free wall thickness, TAPSE = tricuspid annular plane systolic excursion, PAAT = pulmonary artery acceleration time, PAET = pulmonary artery ejection time, CI = cardiac index. Data are mean ± SEM, p value ≤ 0.05 are significant, n = 10, *compared to lean, $^{\$}$compared to normal saline

3.9 Hemodynamic features of MCT induced PH in female Zucker rats

Invasive hemodynamic and right heart hypertrophy parameters were assessed at 5 weeks of normal saline or monocrotaline injection. No differences were seen for the systemic arterial

pressure. In agreement with non-invasive echocardiography data, a significant increase in the RVSP and Fulton's index was observed in MCT injected obese female Zucker rats, compared to their saline controls and lean counterparts. The lean female Zucker rats remained not significantly affected by the MCT injection in the terms of RVSP and Fulton's index (Fig. 20-A and B).

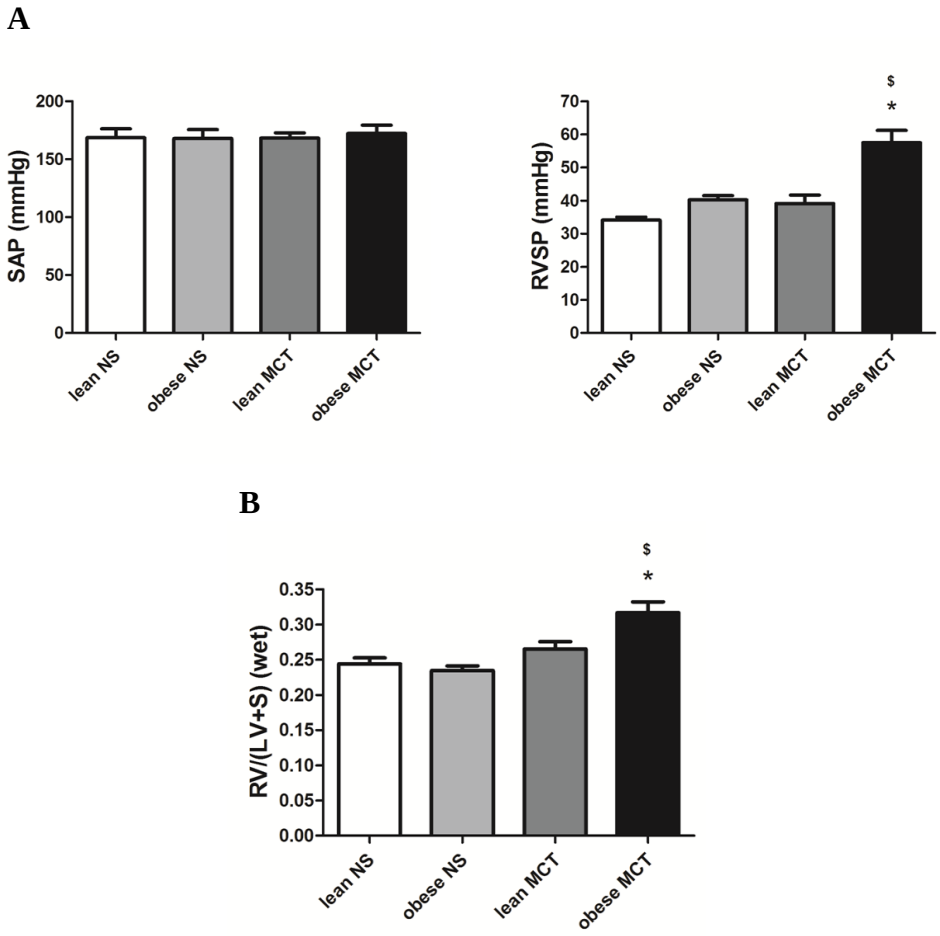

Fig. 20: Hemodynamic measurements and Fulton's index of lean and obese female Zucker rats were assessed after 5 weeks of either NS or MCT treatment. **A.** Systemic arterial pressure and right ventricle systolic pressure measured invasively at 5 weeks after normal saline or monocrotaline injection. **B.** Ratio of right ventricle to left ventricle + septum measured at 5 weeks of normal saline or monocrotaline injection. NS = normal saline, MCT = monocrotaline, SAP = systemic arterial pressure, RV = right ventricle, LV = left ventricle, S = septum. Data are mean ± SEM, p value $\leq$ 0.05 are significant, n = 10, *compared to lean, $^{\$}$compared to normal saline

3.10 Survival curve of MCT induced PH in female Zucker rats

No mortality was seen in female Zucker rats injected with MCT (Fig. 21).

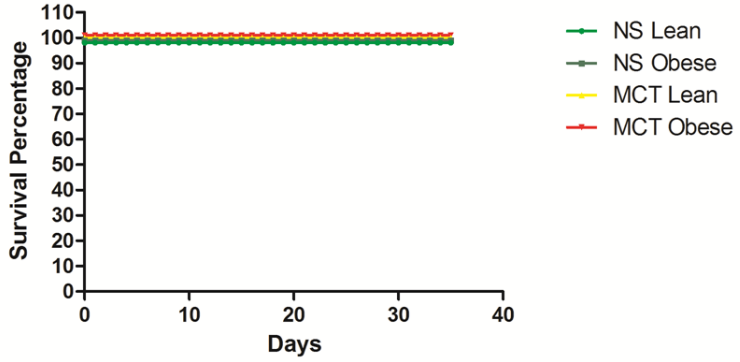

Fig. 21: Survival rate of lean and obese female Zucker rats. Survival percentage was evaluated until 5 weeks of either NS or MCT treatment. NS = normal saline, MCT = monocrotaline. Data are mean ± SEM, p value ≤ 0.05 are significant, n = 10, *compared to lean, $^{\$}$compared to normal saline

3.11 Pulmonary vascular remodeling effects due to MCT in female Zucker rats

Pulmonary vascular remodeling in the distant pulmonary vessels was assessed in female Zucker rats in an identical manner as that of the male Zucker rats. Interestingly, the medial wall thickness was increased in MCT injected lean and obese female Zucker rats compared to their respective saline controls, as well as in normal saline treated obese female group in comparison to its lean counterpart. Importantly and in agreement with physiological *in vivo* data, there was a prominent augmentation of medial wall thickness in the MCT treated obese females, compared to their MCT lean counterparts. Similar results were seen for the fully muscularized vessels (Fig. 22-A).

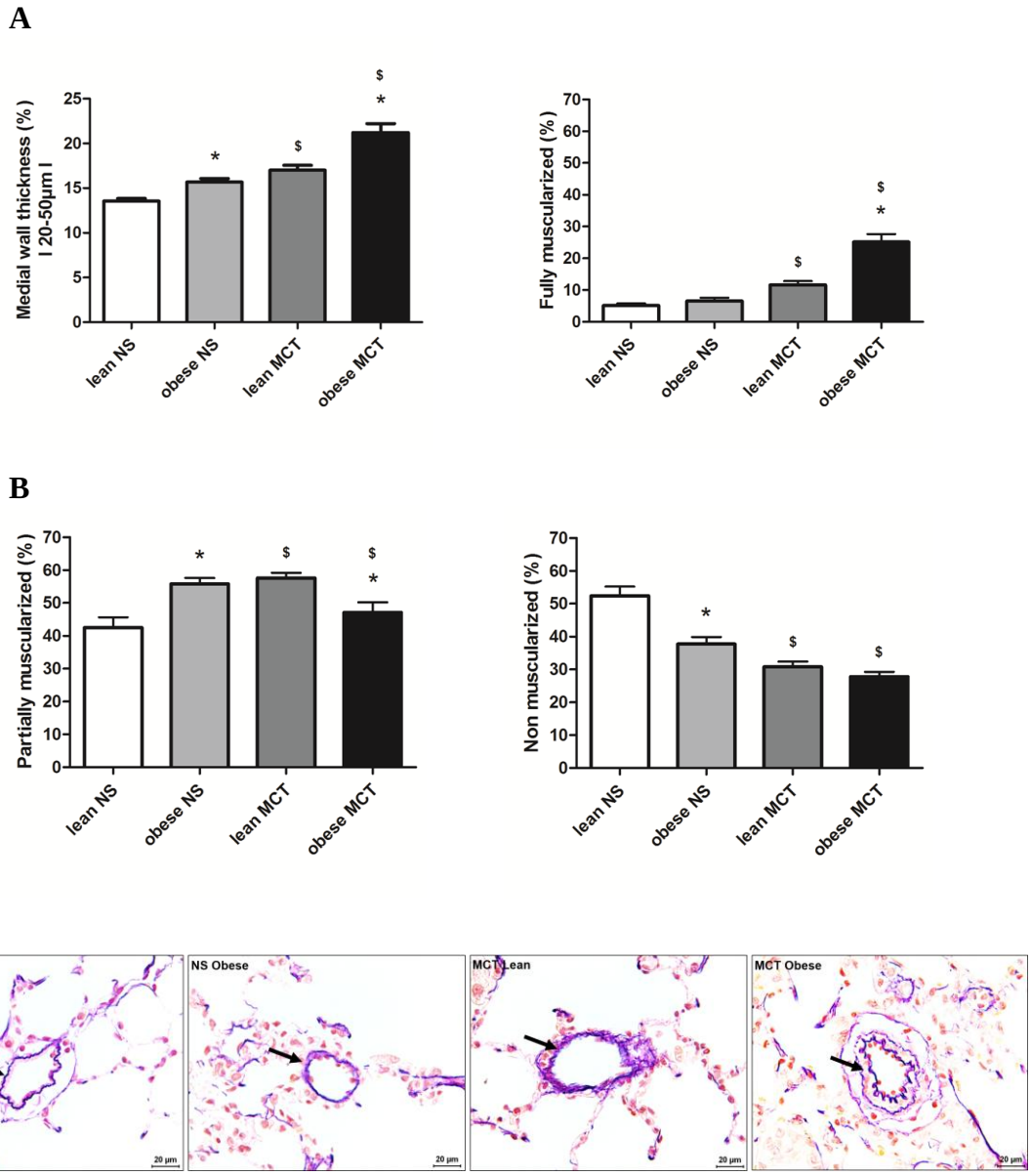

Fig. 22: Medial wall thickness and degree of muscularization of lean and obese female Zucker rats were assessed after 5 weeks of either NS or MCT treatment. Lung tissues were sliced at 3 µm sections for staining. van Gieson's staining was done to measure the medial wall thickness. The distance between lamina elastic interna and externa was measured. Double immuno-staining with anti-alpha smooth muscle actin (α SMA) antibody and anti-von-Willebrand factor (vWF) antibody was done to measure the degree of muscularization. **A and B.** Medial wall thickness and degree of muscularization for lean and obese female Zucker rats treated either with normal saline or monocrotaline solution. **C.** Representative images for medial wall thickness (arrows indicate the pulmonary vessel). NS = normal saline, MCT = monocrotaline. Data are mean ± SEM, p value ≤ 0.05 are significant, n = 10, *compared to lean, $^{\$}$compared to normal saline.

3.12 Inflammatory effect of MCT in female Zucker rats

The inflammatory effects of MCT were traced in identical way as that of male Zucker rats. Higher infiltration of CD68 positive cells were detected in both lean and obese MCT groups compared to their saline injected controls. Furthermore, it was obvious that obesity induced a noticeably increased CD68 positive cell counts in both saline and MCT treated female Zucker rats, in comparison to their lean counterparts (Fig. 23-A).

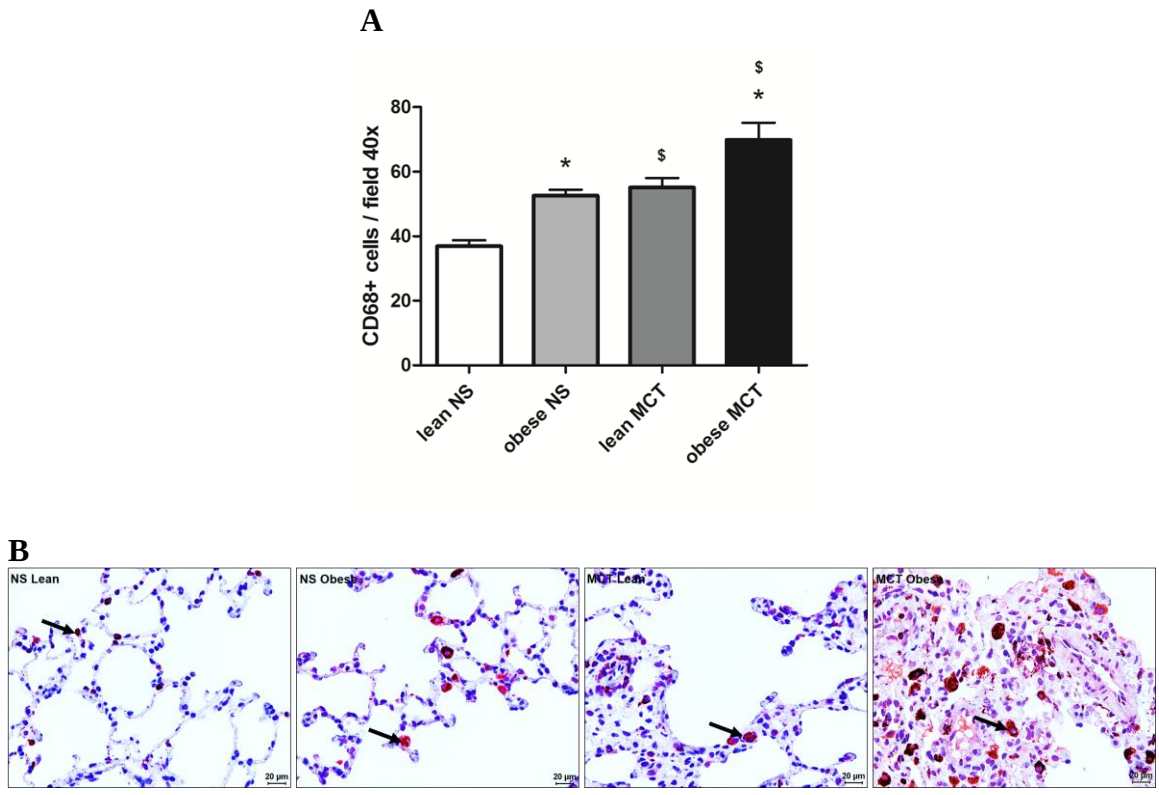

Fig. 23: CD68 (macrophages) positive cells counting in the lung tissues of lean and obese female Zucker rats was assessed after 5 weeks of either NS or MCT treatment. Lung tissues were sliced at 3 µm sections for staining. Staining with anti-CD68 antibody was done. **A.** Quantification of CD68 positive cells from paraffin embedded lung tissues from lean and obese female Zucker rats treated with either normal saline or monocrotaline. **B.** Representative images for CD68 staining in female Zucker rats lung tissues (arrows indicate CD68 positive cells). NS = normal saline, MCT = monocrotaline. Data are mean ± SEM, p value ≤ 0.05 are significant, n = 8-10, *compared to lean, $^{\$}$compared to normal saline.

3.13 Body mass index of lean and obese B6 male mice

The body mass index was measured similar to the Zucker rats, before the final hemodynamic measurements on day 35. The obese mice acquired significantly higher body mass index than their lean counterparts. However, there was a slight decrease of body mass index in obese male mice under hypoxia exposure, compared to their normoxic control (Fig. 24)

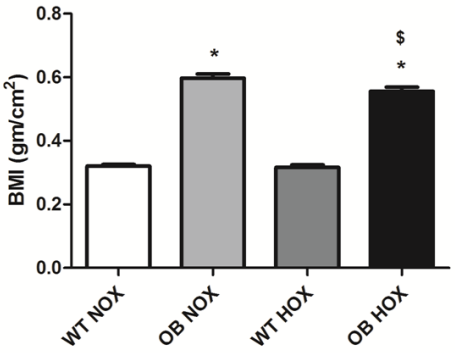

Fig. 24: Body mass index of lean and obese male B6 mice was assessed after 5 weeks of either normoxic or hypoxic (10% Oxygen level) conditions. WT = wild type, OB = obese, NOX = normoxia, HOX = hypoxia, BMI = body mass index. Data are mean ± SEM, p value ≤ 0.05 are significant, n = 10-20, *compared to wild type

3.14 Echocardiographic parameters of hypoxia induced PH in B6 male mice

Echocardiography in male B6 mice was done similar to Zucker rats, at two time points - 3 weeks and 5 weeks after normoxic or hypoxic conditions. Increase in RVID and RVWT was apparent in both lean and obese mice exposed to hypoxia, compared to their normoxic controls. However, the RVID was reduced in obese mice compared to the lean under the hypoxic condition. Surprisingly, RVWT was altered in essentially opposite manner, it was increased in obese versus lean mice under hypoxia. TAPSE and PAAT/PAET were decreased in both hypoxic groups compared to their normoxic controls. However, there was a slight increase in both parameters in obese mice in comparison to their lean

counterparts under the hypoxic condition. Finally, CI was decreased in obese animals compared to the lean groups under both normoxic and hypoxic conditions.

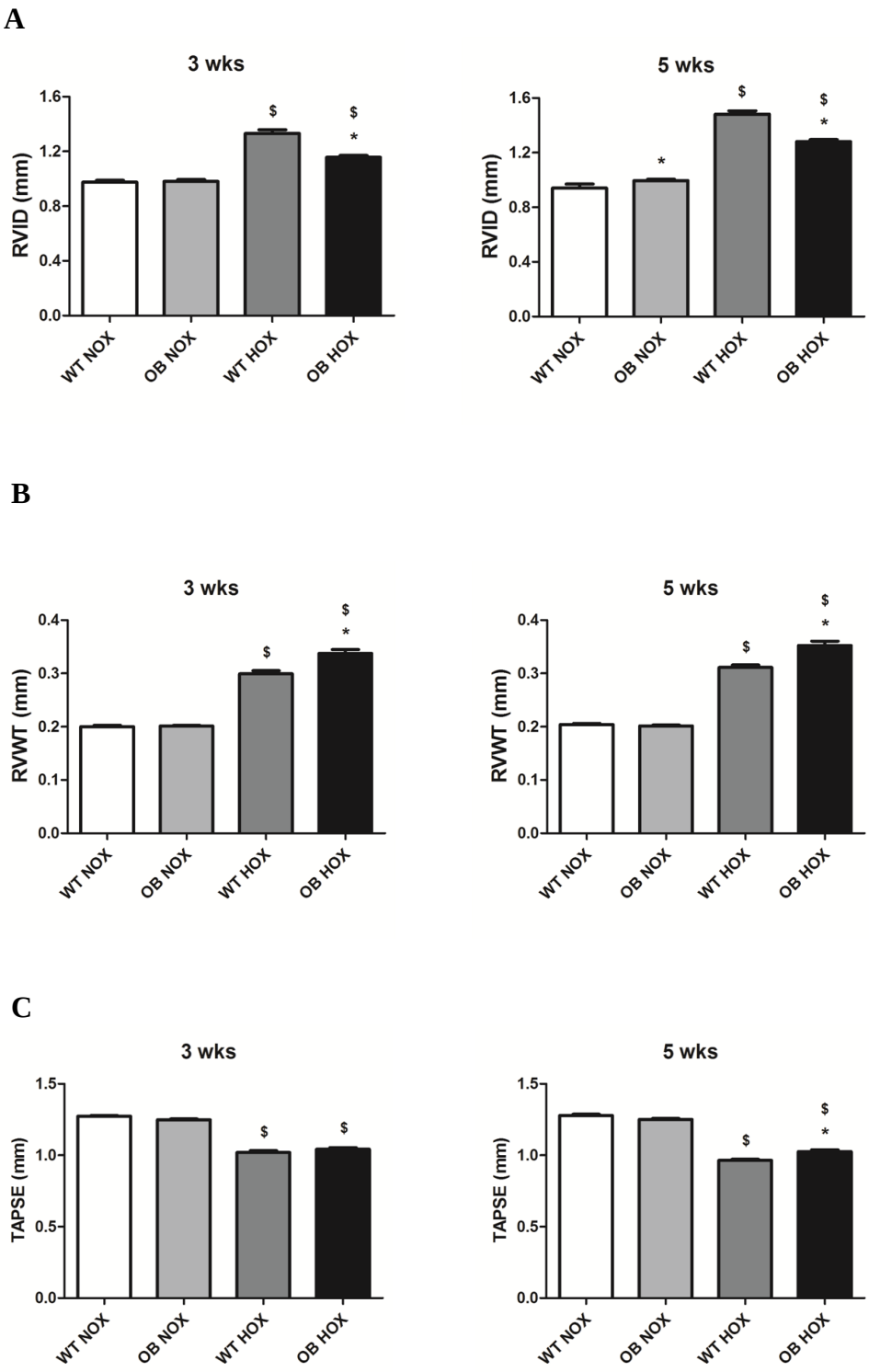

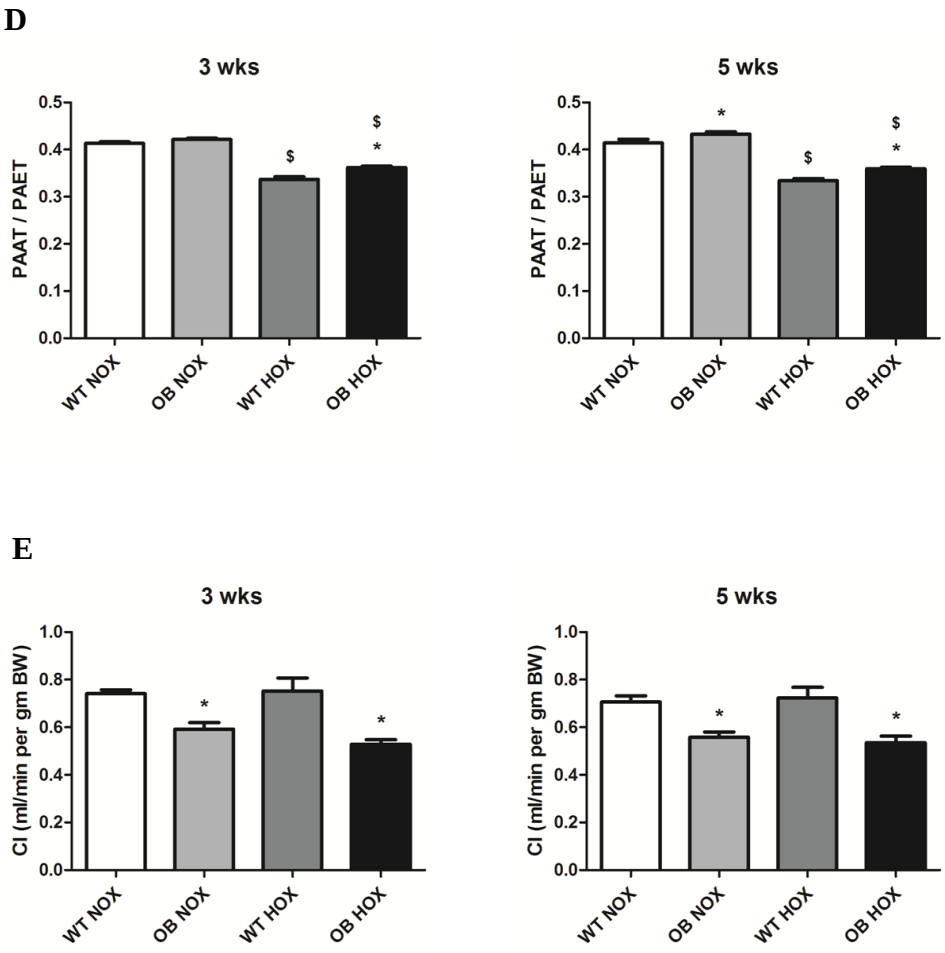

Fig. 25: Echocardiographic parameters of lean and obese male B6 mice were assessed after 3 and 5 weeks of either normoxic or hypoxic (10% Oxygen level) conditions. **A. to E.** Right ventricular internal diameter, right ventricular free wall thickness, tricuspid annular plane systolic excursion, ratio of pulmonary artery acceleration time to ejection time, cardiac output and cardiac index respectively, measured at 3 and 5 weeks. WT = wild type, OB = obese, NOX = normoxia, HOX = hypoxia, RVID = right ventricular internal diameter, RVWT = right ventricular free wall thickness, TAPSE = tricuspid annular plane systolic excursion, PAAT = pulmonary artery acceleration time, PAET = pulmonary artery ejection time, CI = cardiac index. Data are mean ± SEM, p value ≤ 0.05 are significant, n = 9-20, *compared to wild type, $^{\$}$compared to normoxia

3.15 Hemodynamic features of hypoxia induced PH in B6 male mice

Invasive hemodynamic parameters were assessed at 5 weeks of normoxia or hypoxia treatments in lean or obese B6 mice. No differences were seen in any groups for the systemic arterial pressure. A lower RVSP for both normoxic and hypoxic obese mice compared to their respective lean controls and higher RVSP due to hypoxia was observed. Nevertheless, hypoxia rendered significantly higher Fulton's index, but no effects of obesity was seen.

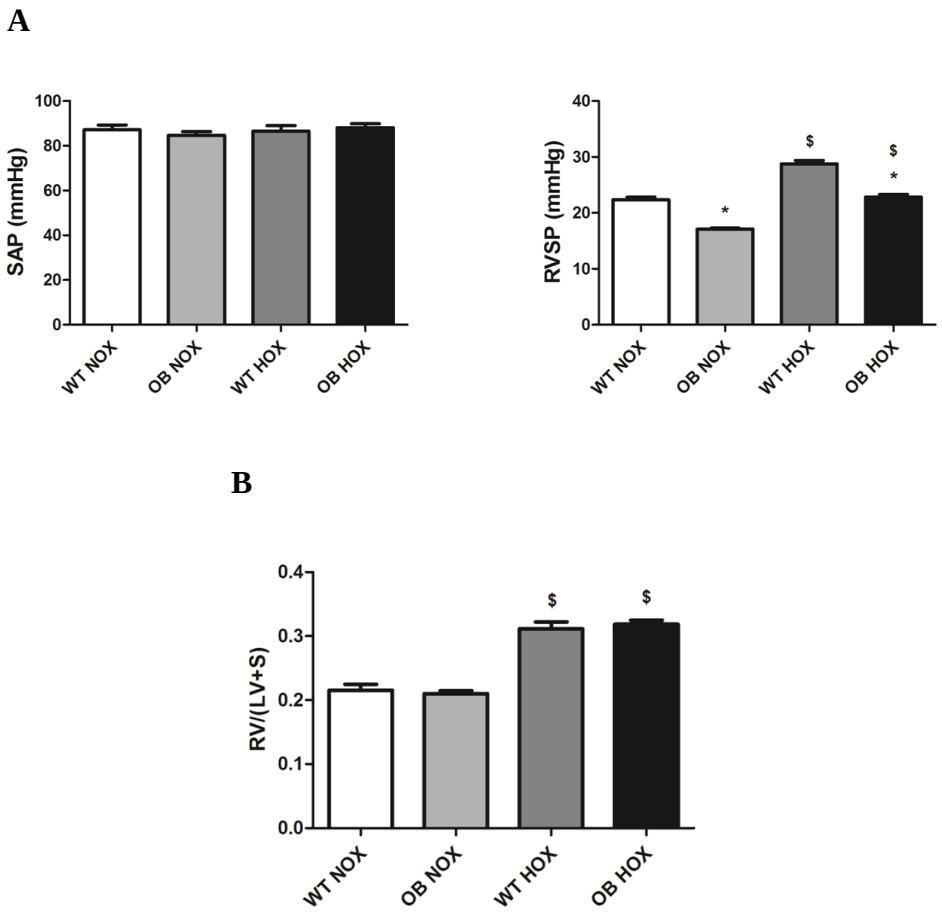

Fig. 26: Hemodynamic measurements and Fulton's index of lean and obese male B6 mice were assessed after 5 weeks of either normoxic or hypoxic (10% Oxygen level) conditions. **A.** Systemic arterial pressure and right ventricle systolic pressure measured invasively at 5 weeks after normoxic or hypoxic conditions. **B.** Ratio of right ventricle to left ventricle + septum measured at 5 weeks of normoxic or hypoxic conditions. WT = wild type, OB = obese, NOX = normoxia, HOX = hypoxia,

SAP = systemic arterial pressure, RV = right ventricle, LV = left ventricle, S = septum. Data are mean ± SEM, p value ≤ 0.05 are significant, n = 8-20, *compared to wild type, $compared to normoxia

3.16 Pulmonary vascular remodeling in hypoxia induced PH in B6 male mice

Pulmonary vascular remodeling in the distant pulmonary vessels was assessed similar to those of Zucker rats. Medial wall thickness and the degree of muscularization were calculated. Increase in medial wall thickness and fully muscularized vessels were found in the groups exposed to hypoxia compared to the normoxic conditions, except for obese mice with regard to the medial wall thickness where the difference was not that prominent. Surprisingly, there was a reduction in medial wall thickness and fully muscularized vessels in obese versus lean mice under hypoxic condition.

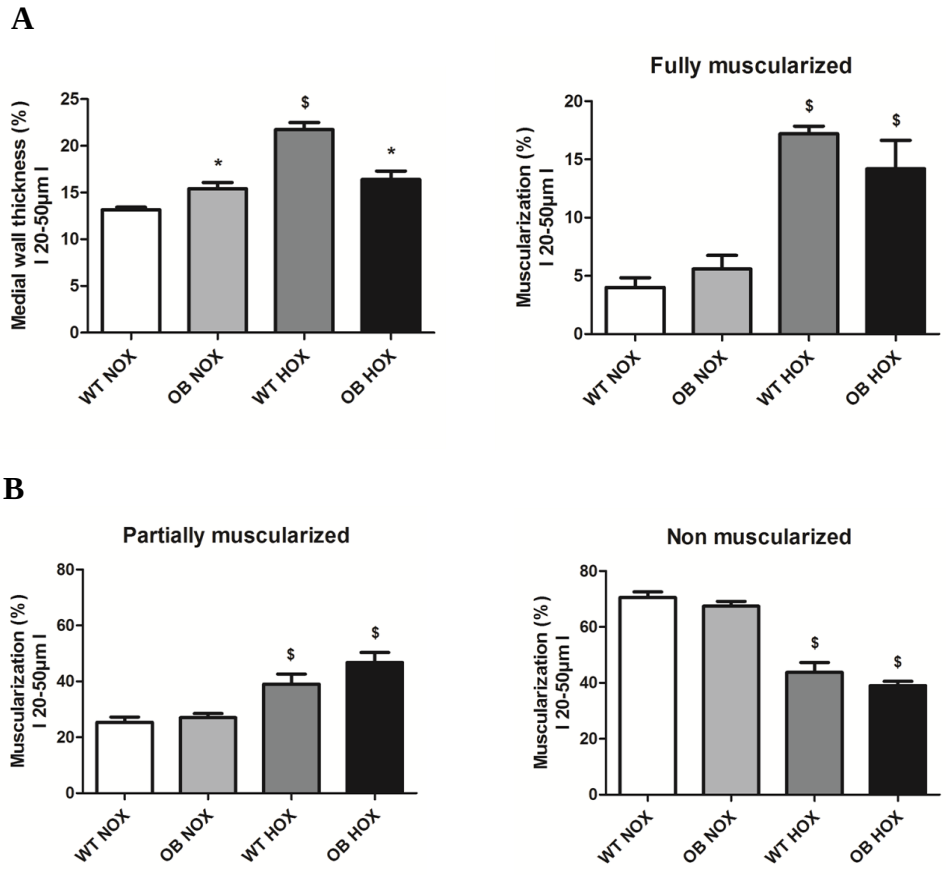

Fig. 27: Medial wall thickness and degree of muscularization of lean and obese male B6 mice were assessed after 5 weeks of either normoxic or hypoxic (10% oxygen level) conditions. Lung tissues were sliced at 3 µm sections for staining. van Gieson's staining was done to measure the medial wall thickness. The distance between lamina elastic interna and externa was measured. Double immuno-staining with anti-alpha smooth muscle actin (α SMA) antibody and anti-von-Willebrand factor (vWF) antibody was done to measure the degree of muscularization. **A and B.** Medial wall thickness and degree of muscularization for lean and obese female Zucker rats treated either with normoxic or hypoxic conditions. WT = wild type, OB = obese, NOX = normoxia, HOX = hypoxia. Data are mean ± SEM, p value ≤ 0.05 are significant, n = 5, *compared to wild type, $compared to normoxia

3.17 Body mass index in lean and obese B6 female mice

The body mass index was measured similar to the male B6 mice. The obese female mice acquired significant higher body mass index than their lean counterparts. A slight effect of hypoxia in terms of decreased body mass index in obese female mice was seen (Fig. 28)

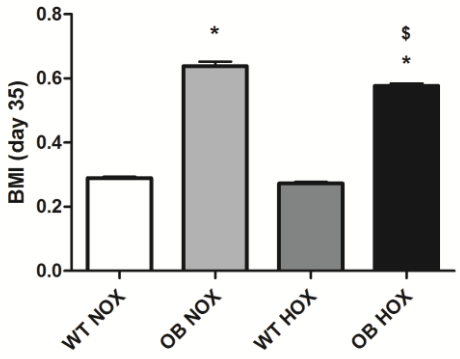

Fig. 28: Body mass index of lean and obese female B6 mice was assessed after 5 weeks of either normoxic or hypoxic (10% Oxygen level) conditions. WT = wild type, OB = obese, NOX = normoxia, HOX = hypoxia, BMI = body mass index. Data are mean ± SEM, p value ≤ 0.05 are significant, n = 10, *compared to wild type, $compared to normoxia

3.18 Echocardiographic parameters of hypoxia induced PH in B6 female mice

Echocardiography in female B6 mice was done identical to the male B6 mice. Increase in RVID and RVWT were apparent after 3 and 5 weeks of hypoxia in both lean and obese mice, compared to the normoxic controls. Interestingly, there was a further increase in both parameters particularly in obese hypoxic mice in comparison to their lean counterparts. Other parameters such as TAPSE and PAAT/PAET were decreased in both lean and obese mice under hypoxic condition, compared to the respective normoxic controls. A slight alteration in TAPSE was also seen in obese mice versus lean under hypoxic condition. CI was decreased in obese group as compared to the lean counterparts. These effects were constant during the 5 week measurements.

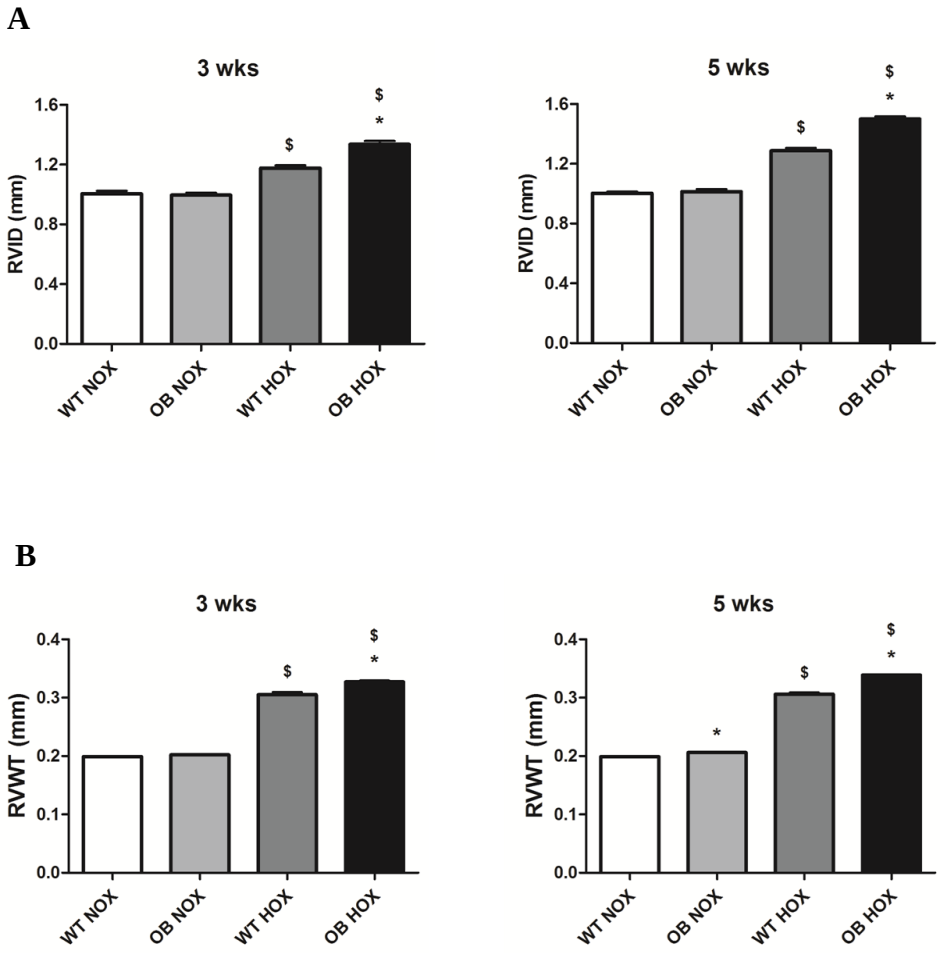

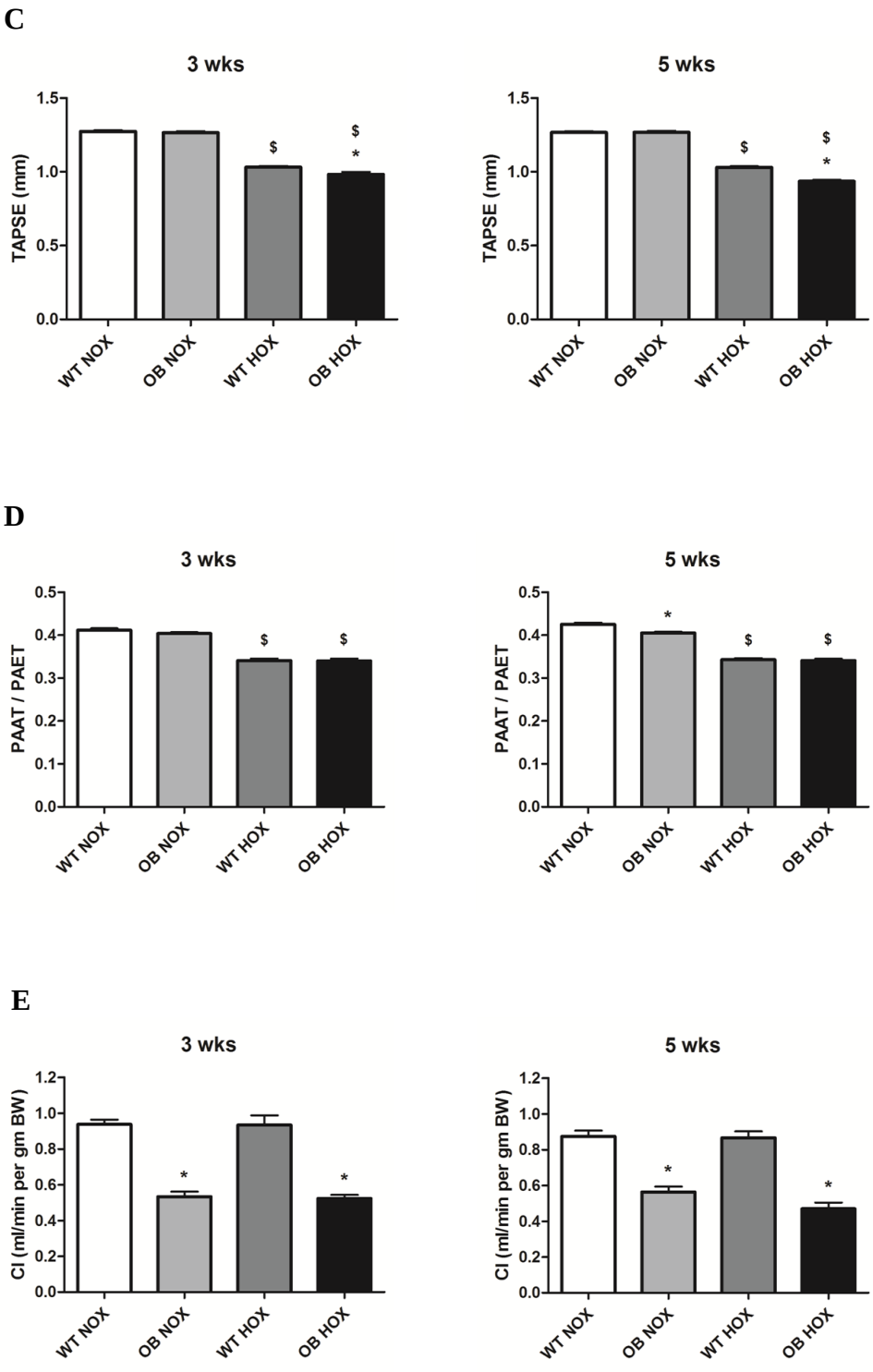

Fig. 29: Echocardiographic parameters of lean and obese female B6 mice were assessed after 3 and 5 weeks of either normoxic or hypoxic (10% Oxygen level) conditions. **A. to E.** Right ventricular internal diameter, right ventricular free wall thickness, tricuspid annular plane systolic excursion, ratio of pulmonary artery acceleration time to ejection time, cardiac output and cardiac index

respectively, measured at 3 and 5 weeks. WT = wild type, OB = obese, NOX = normoxia, HOX = hypoxia, RVID = right ventricular internal diameter, RVWT = right ventricular free wall thickness, TAPSE = tricuspid annular plane systolic excursion, PAAT = pulmonary artery acceleration time, PAET = pulmonary artery ejection time, CI = cardiac index. Data are mean ± SEM, p value ≤ 0.05 are significant, n = 8-10, *compared to wild type, $^{\$}$compared to normoxia

3.19 Hemodynamic features of hypoxia induced PH in B6 female mice

Invasive hemodynamic parameters were assessed similar to male B6 mice. No differences were seen in any groups for the systemic arterial pressure. Hypoxic female mice developed higher RVSP and Fulton's index, compared to the normoxic controls. No prominent effect of obesity was observed under hypoxia, except slight increase of RVSP in obese female mice, compared to the lean control.

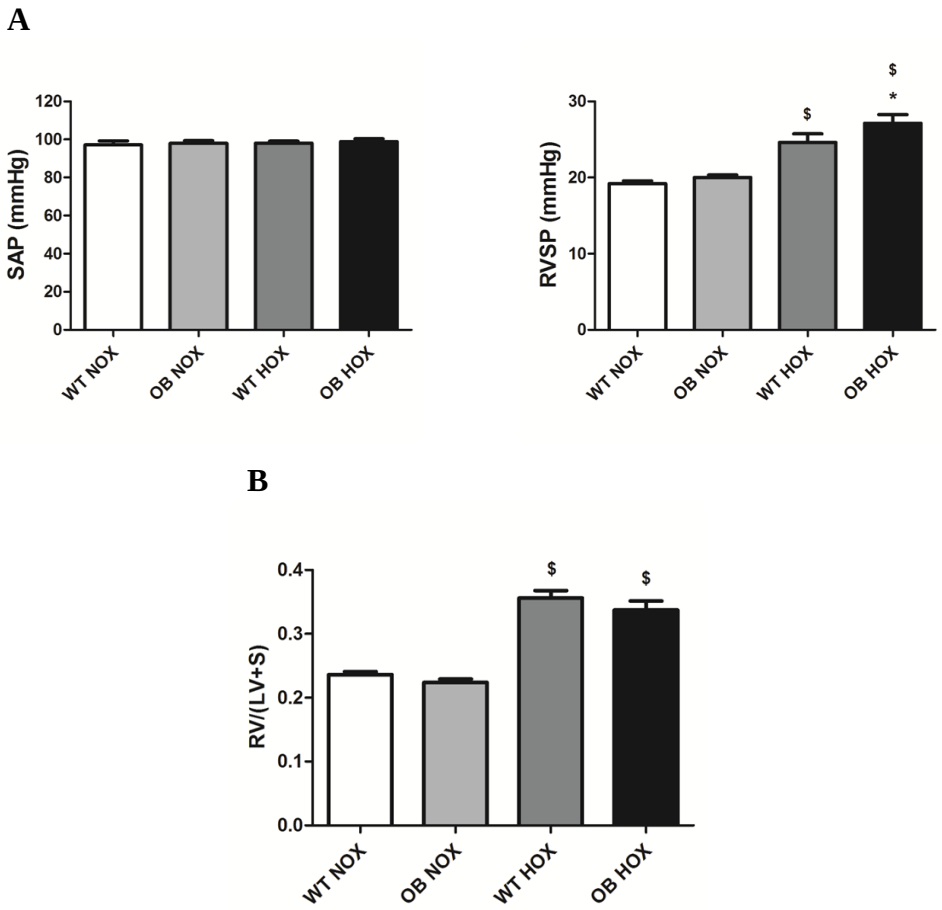

Fig. 30: Hemodynamic measurements and Fulton's index of lean and obese female B6 mice were assessed after 5 weeks of either normoxic or hypoxic (10% Oxygen level) conditions. **A.** Systemic arterial pressure and right ventricle systolic pressure measured invasively at 5 weeks after normoxic or hypoxic conditions. **B.** Ratio of right ventricle to left ventricle + septum measured at 5 weeks of normoxic or hypoxic conditions. WT = wild type, OB = obese, NOX = normoxia, HOX = hypoxia, SAP = systemic arterial pressure, RV = right ventricle, LV = left ventricle, S = septum. Data are mean ± SEM, p value ≤ 0.05 are significant, n = 8-10, *compared to wild type, $compared to normoxia.

3.20 Pulmonary vascular remodeling in hypoxia induced PH in B6 female mice

Pulmonary vascular remodeling in the distant pulmonary vessels were assessed similar to those male B6 mice. Wild type mice developed increased medial wall thickness due to hypoxia but obese mice did not show this increment. Higher degree of fully muscularized vessels were present in both hypoxic wild type and obese mice (Fig. 31-A and B).

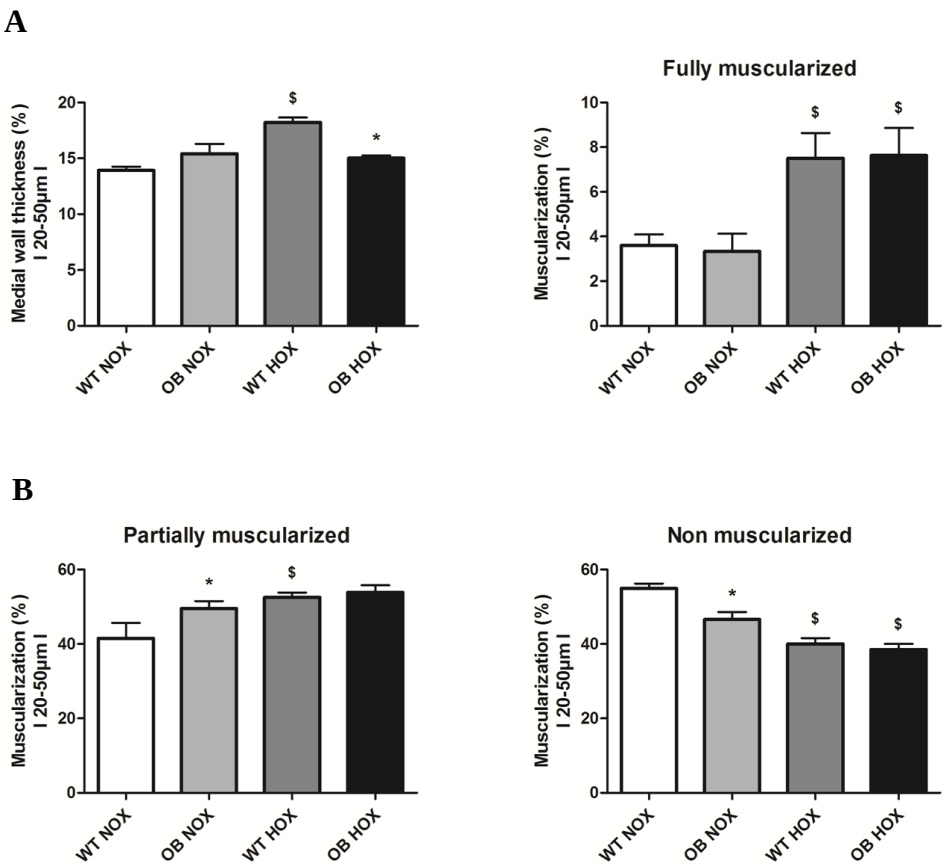

Fig. 31: Medial wall thickness and degree of muscularization of lean and obese female B6 mice were assessed after 5 weeks of either normoxic or hypoxic (10% oxygen level) conditions. Lung tissues were sliced at 3 µm sections for staining. van Gieson's staining was done to measure the medial wall thickness. The distance between lamina elastic interna and externa was measured. Double immuno-staining with anti-alpha smooth muscle actin (α SMA) antibody and anti-von-Willebrand factor (vWF) antibody was done to measure the degree of muscularization. **A and B.** Medial wall thickness and degree of muscularization for lean and obese female B6 mice treated either with normoxic or hypoxic conditions. WT = wild type, OB = obese, NOX = normoxia, HOX = hypoxia. Data are mean ± SEM, p value ≤ 0.05 are significant, n = 5, *compared to wild type, $^{\$}$compared to normoxia

4. Discussion

In general, the results from the study revealed the following findings:

1) Obesity in male Zucker rats did not influence the disease severity in MCT-induced PH. However, there was a clear increase in lung inflammation due to obesity, in comparison to lean controls.

2) Furthermore, the data demonstrated that obesity significantly aggravated the MCT-induced PH in female Zucker rats, compared to their lean controls. These findings indicated potentially different influence of obesity with regard to the gender in the context of inflammatory model of PH, such as MCT.

3) Finally, obesity exhibited negligible effects in hypoxia-induced PH in male and female obese mice, compared to their respective lean controls.

This research was aimed to find the potential relation between obesity and pulmonary hypertension. Along with an obese factor, a clear presentation of male and female characteristics was aimed in the context of PH. To exert an extended explanation for the complex entity of PH, two different models were utilized - MCT and hypoxia model of PH in rats and mice respectively. Both of this models have been successfully and efficaciously used to characterize PH in rats and mice with excellent reproducible results (Dumitrascu et al., 2008; Stenmark et. al., 2006; Schermuly et al., 2004).

MCT, a macrocyclic pyrrolizidine alkaloid, after its application, converts into its active and toxic form, causing inflammatory response and pulmonary injury and non-reversible epithelial damage. Pyrrolizidine alkaloid toxicity, mainly hepatic necrosis, and deaths have also been reported in humans and animals after accidental ingestion of Crotalaria or other related plants (Wilson et al., 1992). Hypoxia, on the other hand, causes different but distinctive form of pulmonary vessels remodeling which presents the differentiation of

immature smooth muscle cells leading to increased migration, proliferation or matrix protein production (Stenmark et al., 2006).

The role of obesity in PH is still unclear, neither suggesting as a friend nor as a foe against this condition. Studies particularly accessing the association between obesity and pulmonary hypertension have shown no relation with class I obesity, but a higher probability of connection with class II or III obesity (Williams III et al., 2010). A typical study done on a moderately high altitude illustrated a higher prevalence of diurnal PH in obese patients. Obesity hypoventilation syndrome was predicted as the main risk factor (Valencia-Flores et al., 2004).

Diet induced obesity in rats have shown to develop various features such as pulmonary artery remodeling, elevated pulmonary artery pressure and right ventricular hypertrophy. The obese rats featured hyperlipidemia, oxidant damage and high circulating inflammatory cytokines but did not show any evidence of hypoventilation or chronic hypoxia-like features (Irwin et al., 2014). High fat diet fed obese mice demonstrated an upregulation of the genes of cardiac endothelin system. The plasma levels of endothelin-1 as well as endothelin receptors A and B protein expression were also higher in those mice (Catar et. al., 2014) suggesting a predisposition for PH or pulmonary disease. Increased inflammation and oxidative stress are associated independently with obesity or PH and administration of antioxidant supplementation in either case is shown to be beneficial (Bowers et al., 2004; Musaad and Haynes 2007). Obesity with the association of inflammatory markers and oxidative stress might be an essential factor for PH development.

The gender in humans also affect the prevalence or survival due to PH. Earlier believed to be more frequent in younger females, PAH has gradually lurched to nullify this gender dominance. Equally balanced gender patients at older age but with higher severity and lower therapy response was observed by European based medial therapies for PH - COMPERA (Comparative, Prospective Registry of Newly Initiated Therapies for Pulmonary Hypertension) (Hoeper, et al., 2013). A radically distinctive study has shown a greater percentage of females within the patients who were obese but not diabetic (Poms et

al., 2013). Intriguingly, females show better survival probabilities than the males. Interestingly, animal studies have shown for estrogens to have protective role in animal models of PH (Lahm et al., 2014).

Having these confounding results both with regard to obesity and gender versus PH, it gives a great opportunity to unravel these research questions. In general, the results of MCT-induced PH in Zucker male rats revealed that the obesity did not influence significantly the disease severity. However, more prominent inflammation was still present in the lungs of obese versus lean male rats upon MCT injections. Female Zucker rats, on the other hand, showed less effects of MCT-induced PH, but a higher severity of the disease in the obese females than those of leans. Both obesity and gender appeared to alter the normal and established norms and understanding on the topic. Therefore, obesity may represent an important factor which modulates the PH development in the context of females. In the case of hypoxia-induced PH, obesity was not shown to play an important role neither in male nor female gender.

4.1 MCT-induced PH in lean and obese male Zucker rats

For inducing obesity in male rats, leptin receptor recessive Zucker rats (Crl:ZUC-*Lepr*^{fa}) were used from Charles River Laboratories together with their lean counterpart. For PH development in rats, widely used MCT model at a dose of 60 mg MCT per kg body weight was followed. It has been successfully utilized in several experiments showing prominent features of PH in various rat species (Gomez-Arroyo et al., 2012; Kosanovic et al., 2011; Schermuly et al., 2004). The difference of final body mass index for lean and obese groups were significant for the evaluation of the results. In order to track down the potential magnitude of disease progression, assessment of the echocardiography data were done at two instances - 3 weeks and 5 weeks.

Both the lean and obese groups of Zucker rats injected with MCT presented severe form of PH as revealed by increase in RVID and RVWT as well as decrease in TAPSE, PAAT/PAET and CI (Fig. 13-A to E). The severity of PH was confirmed by elevation of

right ventricular systolic pressure and Fulton's index (Fig. 14-A and B) and with the assessment of the pulmonary vascular remodeling of distal pulmonary vessels (Fig. 16-A and B).

However, the difference between the end stage severity of lean and obese male Zucker rats in terms of echocardiographic parameters, hemodynamic measurements and pulmonary vascular remodeling was not evident. In addition, there was little or non-significant fluctuations of 3 weeks echocardiographic parameters except PAAT to PAET ratio, in which obese male Zucker rats had significantly better performance (Fig. 13-D). CI in obese male rats was also slightly better, albeit not significant (Fig. 13-E).

The survival percentage in MCT injected lean and obese male Zucker rats were recorded. After the MCT injection, the rats were observed in daily basis and duly assigned a score for its body condition to access the distress in the body. The mortality in MCT injected lean male Zucker rats started at day 28, couple of days earlier than MCT injected obese male Zucker rats. However, the end stage mortality (day 35) in obese ones was higher than those of leans (73.3% survival rate of lean rats versus 46.7% survival rate of obese) (Fig. 15). With similar end stage severity of PH parameters in both the groups, but higher mortality in obese male Zucker rats, it reserves a more profound study in the future to reveal if this observation is important.

4.2 Higher inflammation in lung tissues of obese male Zucker rats

To gain the insightful perspective for stimulation of immune system and degree of inflammation, macrophage specific CD68 positive cells were measured in the paraffin embedded lung tissues. Significant increase in the CD68 positive cells were seen. Infiltration of perivascular inflammatory cells in idiopathic PAH patients and MCT model have been characterized (Savai et al., 2012). Increased macrophages have been seen in the bronchoalveolar lavage fluid in the murine model (Tilton et al., 2013). Interestingly, obese male Zucker rats revealed significantly higher CD68 positive cells suggesting higher degree of inflammation or activation of the immune system, compared to their lean

counterparts (Fig. 17-A). This provides a clue of heightened inflammatory effects which might play crucial role for exasperation of disease severity in obesity in its chronic form.

4.3 Milder PH features in female Zucker rats

For inducing obesity in female rats, I used the females of the same variant of male Zucker rats. These leptin receptor recessive female Zucker rats (Crl:ZUC-*Lepr*^{fa}), together with the lean counterpart, were also ordered from Charles River Laboratories. For PH development in female rats, the same MCT-model at a dose of 60 mg per kg body weight was implemented, similar to that of males. The difference of final body mass index for lean and obese groups was significant and echocardiography data were assessed at two instances - 3 weeks and 5 weeks. The lean female Zucker rats were characterized by milder disease severity due to MCT administration compared to the males, as seen in the RVID, RVWT and PAAT/PAET. Furthermore, relatively less effects of MCT in the terms of Fulton's index or RVSP were also noted in the lean female groups. Pulmonary vascular remodeling (as assessed by increase in medial wall thickness and muscularization) was demonstrated, however, in less extent. This data corresponds with previous studies where researches were not able to show MCT effects in female Wistar rats (Lookin et. al., 2015).

Female hormones have been attributed for this difference of MCT induced PH in male and female rats (Bal et al., 2013; Lookin et al., 2015). The group of Won-Jung Lee were able to show development of PH when both the ovaries from Sprague-Dawley rats were removed highlighting the importance of female hormones in PH progression (Ahn et al., 2003).

4.4 Higher severity of disease in obese female Zucker rats

Effects of MCT in obese female rats have not been documented earlier. This study provides important data about obese female Zucker rats which shows they are more prone to heart function damage and vascular remodeling following MCT injection. Consistent results of increased severity were found in terms of echocardiographic parameters, hemodynamic measurement, distal pulmonary vascular remodeling and CD68 positive macrophages.

Compared to their lean counterparts, 5 weeks post MCT data shows obese female Zucker rats had significantly higher RVID, RVWT as well as lower TAPSE and PAAT/PAET. A significant increase in Fulton's index and RVSP was also clearly observable in the obese female Zucker rats after the MCT injection. Likewise, medial wall thickening and muscularization of distal pulmonary arteries were also increased in the obese MCT female groups than those of the lean counterparts.

The striking characteristics of MCT-induced PH in male Zucker rats were still not found in the female Zucker rats. The overall severity as compared to the male Zucker rats was less in females. The mean RVSP of female obese Zucker rats after 5 weeks of receiving MCT was 57.5 mmHg while this value for male obese Zucker rats after 5 weeks of receiving MCT was 71.33 mmHg. The Fulton's index of males were 0.43 versus 0.32 of females. There were no mortality due to MCT injection in the female group of rats while the mortality following MCT injection in males were 53%. This overall results implicated a milder form of disease in the obese females compared to that of obese males, but obesity is shown to modulate the PH development in the context of females and not in the males.

4.5 Increased inflammation in obese female Zucker rats

Macrophage specific CD68 positive cells were counted in the paraffin embedded lung tissues of female Zucker rats treated for 5 weeks with either normal saline or MCT. The procedures were similar to those adopted for male Zucker rats. An increase in the CD68 positive cells were seen in all the female groups as compared to the lean females. This indicated increased inflammation and stimulation of immune system in obese females as well as MCT treated lean and obese females. A clearly alike augmentation of CD68 positive cells infiltration was seen in the obese females treated with MCT as that of obese male Zucker rats. Therefore, it seems that inflammation may be one of the potential links between obesity and PH, and that gender difference in indeed an important factor.

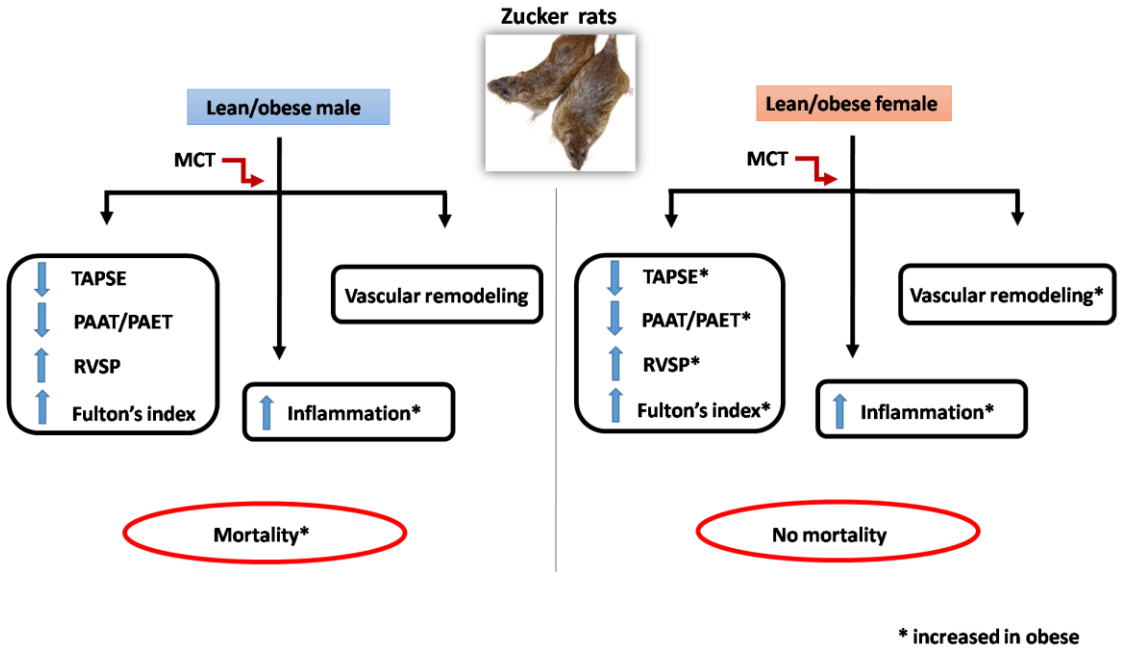

Fig. 32: Scheme for the characterization of MCT induced PH in lean and obese Zucker rats of both of the genders. MCT = monocrotaline, TAPSE = tricuspid annular plane systolic excursion, PAAT = pulmonary artery acceleration time, PAET = pulmonary artery ejection time, RVSP = right ventricular systolic pressure.

4.6 Hypoxia induced PH in lean and obese male mice

Lean and obese male B6 mice were exposed to hypoxia (10% oxygen) for 5 weeks. PH due to hypoxia is officially listed in Group 3 in the updated clinical classification of PH (Simonneau et al., 2013). Hypoxia exposure to mouse has been robustly used as a model of PH in several studies (Dahal et al., 2012; Pak et al., 2010; Sommer et al., 2008). The body mass index in obese male mice was significantly higher than in their lean counterparts (Fig. 24). 5 weeks long hypoxia exposure did not alter the BMI of lean or obese groups of mice. To access the development of PH, echocardiographic measurements were done at 3 and 5 weeks, as well as hemodynamic measurements at 5 weeks after hypoxia exposure.

Evaluation of echocardiographic results at 3 weeks of hypoxic exposure showed clear manifestation of PH features with increase in RVID and RVWT and decrease in PAAT/PAET and TAPSE. Hypoxia has been known to develop clear PH features after 3 weeks (Xia et al., 2014; Zhao et al., 2001). Increase in RVSP has been shown as early as 1 week of hypoxia exposure (Xia et al., 2014). Echocardiographic features stayed mostly similar at 5 weeks of hypoxia exposure as that of 3 weeks for both the lean and obese mice. Hemodynamic measurements were done after 5 weeks of normoxia or hypoxia treatment. SAP were similar in all groups negating the changes of systemic hypertension. Both lean and obese mice showed elevated RVSP than the normoxic mice, however, the obese mice, both in normoxic or hypoxic conditions, presented lower RVSP than their lean counterparts. Fulton's index were higher for both groups of hypoxic mice, but no differences were seen between lean and obese mice.

Remodeling of distal pulmonary arteries were evaluated in the same manner as Zucker rats. Increased medial wall thickness and muscularization was visible in both lean and obese hypoxic mice, compared to the normoxic groups.

4.7 Hypoxia induced PH in lean and obese male mice

Although some echocardiographic data (such as RVID, TAPSE and PAAT/PAET) and pulmonary vascular remodeling results show some mild "improvements" in obese versus lean male mice under hypoxia, other important measures, such as RVWT, RVSP and Fulton's index, do not reveal clear effects of obesity on hypoxia-induced PH. Therefore, our data do not convincingly support the significant influence of obesity in the context of chronic hypoxia exposure. In the line with these findings, it was demonstrated that mild form of PH is higher in obese patients who live at higher altitude with low oxygen level in the environment (Valencia-Flores et al., 2004). Chronic obesity in rats have also shown that hypoxic conditions do not contribute to obesity related PH but are related to increased inflammatory cytokines and oxidant damage (Irwin et al., 2014).

4.8 Hypoxia induced PH in lean and obese female mice

Lean and obese female B6 mice were exposed to hypoxia (10% oxygen) for 5 weeks. Obese female mice gained significant higher body mass index than their lean counterparts (Fig. 28). Similar to male mice, female mice were subjected to 5 weeks long hypoxia exposure. BMI of lean was fully unaffected due to hypoxia, but slight reduction of BMI was visible in obese mice. Echocardiographic measurements were done at the same time periods of 3 and 5 weeks, and hemodynamic measurements at 5 weeks after hypoxia exposure.

A readily apparent PH was established at 3 weeks of hypoxia exposure in both lean and obese female mice. This was evident by significant increase in RVID and RVWT and decrease in TAPSE and PAAT/PAET. These conditions were stable until 5 weeks of hypoxia continuation in both of the groups. Hemodynamic measurements were done after 5 weeks of normoxia or hypoxia treatment. SAP was similar in all the groups. Lean and obese female mice had elevated RVSP and Fulton's index under hypoxic condition, but no differences between these two groups were observed.

The levels of distal pulmonary arteries remodeling were evaluated similar to those of male mice. Increased medial wall thickness and muscularization was present in both lean and obese hypoxic female mice except medial wall thickness in hypoxic obese mice where no increase was observed. However, the obese females had a bit lesser degree of medial wall thickness. In contrast, the right ventricle structure and functions were a bit worse for obese female mice. RVID and RVWT were higher, PAAT/PAET and TAPSE were lower for obese females. Therefore, there was no convincing evidence that obesity further altered or modified chronic hypoxia-induced PH and finally, the gender factor did not seem involved either.

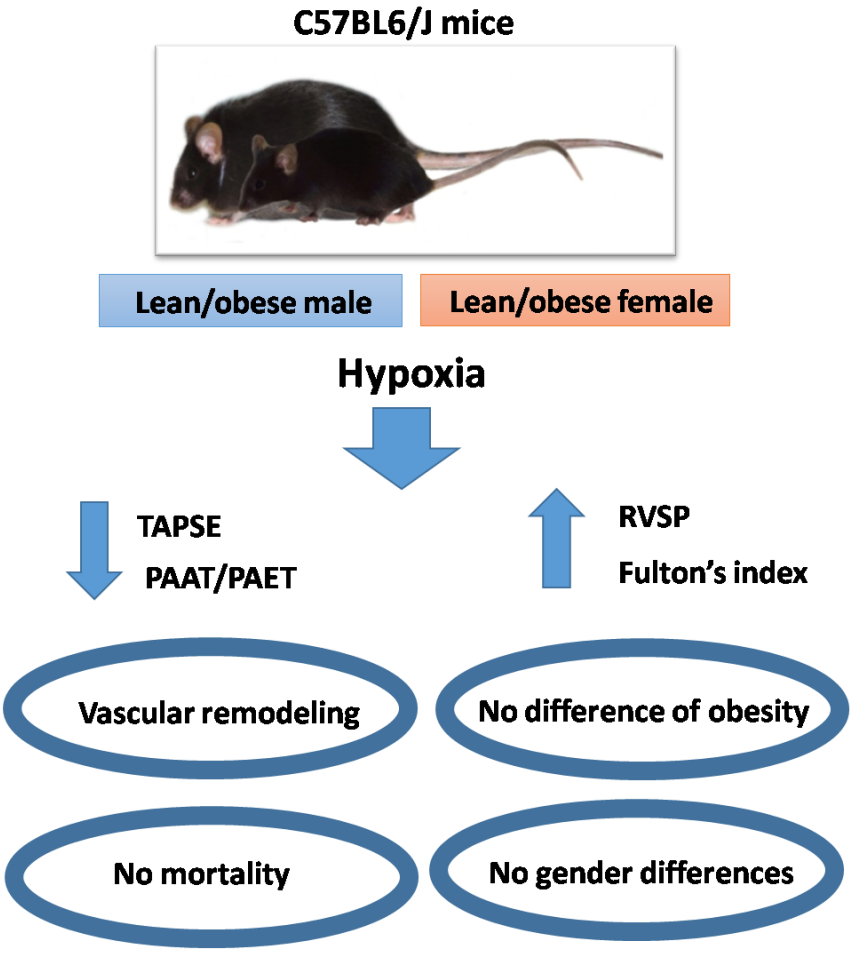

Fig. 33: Scheme for the characterization of hypoxia induced PH in lean and obese B6 mice of both of the genders. TAPSE = tricuspid annular plane systolic excursion, PAAT = pulmonary artery acceleration time, PAET = pulmonary artery ejection time, RVSP = right ventricular systolic pressure

4.9 Conclusion, limitations and future perspectives

The study on male and female obesity in murine models of PH revealed important differences with regard to gender and animal model (MCT- versus chronic hypoxia-induced PH). MCT presented a more severe form of PH with significantly higher remodeling and worsening of hemodynamic parameters in males, compared to the females. However, obesity was not found to be an important modulator of PH in males. Conversely,

obesity was found to be an important factor for the disease pathology in females. Interestingly, higher degree of inflammation was evident in obese animals of both male and female Zucker rats. On the other hand, hypoxia induced PH in obese male and female mice resulted in negligible differences between lean and obese or males and females. Therefore, in contrast to inflammatory-driven pathology (such as in MCT-model), obesity was not demonstrated as significant pathological factor for chronic hypoxia-induced PH.

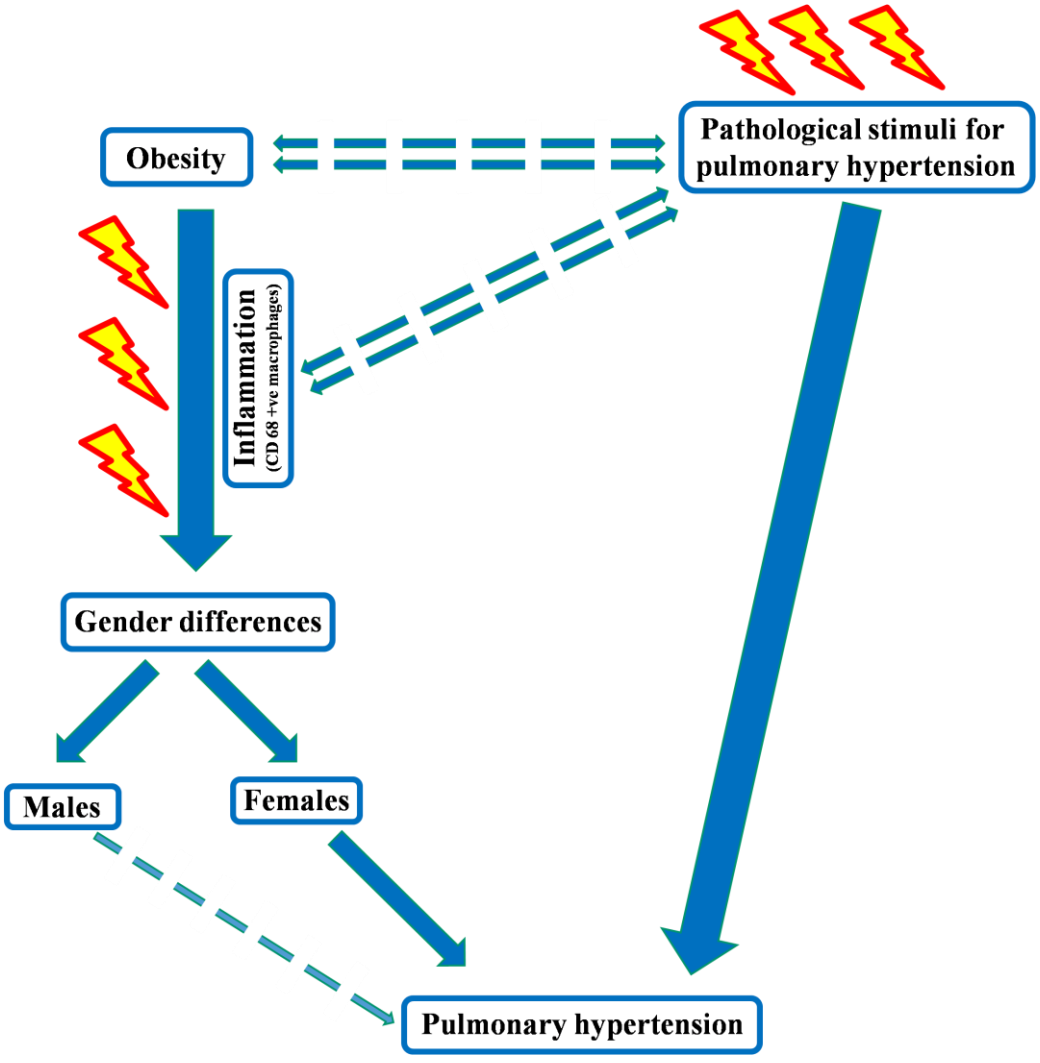

Fig. 34: Scheme for the characterization of obesity related pulmonary hypertension. The lightning bolt in yellow with red outline represents various pathological mediators.

This study was not free of limitations. As an established protocol for MCT administration of 300-350 gm body weight in rats (Schermuly et al., 2005), same range of body weight was chosen to avoid any variance in the MCT model itself. This urged to administer MCT into rats which had relatively lesser BMI and gained the body weight during the 35 days experimental stint. Researchers exploit obesity induced over longer period (greater than 5 months) to have more concrete results (Irwin et al., 2014; Khoo et al., 2012). Due to time and resource constraints, the study used only two animal models of PH namely, MCT model of PH in rats and hypoxia model of PH in mice.

This study reserves the molecular pathway scrutiny for further elucidation of obesity related pathobiology in PH. Because of the complexity of PH as well as the variation of species in obesity effects, different species as well as new models of PH would provide interesting insights about its characteristics.

5. Summary

Obesity and pulmonary hypertension (PH) are medical conditions, both characterized by augmented inflammation and oxidative stress. Some of the studies showed a possible correlation between obesity and PH. However, the exact role or contribution of obesity to the pathology of this pulmonary vascular disease is still unknown and needs further research.

Animal experiments were conducted on monocrotaline (MCT) and hypoxia models of PH. Lean and obese Zucker rats or B6 mice of both gender were used for MCT or chronic hypoxia models, respectively. Lean and obese (male or female) Zucker rats or B6 mice were further divided into two groups, receiving either normal saline/normoxia exposure or MCT injection/hypoxia exposure for 5 weeks. Echocardiography, hemodynamic measurements and histology were performed to analyze various parameters, such as heart function and hypertrophy, hemodynamics, pulmonary vascular remodeling and lung inflammation.

MCT injection resulted in the development of PH in both lean and obese male and female rats. Negligible differences in terms of PH severity were observed between lean and obese male rats at the end stage of the disease. Conversely, obese female rats developed more prominent and severe PH compared to their lean counterparts. On the other hand, no apparent differences were found between lean and obese mice and gender factor also appeared to have negligible influence in the context of chronic hypoxia-induced PH.

As a conclusion, obesity is found to be important factor associated with altered inflammation. In addition, significant differences between genders existed in the MCT model with regard to the severity of this life-threatening pulmonary vascular disease. However, future studies are needed to substantiate these findings and to reveal the underlying mechanisms.

6. Zusammenfassung

Adipositas und Pulmonale Hypertonie (PH) sind Erkrankungen, die beide durch vermehrte Inflammation und oxidativem Stress charakterisiert sind. Einige Studien zeigten eine mögliche Korrelation zwischen Adipositas und PH. Allerdings sind die exakten Auswirkungen der Fettleibigkeit auf die Pathologie dieser Lungengefäßerkrankung noch nicht bekannt und bedürfen weiterer Forschung.

In dieser Arbeit wurden zwei verschiedene tierexperimentelle Modelle zur Nachahmung der PH verwendet. Das Monocrotalin (MCT)-Modell wurde in schlanken und fettleibigen Zucker Ratten beiderlei Geschlechts angewendet. In ebenfalls beiden Geschlechtern von C57Bl6 Mäusen wurde das Modell der chronischen Hypoxie verwendet. Beide Modelle hatten eine Laufzeit von 5 Wochen. Beide Kohorten (männlich und weiblich) wurden in zwei Gruppen aufgeteilt. Die schlanken und fettleibigen Zucker Ratten erhielten entweder die MCT-Injektion oder die Kochsalzlösung-Injektion. Die C57Bl6N-Mäuse wurden entweder unter normoxischen oder hypoxischen Bedingungen gehalten. Echokardiographie, hämodynamische Druckmessungen und histologische Untersuchungen wurden durchgeführt, um verschiedene Parameter, wie die Herzfunktion, Rechtsherzhypertrophie, vaskuläres Remodelling und inflammatorische Prozesse in der Lunge, zu analysieren.

Die MCT-Injektion führte bei schlanken und fettleibigen männlichen und weiblichen Ratten zur Entwicklung einer PH. Es wurden unbedeutende Unterschiede in Bezug auf den Schweregrad der PH zwischen schlanken und übergewichtigen männlichen Ratten im Endstadium der Krankheit beobachtet. Im Gegensatz dazu entwickelten weibliche adipöse Ratten eine schwerere PH im Vergleich zu den schlanken Pendants. Bei der Induktion einer PH mittels chronischer Hypoxie wurden keine offensichtlichen Unterschiede zwischen schlanken und fettleibigen Mäusen beiden Geschlechts gefunden.

Abschließend ist zu sagen, dass die Adipositas ein wichtiger Faktor in Verbindung mit einer veränderten Entzündungsreaktion ist. Im Hinblick des Schweregrades dieser lebensbedrohlichen Lungengefäßkrankheit bestehen darüber hinaus signifikante Unterschiede zwischen beiden Geschlechtern im MCT-Modell. Allerdings sind weitere Studien notwendig, um die Ergebnisse dieser Arbeit zu untermauern und die zugrundeliegenden Mechanismen im Detail zu verstehen.

7. List of abbreviations

ALK-1 = activin receptor-like kinase 1

Ang = angiotensinogen

ANOVA = analysis of variance

bFGF = basic fibroblast growth factor

BMI = body mass index

BMPR2 = bone morphogenetic protein receptor type II

BSA = body surface area

BSA = bovine serum albumin

CAV1 = caveolin-1

cc = cubic centimeter

CD 68 = cluster of differentiation 68

cGMP = cyclic guanosine monophosphate

CI = cardiac index

cm = centimeter

CO = cardiac output

CO_2 = carbon dioxide

COMPERA = Comparative, Prospective Registry of Newly Initiated Therapies for PH

COPD = chronic obstructive pulmonary disease

CRP = c reactive protein

DAB = 3,3'-Diaminobenzidine

EDTA = ethylenediaminetetraacetate

ENG = endoglin

eNOS = endothelial nitric oxide synthase

F_2 IsoPs = F_2 isoprostanes

Fig. = figure

gm = gram

H_2O = hydrogen monoxide (water)

H_2O_2 = hydrogen peroxide

HCl = hydrogen chloride

HIV = human immuno-deficiency virus

HOX = hypoxia

HR = heart rate

i.e. = id est (that is)

IL-6 interleukin 6

KCl = potassium chloride

KCNK3 = Potassium channel subfamily K member 3

Kg = kilogram

KH2PO4 = potassium dihydrogen phosphate

LA = left atrium

LV = left ventricle

LV+S = left ventricle plus septum

m = meter

MCP-1 = monocyte chemoattractant protein-1

MCT = monocrotaline

ml = milli liter

mRNA = micro ribonucleic acid

N_2 = nitrogen

Na2HPO4 = sodium hydrogen phosphate

NaCl = sodium chloride

NaOH = sodium hydroxide

NOX = normoxia

NS = normal saline

O_2 = oxygen

OB = obese

^{O}C = degree centigrade

oxLDL = oxidized low density lipoprotein

PA = pulmonary artery

PAAT = Pulmonary artery acceleration time

PACP = pulmonary artery capillary pressure

PAET = pulmonary artery ejection time

PAH = pulmonary arterial hypertension

PAWP = pulmonary artery wedge pressure

PBS = phosphate buffer saline

PDE5 = phosphodiesterase 5

PDGF = platelet derived growth factor

PH = pulmonary hypertension

PPAR-β = peroxisome proliferator-activated receptors - beta

PV = pulmonary vein

PVRI = Pulmonary Vascular Research Institute

RA = right atrium

rpm = revolutions per minute

RV = right ventricle

RVID = right ventricle internal diameter

RVSP = right ventricular systolic pressure

RVWT = right ventricle free wall thickness

SA node = sino-artrial node

SAP = systemic arterial pressure

SEM = standard error of mean

SMAD9 = mothers against decapentaplegic homolog 9

SU5416 = 3-[(2,4-dimethylpyrrol-5-yl) methylidenyl]-indolin-2-one

SV = stroke volume

TAPSE = tricuspid annular plane systolic excursion

TGF-β = transforming growth factor - beta

TNF-α = tumor necrosis factor-alpha

VEGF = vascular endothelial growth factor

VEGFR = vascular endothelial growth factor receptor

vWF = von-Willebrand factor

WHO = World Health Organization

WT = wild type

α-SMA = alpha smooth muscle actin

μm = micro meter

8. References

Ahn, B. H. et al. Estrogen and enalapril attenuate the development of right ventricular hypertrophy induced by monocrotaline in ovariectomized rats. *J. Korean Med. Sci.* **18,** 641–48 (2003).

Austin, E. D. et al. Gender, sex hormones and pulmonary hypertension. *Pulm. Circ.* **3,** 294–314 (2013).

Badri, M. et al. Effect of obesity on mortality in pulmonary arterial hypertension: a retrospective analysis. *J. Am. Coll. Cardiol.* **59,** E1590 (2012).

Bal, E. et al. The effects of gender difference on monocrotaline-induced pulmonary hypertension in rats. *Hum. Exp. Toxicol.* **32,** 766-74 (2013).

Banks, W. A. et al. Triglycerides induce leptin resistance at the blood-brain barrier. *Diabetes* 1253–60 (2004).

Belke, D. D. et al. Altered metabolism causes cardiac dysfunction in perfused hearts from diabetic (db/db) mice. *Am. J. Physiol. Endocrinol. Metab.* **279,** E1104–13 (2000).

Berbari, N. F. et al. Leptin resistance is a secondary consequence of the obesity in ciliopathy mutant mice. *Proc. Natl. Acad. Sci. U. S. A.* **110,** 7796–801 (2013).

Böhm, C. et al. Sexual dimorphism in obesity-mediated left ventricular hypertrophy. *Am. J. Physiol. Heart Circ. Physiol.* **305,** H211–18 (2013).

Bowers, R. et al. Oxidative stress in severe pulmonary hypertension. *Am. J. Respir. Crit. Care Med.* **169,** 764–9 (2004).

Catar R. A. et al. Increased gene expression of the cardiac endothelin system in obese mice. *Horm. Metab. Res.* **47,** 509-15 (2014).

Dahal, B. K. *et al.* Hypoxic pulmonary hypertension in mice with constitutively active platelet-derived growth factor receptor-β. *Pulm. Circ.* **1,** 259–68 (2011).

Dahal, B. K. et al. Involvement of mast cells in monocrotaline-induced pulmonary hypertension in rats. *Respir. Res.* **12:60** (2011).

Dahal, B. K. et al. Role of epidermal growth factor inhibition in experimental pulmonary hypertension. *Am. J. Respir. Crit. Care Med.* **181,** 158–67 (2010).

Devaraj, S. et al. Adiponectin decreases C-reactive protein synthesis and secretion from endothelial cells: evidence for an adipose tissue-vascular loop. *Arterioscler. Thromb. Vasc. Biol.* **28,** 1368–74 (2008).

Dewachter, L. & Naeije, R. The newborn piglet: a large animal model of paediatric pulmonary hypertension. *Drug Discov. Today Dis. Model.* **7,** 107–113 (2010).

Dorfmüller, P. et al. Increased oxidative stress and severe arterial remodeling induced by permanent high-flow challenge in experimental pulmonary hypertension. *Respir. Res.* **12:119** (2011).

Dumitrascu, R. et al. Characterization of a murine model of monocrotaline pyrrole-induced acute lung injury. *BMC Pulm. Med.* **8,** 25 (2008).

Elizabeth, K. E. & Muraleedharan, M. Three-in-one weight, height and body mass index charts for children and adults. *J. Trop. Pediatr.* **49,** 224–27 (2003).

Forfia, P. R. et al. Tricuspid annular displacement predicts survival in pulmonary hypertension. *Am. J. Respir. Crit. Care Med.* **174,** 1034–41 (2006).

Furuya, Y., Satoh, T. & Kuwana, M. Interleukin-6 as a potential therapeutic target for pulmonary arterial hypertension. *Int. J. Rheumatol.* **2010(720305)** (2010).

Galiè, N. et al. Updated treatment algorithm of pulmonary arterial hypertension. *J. Am. Coll. Cardiol.* **62,** D60–72 (2013).

Ghamra, Z. W. & Dweik, R. A. Primary pulmonary hypertension: an overview of epidemiology and pathogenesis. *Cleve. Clin. J. Med.* **70** (2003).

Ghofrani, H. A. et al. Future perspectives for the treatment of pulmonary arterial

hypertension. *J. Am. Coll. Cardiol.* **54,** S108–17 (2009).

Ghofrani, H. A. et al. Nitric oxide pathway and phosphodiesterase inhibitors in pulmonary arterial hypertension. *J. Am. Coll. Cardiol.* **43,** (2004).

Ghofrani, H. A. et al. Riociguat for the treatment of pulmonary arterial hypertension. *N. Engl. J. Med.* **369,** 330–40 (2013).

Ghofrani, H. A. et al. Sildenafil for treatment of lung fibrosis and pulmonary hypertension: a randomised controlled trial. *Lancet* **360,** 895–900 (2002).

Gomez-Arroyo, J. G. et al. The monocrotaline model of pulmonary hypertension in perspective. *AJP Lung Cell. Mol. Physiol.* **302,** L363–69 (2012).

Grant, R. W. & Dixit, V. D. Adipose tissue as an immunological organ. *Obesity* **23,** 512–18 (2015).

Guyton, A. C. & Hall, J. E. Textbook of Medical Physiology. 11th Ed. Elsevier Inc. (2006).

Hansmann, G. & Rabinovitch, M. The protective role of adiponectin in pulmonary vascular disease. *Am. J. Physiol. Lung Cell. Mol. Physiol.* **298,** L1-2 (2010).

Hayashi, S. et al. Establishment of an animal model for pulmonary fibrosis in mice using monocrotaline. *Toxicologic. Pathology* **23,** 63–71 (1995).

Hoeper, M. M. et al. Definitions and diagnosis of pulmonary hypertension. *J. Am. Coll. Cardiol.* **62,** D42–D50 (2013).

Hoeper, M. M. et al. Elderly patients diagnosed with idiopathic pulmonary arterial hypertension: results from the COMPERA registry. *Int. J. Cardiol.* **168,** 871–80 (2013).

Ikeda, Y. et al. Anti-monocyte chemoattractant protein-1 gene therapy attenuates pulmonary hypertension in rats. *Am. J. Physiol. Lung Cell. Mol. Physiol.* **286,** L1038–44 (2004).

Irwin, D. C. et al. Obesity-related pulmonary arterial hypertension in rats correlates with

increased circulating inflammatory cytokines and lipids and with oxidant damage in the arterial wall but not with hypoxia. *Pulm. Circ.* **4,** 638–653 (2014).

Itoh, T. et al. Increased plasma monocyte chemoattractant protein-1 level in idiopathic pulmonary arterial hypertension. *Respirology* **11,** 158–63 (2006).

Kauppert, C. A. et al. Pulmonary hypertension in obesity-hypoventilation syndrome. *Respir. Med.* **107,** 2061–70 (2013).

Kessler, R. et al. Pulmonary hypertension in the obstructive sleep apnoea syndrome: prevalence, causes and therapeutic consequences. *Eur. Respir. J.* **9,** 787–94 (1996).

Khoo, N. K. H. et al. Obesity-induced tissue free radical generation: an in vivo immuno-spin trapping study. *Free Radic. Biol. Med.* **52,** 2312–19 (2012).

Kojonazarov, B. et al. Effects of multikinase inhibitors on pressure overload-induced right ventricular remodeling. *Int. J. Cardiol.* **167,** 2630–37 (2013).

Konter, J. M. et al. Adiponectin attenuates LPS-induced acute lung injury through suppression of endothelial cell activation. *J. Immunol.* **188,** 854–63 (2012).

Kosanovic, D. et al. Histological characterization of mast cell chymase in patients with pulmonary hypertension and chronic obstructive pulmonary disease. *Pulm. Circ.* **4(1),** 128-36 (2014).

Kosanovic, D. et al. Therapeutic efficacy of TBC3711 in monocrotaline-induced pulmonary hypertension. *Respir. Res.* **12,** 87 (2011).

Lahm, T., Tuder, R. M. & Petrache, I. Progress in solving the sex hormone paradox in pulmonary hypertension. *Am. J. Physiol. Lung Cell. Mol. Physiol.* **307,** L7–26 (2014).

Lavie, C. J. et al. Obesity and cardiovascular disease: risk factor, paradox, and impact of weight loss. *J. Am. Coll. Cardiol.* **53,** 1925–32 (2009).

Lavie, C. J. et al. Obesity and cardiovascular diseases: Implications regarding fitness, fatness, and severity in the obesity paradox. *J. Am. Coll. Cardiol.* **63,** 1345–54 (2014).

Lee, J. et al. Golgi, trafficking, and mitosis dysfunctions in pulmonary arterial endothelial cells exposed to monocrotaline pyrrole and NO scavenging. *Am. J. Physiol. Lung Cell. Mol. Physiol.* **297,** L715–28 (2009).

Li, R. et al. Adiponectin improves endothelial function in hyperlipidemic rats by reducing oxidative/nitrative stress and differential regulation of eNOS/iNOS activity. *Am. J. Physiol. Endocrinol. Metab.* **293,** E1703–08 (2007).

Lookin, O. et al. Sex differences in stretch-dependent effects on tension and Ca^{2+} transient of rat trabeculae in monocrotaline pulmonary hypertension. *J. Physiol. Sci.* 89–98 (2015).

Lookin, O. et al. The length-dependent activation of contraction is equally impaired in impuberal male and female rats in monocrotaline-induced right ventricular failure. *Clin. Exp. Pharmacol. Physiol.* **42,** 1198–206 (2015).

Mancuso, P. Obesity and lung inflammation. *J. Appl. Physiol.* **108,** 722–28 (2010).

Medoff, B. D. et al. Adiponectin deficiency increases allergic airway inflammation and pulmonary vascular remodeling. *Am. J. Respir. Cell Mol. Biol.* **41,** 397–406 (2009).

Musaad, S. & Haynes, E. N. Biomarkers of obesity and subsequent cardiovascular events. *Epidemiol. Rev.* **29,** 98–114 (2007).

Ouchi, N. & Walsh, K. A novel role for adiponectin in the regulation of inflammation. *Arterioscler. Thromb. Vasc. Biol.* **28,** 1219–21 (2008).

Pak, O. et al. Animal models of pulmonary hypertension: role in translational research. *Drug Discov. Today Dis. Model.* **7,** 89–97 (2010).

Palmer, B. F. & Clegg, D. J. The sexual dimorphism of obesity. *Mol. Cell. Endocrinol.* **402,** 113–19 (2015).

Poms, A. D. et al. Comorbid conditions and outcomes in patients with pulmonary arterial hypertension: a REVEAL registry analysis. *Chest* **144,** 169–76 (2013).

Pulido, T. et al. Medical therapies for pulmonary arterial hypertension. *Heart Fail. Rev.* (2016).

Pullamsetti, S. S. et al. Inflammation, immunological reaction and role of infection in pulmonary hypertension. *Clin. Microbiol. Infect.* **17,** 7–14 (2011).

Ramos, M. et al. Monocrotaline pyrrole induces smad nuclear accumulation and altered signaling expression in human pulmoanry arterial endothelial cells. *Vasc. Pharmacol.* **46,** 439–48 (2007).

Reichenberger, F. et al. Sildenafil treatment for portopulmonary hypertension. *Eur. Respir. J.* **28,** 563–67 (2006).

Reis, G. S. et al. Oxidative-stress biomarkers in patients with pulmonary hypertension. *Pulm. Circ.* **3(4),** 856–61 (2013).

Reuter, S. et al. Oxidative stress, inflammation, and cancer: How are they linked? *Free Radic. Biol. Med.* **49(11),** 1603-16 (2010).

Reynolds, S. D. & Malkinson, A. M. Clara cell: progenitor for the bronchiolar epithelium. *Int. J. Biochem. Cell Biol.* **42,** 1–4 (2010).

Satoh, K. et al. Basigin mediates pulmonary hypertension by promoting inflammation and vascular smooth muscle cell proliferation. *Circ. Res.* **115,** 738–50 (2014).

Savai, R. et al. Immune and inflammatory cell involvement in the pathology of idiopathic pulmonary arterial hypertension. *Am. J. Respir. Crit. Care Med.* **186,** 897–908 (2012).

Savai, R. et al. Pro-proliferative and inflammatory signaling converge on FoxO1 transcription factor in pulmonary hypertension. *Nat. Med.* **20,** 1289–300 (2014).

Scanlon, V. C. & Sanders, T. Essentials of Anatomy and Physiology. 5th Ed. F. A. Davis Company (2007).

Schermuly, R. T. et al. Chronic sildenafil treatment inhibits monocrotaline-induced pulmonary hypertension in rats. *Am. J. Respir. Crit. Care Med.* **169,** 39–45 (2004).

Schermuly, R. T. et al. Mechanisms of disease: pulmonary arterial hypertension. *Nat. Rev. Cardiol.* **8,** 443–55 (2011).

Schermuly, R. T. et al. Reversal of experimental pulmonary hypertension by PDGF inhibition. **115,** 2811–21 (2005).

Simonneau, G. et al. Continuous subcutaneous infusion of treprostinil, a prostacyclin analogue, in patients with pulmonary arterial hypertension. *Am. J. Respir. Crit. Care Med.* **165,** 800–804 (2002).

Simonneau, G. et al. Updated clinical classification of pulmonary hypertension. *J. Am. Coll. Cardiol.* **62,** D34–41 (2013).

Sitbon, O. et al. Selexipag for the treatment of pulmonary arterial hypertension. *N. Engl. J. Med.* **373(26),** 2522-33 (2015).

Sommer, N. et al. Regulation of hypoxic pulmonary vasoconstriction: basic mechanisms. *Eur. Respir. J.* **32,** 1639–51 (2008).

Soon, E. et al. Elevated levels of inflammatory cytokines predict survival in idiopathic and familial pulmonary arterial hypertension. *Circ.* **122,** 920–927 (2010).

Steinhorn, R. H. Lamb models of pulmonary hypertension. *Drug Discov. Today Dis. Model.* **7,** 99–105 (2010).

Stenmark, K. R. et al. Animal models of pulmonary arterial hypertension: the hope for etiological discovery and pharmacological cure. *Am. J. Physiol. Lung Cell. Mol. Physiol.* **297,** 1013–32 (2009).

Stenmark, K. R., Fagan, K. A. & Frid, M. G. Hypoxia-induced pulmonary vascular remodeling: cellular and molecular mechanisms. *Circ. Res.* **99,** 675–91 (2006).

Stevan, T. P. et al. Progesterone inhibits vascular remodeling. *Prilozi* **43,** 25–43 (2009).

Summer, R. et al. Adiponectin deficiency: a model of pulmonary hypertension associated with pulmonary vascular disease. *Am. J. Physiol. Lung Cell. Mol. Physiol.* **297,** L432–38 (2009).

Summer, R. et al. Obesity and pulmonary arterial hypertension: Is adiponectin the molecular link between these conditions? *Pulm. Circ.* **1,** 440–47 (2012).

Tam, A. et al. The airway epithelium: more than just a structural barrier. *Ther. Adv. Respir. Dis.* **5,** 255–73 (2011).

Tang, B. et al. Ellagic acid prevents monocrotaline-induced pulmonary artery hypertension via inhibiting NLRP3 inflammasome activation in rats. *Int. J. Cardiol.* **180C,** 134–41 (2014).

Taraseviciene-Stewart, L. et al. Inhibition of the VEGF receptor 2 combined with chronic hypoxia causes cell death-dependent pulmonary endothelial cell proliferation and severe pulmonary hypertension. *FASEB J.* **15,** 427–38 (2001).

Tilton, S. C. et al. Diet-induced obesity reprograms the inflammatory response of the murine lung to inhaled endotoxin. *Toxicol. Appl. Pharmacol.* **267,** 137–48 (2013).

Tonelli, A. R. et al. Leptin levels predict survival in pulmonary arterial hypertension. *Pulm. Circ.* **2,** 214–19 (2012).

Tschöp, M. et al. Ghrelin induces adiposity in rodents. *Nature* **407,** 908–13 (2000).

Tuder, R. M. et al. Relevant issues in the pathology and pathobiology of pulmonary hypertension. *J. Am. Coll. Cardiol.* **62,** (2013).

Valencia-Flores, M. et al. Prevalence of pulmonary hypertension and its association with respiratory disturbances in obese patients living at moderately high altitude. *Int. J. Obes. Relat. Metab. Disord.* **28,** 1174–80 (2004).

Vgontzas, A. N. et al. Sleep apnea and daytime sleepiness and fatigue: relation to visceral obesity, insulin resistance, and hypercytokinemia. *J. Clin. Endocrinol. Metab.* **85,** 1151–58 (2000).

Vitali, S. H. et al. The Sugen 5416/hypoxia mouse model of pulmonary hypertension revisited: long-term follow-up. *Pulm. Circ.* **4,** 619–29 (2015).

Vonk-Noordegraaf, A. et al. Right heart adaptation to pulmonary arterial hypertension: physiology and pathobiology. *J. Am. Coll. Cardiol.* **62,** 22–33 (2013).

Wang, L. et al. Sex difference in the association between obesity and asthma in U.S. adults: findings from a national study. *Respir. Med.* **109,** 955–62 (2015).

Wang, Q. et al. Monocrotaline-induced pulmonary arterial hypertension is attenuated by TNF-α antagonists via the suppression of TNF-α expression and NF-κB pathway in rats. *Vascul. Pharmacol.* **58,** 71–77 (2013).

Weibel, E. R. What makes a good lung? *Swiss Med. Wkly.* **139,** 375–86 (2009).

Weng, M. et al. Adiponectin decreases pulmonary arterial remodeling in murine models of pulmonary hypertension. *Am. J. Respir. Cell Mol. Biol.* **45,** 340–47 (2011).

Williams III, W. H. et al. Pulmonary arterial hypertension and obesity. *The Open Obes. J.* 132–36 (2010).

Wilson, D. W. et al. Mechanisms and pathology of monocrotaline pulmonary toxicity. *Crit. Rev. Toxicol.* **22,** 307–25 (1992).

Xia, Y. et al. Classical transient receptor potential 1 and 6 contribute to hypoxic pulmonary hypertension through differential regulation of pulmonary vascular functions. *Hypertension* **63,** 173–80 (2014).

Yazdi, F. T. et al. Obesity genetics in mouse and human: back and forth, and back again. *PeerJ* **3,** e856 (2015).

Yuan, P. et al. Oestradiol ameliorates monocrotaline pulmonary hypertension via NO, prostacyclin and endothelin-1 pathways. *Eur. Respir. J.* **41,** 1116–25 (2013).

Zafrir, B. et al. The association between obesity, mortality and filling pressures in pulmonary hypertension patients; the 'obesity paradox'. *Respir. Med.* **107,** 139–46 (2013).

Zhao, L. et al. Sildenafil inhibits hypoxia-induced pulmonary hypertension. *Circulation* **104,** 424–28 (2001).

9. Declaration

I declare that I have completed this dissertation single-handedly without the unauthorized help of a second party and only with the assistance acknowledged therein. I have appropriately acknowledged and referenced all text passages that are derived literally from or are based on the content of published or unpublished work of others, and all information that relates to verbal communications. I have abided by the principles of good scientific conduct laid down in the charter of the Justus Liebig University of Giessen in carrying out the investigations described in the dissertation.

.....

Balram Neupane 2016, Giessen

10. Acknowledgements

I want to express my gratitude to all the people who have in one or another way bestowed their valuable assistance during this study till the thesis completion. First and foremost I owe my deepest gratitude to Prof. Dr. Ralph Theo Schermuly for accepting me in his laboratory to do this dissertation. He has been immensely supportive throughout and I could not have asked more. He is a great source of inspiration and I will have pleasant memories throughout my life. My sincere thanks to Prof. Dr. Christiane Herden for her invaluable assistance during my PhD studies. Her pleasant demeanor and readiness to help has provided me the mark of confidence.

I am heartily thankful to Dr. Djuro Kosanovic whose guidance and support from the initial to the final level of lab and thesis work enabled me to develop an understanding of the subject and prepare my thesis manuscript. I wish to express my sincere thanks to Dr. Akylbek Sydykov for helping me for echocardiographic measurements and for critical discussions and advices. Many thanks to Christina Vroom for all her help in the lab. Her supportive manner and handiness always created a joyful atmosphere in the lab. I am extremely thankful to Prof. Werner Seeger and Dr. Rory E. Morty for the international MBML program and Dr. Lorna Lück and all the GGL team for all support during my studies. I would also like to thank all the AG Schermuly group for making the life easier both inside and outside the lab.

I gratefully express my gratitude to Dr. Adam Schikora from the Julius Kühn Institute, Braunschweig. Adam not only taught and improved my scientific skills but has also helped me approach the law to fight against the offense. Without his motivation, I would not have been able to continue my doctoral studies. Thank you Adam for being a teacher, a guardian and a friend. My heartfelt applause to you for what you do every day.

I am most grateful to my parents - Bishnu Ballav Neupane and Namakala Neupane, my brothers- Yagya Prasad Neupane and Narayan Neupane and my parent in-laws -Adarsha Pradhan and Hira Maya Shrestha for their continuous love and endorsement. I express my appreciation to my wife Kabita Pradhan whose dedication, love and persistent confidence in me, has taken the load off my shoulder during my studies and preparation of this thesis manuscript. Finally I can’t forget my sons Bichar and Bigyan who have made my life full of joy during this period.

Balram Neupane

11. Curriculum vitae

The curriculum vitae is removed from the online version of this thesis.